Concawe
Environmental Science for European Fuel Manufacturing

Report

Report no. 1/24

Influence of aviation fuel composition on the formation and lifetime of contrails - A literature review

ISBN 978-2-87567-181-3

Influence of aviation fuel composition on the formation and lifetime of contrails — a literature review

This report was prepared by:

K. Gierens[1], R. Sausen[1], U. Bauder[2], G. Eckel[2], K. Großmann[2], P. Le Clercq[2], D.S. Lee[3], B. Rauch[2], D. Sauer[1], C. Voigt[1], A. Schmidt[1]

[1] Deutsches Zentrum für Luft- und Raumfahrt e.V., Institut für Physik der Atmosphäre, Oberpfaffenhofen, Germany
[2] Deutsches Zentrum für Luft- und Raumfahrt e.V., Institut für Verbrennungstechnik, Stuttgart, Germany
[3] Manchester Metropolitan University, Manchester M1 5GD, United Kingdom
[*] Corresponding author: klaus.gierens@dlr.de

Under the supervision of: T. Megaritis (Concawe Science Associate)

At the request of:

Concawe Special Task Force on Aviation Fuels (FE/STF-28) with the collaboration of Safran and Airbus as members of the Steering Committee

Thanks for their contribution to:

- Members of FE/STF-28
- Members of SAFRAN
- Members of Airbus

SUMMARY

The question of how aviation fuel composition affects the formation and lifetime of contrails is a complex one. Although the theory regarding initial contrail formation is well-founded in thermodynamics and proven to be correct by measurements, there remain large uncertainties in terms of persistent contrails forming contrail cirrus. These originate both from processes which are not yet fully understood and from the complexity of quantifying the many factors of influence on their effect on climate. There is an extended cause-effect chain from fuel composition through its combustion and consequential emissions, to contrail formation and their spreading in the atmosphere, and microphysical and optical properties. These properties affect the lifetime and radiative effect of single contrails to the global and multi-annual average of the radiative effects of all contrails, and thus eventually to their climate impact. This problem extends over 17 orders of magnitude in space and time, from the scales of single molecules (about 0.1 nm) and their elementary interactions (say, 1 ns) to the global scales of climate (say, 10,000 km and 10-30 years). It is not possible to cover such a vast range with a single numerical model or with relatively few measurements.

Fortunately, in addition to the thermodynamics of contrail formation, there are other results in this context where the science is relatively robust. This is the fact, shown by measurements, that using sustainable aviation fuels lead to a reduction of soot emission and in consequence to a reduced initial number of ice crystals in the contrails, as long as the reduction of the soot emission does not lead into a regime where co-emitted volatile particles and ambient particles take over the role of condensation nuclei (generally $<10^{14}$ particles per kg fuel). Reduction of the contrail ice crystal concentration in the 'soot rich' regime ($>10^{14}$ particles per kg fuel) has been calculated to result in a lower radiative impact and shorter lifetime, with a lower impact on climate. Whether therefore it would be beneficial for climate to drive aircraft with more and more sustainable aviation fuels, depends on further questions, namely whether these can be produced in a CO_2-neutral way and whether the additional functions that fuels fulfil (e.g., lubrication) are fulfilled by alternative fuels as well. In all cases, safety of flying must not be compromised. While changes in aviation fuel can reduce soot number concentrations by many 10s of percent, lean-burn combustors have the potential to reduce soot number emissions by orders of magnitude.

Aviation contributes about 3.5% to total effective radiative forcing (ERF) from its historical CO_2 emissions and current non-CO_2 effects. A recent assessment by Lee et al. (2021) suggests that the ERF from aircraft non-CO_2 effects in 2018 (mainly contrails and nitrogen oxides) could be larger than the effective radiative forcing from aviation's CO_2 emissions since historical start of air traffic. The magnitude of aviation's non-CO_2 ERF effects is considerably more uncertain than that from CO_2, but could be of the same order of magnitude or even larger. CO_2 is well mixed in the global atmosphere and persists for many millennia from a fossil fuel-based CO_2 emission. Non-CO_2 effects are short-lived (about hours to a decade) and the individual effect of a single emission depends strongly on the local ambient situation (meteorology, sun position, chemical composition of the ambient air).

Contrails form when soot and aerosol particle emissions from the engines mix with ambient air and cool down. Small liquid droplets form on the exhaust particles when liquid water saturation is reached in the expanding plume and instantaneously freeze into ice crystals at temperatures below about -38°C. If the ambient air remains supersaturated with respect to ice, the contrails spread out into persistent contrail cirrus. They may change the energy budget of the atmosphere by trapping

longwave radiation, which leads to an energy input to the atmosphere and to a warming. During the day, the small ice crystals may act as mirrors and reflect a part of the solar radiation, less solar energy reaches the ground, which leads to a slight cooling. On the global annual mean, the warming effect of contrails dominates and the ERF might be in the order of the ERF of aviation's CO_2 emissions.

Details of the radiative impact of persistent contrails depend on their optical and microphysical properties. These are controlled in particular by the amount and type of particulate matter that is emitted from an aircraft engine, which in turn depends indirectly on the type and composition of the fuel and on the combustion process. In this way the number and type of particulate matter have an impact on the magnitude of the contrail-induced climate change. Contrails can form even if no particles are emitted, because the ambient atmosphere contains aerosol, that is, particles that in such a case serve as condensation nuclei. This becomes important if non-hydrocarbon fuels such as liquid hydrogen are used.

Sustainable aviation fuels (SAF) from biogenic feedstocks and produced with renewable energy have significantly lower aromatic and sulphur fuel contents compared with fossil fuel-based kerosene. As the temperature distribution in the engine is not significantly modified by SAF, NO_x emissions are not expected to change when burning SAF. With respect to contrail formation, the cyclic aromatic ring structures in the fuel have a higher bonding energy and are therefore more efficient soot precursors compared to the large fraction of chain-like hydrocarbon molecules within the fuel. Ground tests as well as in-flight measurements have shown that the reduced aromatic content of SAF (indicated by a higher hydrogen content of the fuel), leads to a reduction in soot particle emissions. Initial in-flight measurements have shown a reduction in the number of ice crystals in contrails - as long as the soot emissions remain in the high soot regime of the current fleet ($>10^{14}$ soot particles per kg of fuel burnt).

Initial ice crystal number concentrations are proportional to soot particle number emissions in the "soot-rich" regime with more than 10^{14} soot particles emitted per kg kerosene burnt. It is plausible to assume that reducing the soot emission within the soot-rich regime is beneficial for climate. Generally, this implies larger ice crystals with smaller radiative effects and higher fall-velocity, thus less horizontal spreading and a shorter contrail lifetime. To compute the benefit for climate is complicated, both for individual cases and for the global average, because of the large number of influential factors and processes. In any case, the benefit is not simply proportional to a reduction of soot in the soot-rich regime.

The concentration of ice crystals is not proportional to the soot number emission in the soot-poor regime, because also volatile particles in the exhaust and ambient aerosol particles may serve as condensation nuclei, as shown by modelling. As there are about 100 times more volatile than non-volatile particles emitted, the number of droplets and ice crystals can increase dramatically in the soot-poor regime. However direct measurements and observations of this are lacking and first experiments are currently being analysed and evaluated. Consequently, models for the climate impact of such contrails are not yet available.

Eventually, it is not only the radiative impact of contrails which is of interest but the actual climate change that they cause (e.g., rise of the mean temperature at Earth surface, or sea-level rise). So far, there is only one study, using a global model, that tries to quantify the effect on the ground temperature. This study indicates that the temperature effect of the ERF from contrail cirrus is approximately 0.4 of that from an equal forcing from CO_2. As this is the only study

of this kind so far, more simulations of contrails climate impacts with other climate models are urgently needed to corroborate or question these results.

This report makes clear that reducing fuel constituents that lead to the formation of soot in the exhaust leads to lower concentrations of ice crystals in the contrail. This statement refers, however, to soot-rich regime only, that is, where more than 10^{14} soot particles are emitted for each kg fuel burnt. In this regime, the initial reduction of ice crystals numbers is proportional to the reduction of soot particle number. However, the final reduction of ice crystal number after the vortex phase is weaker and the eventual climate benefit for a single case depends on factors such as ambient temperature and contrail dissipation mechanism. Thus, to estimate the climate benefit, either in terms of RF or ERF, from a reduction of fuel constituents (e.g., aromatics) is not a simple calculation. Many processes are involved, starting with the uncertainty at the very beginning, namely the soot formation itself. For example, the effect of a reduction on aromatics to emission index of soot ($EI_{n,soot}$) cannot be calculated simply, since it depends on the combustion process and other factors. The quoted measurements show lower soot numbers for lower aromatics, but in a complicated way. Then, the processing of initial ice crystals in wing vortices depends on a number of factors, including aircraft size, speed, ice size distribution, air temperature, etc. The later fate of the contrail depends primarily on the meteorological situation. Thus, even in the simpler and better-known soot-rich regime there are still difficult problems to be overcome that require better theories (soot formation), measurements (to confirm the theories) and global modelling of contrails to catch the large meteorological variability that affects contrail evolution and their individual radiative effect. Even this latter effect depends not only on N_{ice} but also size distribution and crystal habit (shape), which may be changed with SAF/low aromatic fuel usage.

The uncertainties are even larger in the soot-poor regime, for which only preliminary measurement results exist so far. Theory predicts that ice crystal numbers can even rise with decreasing soot emissions, since this allows ultrafine aqueous particles in the exhaust and ambient aerosol to take over the role of condensation nuclei from the soot particles. The radiative consequences of such a strong soot reduction is not known so far, since corresponding simulations with global models do not exist. Further measurements need to be made and the results incorporated in such models before they can be used for such a purpose. Ideally, global models of several independent groups should be used, in order to get an estimate of the uncertainty of the results.

KEYWORDS

Contrails, Soot particles, aromatics, non-CO_2, ice-crystals, nucleation, fuels specifications, soot-poor regime, soot-rich regime,

INTERNET

This report is available as an Adobe pdf file on the Concawe website (www.concawe.org).

CONTENTS

1. INTRODUCTION

The influence of aviation on climate is shown to be greater than that from its CO_2 emissions alone but with large uncertainties on the non-CO_2 effects (IPCC, 1999; Sausen et al., 2005; Lee et al, 2009; Lee et al., 2021). The aviation non-CO_2 effects comprise changes of the atmospheric concentrations of O_3, CH_4 and H_2O resulting from NO_x emissions, the formation of contrails and contrail cirrus, the direct emission of H_2O, the emission of aerosols and aerosol precursors with their direct radiative effects, and the indirect cloud effects resulting from aviation induced aerosols (e.g., Prather et al., 1999; Sausen et al., 2005; Lee et al., 2009; Lee et al., 2021).

Figure 1.1 shows the various contributions of aviation to climate change in terms of effective radiative forcing (ERF) as presented in a recent paper by Lee et al. (2021). The results show that contrails and contrail cirrus, while short-lived relative to CO_2, are currently respectively the largest contributors to the total radiative forcing (RF) and effective radiative forcing (ERF), from aviation, if the best estimates are considered. Nevertheless, the uncertainty of the magnitude of the contrail (and contrail cirrus) induced RF and ERF, is large in comparison to CO_2. The uncertainty further increases if RF or ERF are to be transferred into climate change effects, e.g., in terms of global mean temperature change due to the associated efficacy. Note that the efficacy of contrails and contrail cirrus is significantly smaller than 1, i.e. the temperature response is smaller than would be expected from RF or ERF (e.g., Ponater et al., 2005; Rap et al., 2010; Bickel et al., 2020; Bickel, 2023).

In addition to the impact of atmospheric conditions, the magnitude of the RF and ERF from contrails and contrails cirrus depends on fuel composition, engine type, and consequential soot emissions, an effect which requires a better quantification (e.g., Burkhard et al., 2018). Arrowsmith et al. (2020) suggested the use of lower C footprint alternative (hydrocarbon) fuels may have the co-benefit of mitigating contrails. (For details see Sections 5.8 and 5.9).

This report puts into perspective the role of jet fuel composition to the associated aviation emissions, with a particular focus on the (poly)aromatic / naphtalenic fuel content, the sulphur content and particulate matter (i.e. soot) emissions, including their effect on contrail formation and lifetime, and the associated forcing. This will shed light on a potential mitigation strategy for the aviation climate impact, i.e., by using alternative fuels.

After a definition of terms, which are of central importance in the study (Section 2), we describe in Section 3 the basic chemistry and microphysics that play an important role in particle formation, ice nucleation, cloud formation, and the associated radiative effects. Sections 4 and 5 elaborate on jet fuel composition and its impact on aviation emissions, and on the impact of jet fuel composition on contrail formation and lifetime, respectively, including the associated radiative forcing. The uncertainties and limitations with respect to the contrail RF and ERF are reported in Section 6. Finally, future implications and challenges, and future research opportunities are discussed in Sections 7 and 8, respectively.

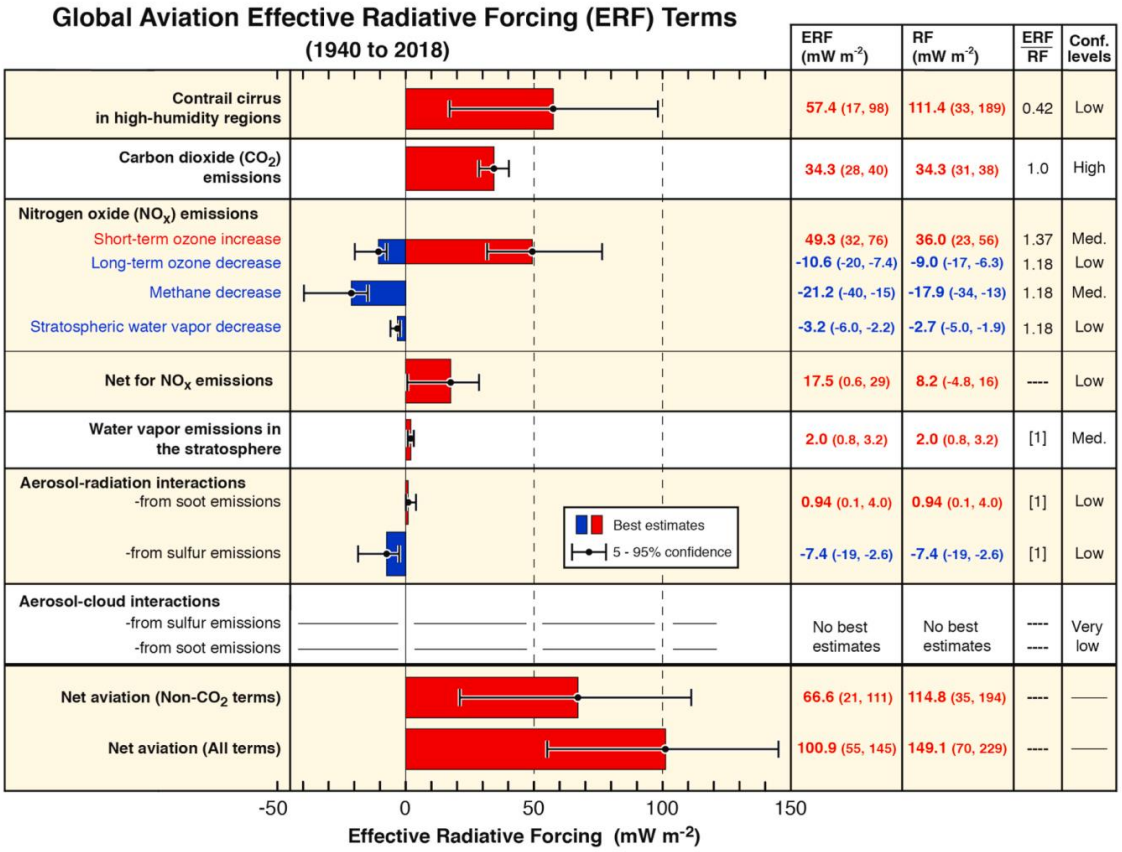

Figure 1.1 Best-estimates for climate forcing terms from global aviation from 1940 to 2018. The bars and whiskers show ERF best estimates and the 5–95% confidence intervals, respectively. Red bars indicate warming terms and blue bars indicate cooling terms. Numerical ERF and RF values are given in the columns with 5–95% confidence intervals along with ERF/RF ratios and confidence levels. RF values are multiplied by the respective ERF/RF ratio to yield ERF values. ERF/RF values designated as [1] indicate that no estimate is available yet (from Lee et al., 2021).

2. DEFINITIONS

In this section, the definitions of selected terms, which are of central importance in the study are provided.

Sustainable aviation fuel (SAF) is a broad term used by the aviation sector to refer to fuels that have a lower, or zero fossil carbon footprint. This may include novel fuels such as liquid hydrogen (LH_2). Here, we use the term 'SAF' only in terms of liquid hydrocarbon fuels, designed to be 'drop in' replacements to fossil aviation kerosene. Such fuels may be produced by the hydrotreatment of bio or waste-based sources; along with so-called 'e-fuel' or 'power-to-liquid' fuels. The lower (fossil) C footprint of such fuels is usually presented on a life-cycle analysis (LCA) basis, which accounts for the production and transport of such fuels on a CO_2 equivalent (CO_2-e) basis (see "metrics", below). This is not further discussed here but the reader is referred to the recent assessment of aviation fuels in a 'net zero' context by Hutchings et al. (2023). Presently, SAFs are required to be blended with conventional fossil-based fuels to be drop-in. The resulting SAF blends can have lower aromatic content and sulphur content compared with conventional jet fuels. This alters their soot-forming propensity (see "soot", below).

Particulate matter (PM) designates microscopic particles suspended in air covering a large range of sizes from a few nanometres to hundreds of micrometres. PM is omnipresent throughout the atmosphere and has a variety of origins, both natural and anthropogenic. Depending on the formation process, PM is categorized as primary and secondary PM, where the former refers to particles which are directly suspended into the atmosphere such as soot or mineral dust, while the latter are particles created through chemical transformation of precursor gases, e.g. sulphur or nitrogen oxides or oxidation of volatile organic compounds (VOC).

Non-volatile particulate matter (nvPM) is sometimes used interchangeably with soot (see below) in the context of aviation exhaust, however, nvPM has a strict regulatory definition made under measurement conditions specified by ICAO[1] Annex 16, i.e., PM exiting the engine exhaust that does not volatilize when heated to 350°C (ICAO, 2021)

Soot (particles) forms as a result of incomplete combustion of carbonaceous components. It is generally produced through condensation of vaporized organic matter, usually through a number of polycyclic aromatic hydrocarbons (PAH). As condensation nuclei, soot particles play an important role in the formation of contrails (see Section 3.2).

Relative humidity is a measure of the concentration of water vapour. It is expressed as a fraction (or in percent) of a concentration at which the vapour is saturated. Saturation, in turn, is a state where a net exchange rate between the water vapour and surfaces of condensed water (either liquid water or ice) becomes zero; that is, the vapour concentration is such that on average the same number of water molecules go from the vapour into the condensed phase as the opposite direction. As the condensed phase can be liquid or ice, there are two forms of relative humidity: RH with respect to liquid water and RHi with respect to ice. A certain water vapour concentration (or partial pressure) can be expressed both as RH and RHi; in this case RHi has the higher value. RH only slightly exceeds 100% in the

[1] The International Civil Aviation Organization, a specialist agency of the United Nations, with responsibility for international civil aviation.

atmosphere (formation of liquid clouds), but RHi can attain quite high values exceeding 150%. States with RHi>100% are labelled “ice-supersaturated”.

Contrails are line shaped ice clouds triggered by the emission of water vapour by aircraft engines under specific atmospheric conditions within the atmosphere, in particular in sufficiently cold air (specified in the so-called Schmidt-Appleman criterion, see section 5.1). Persistent contrails can horizontally spread in the air, such that they no longer appear line-shaped after a while. These clouds are termed contrail cirrus. Other forms of condensation caused by aerodynamic effects around aircraft are not considered in this study.

Radiative forcing (RF) characterizes the size of the perturbation to the planetary radiation budget due to the imposed effect, relative to pre-industrialization (unit: watts per square metre, W m^{-2}). The climate system then responds to RF leading to a surface temperature change (a positive RF leads to a warming, and vice versa). The concept is discussed at length in IPCC assessments, including Myhre et al. (2013) and Forster et al. (2021). RF enables a comparison of the size of different climate-change drivers, e.g., greenhouse gases, and also both within and between sectors. RF is proportional to the expected equilibrium surface temperature change (ΔT) relative to (say) pre-industrial temperature (T-T_{pi}), that would result if the atmospheric perturbation resulting to that RF was applied for many decades, so that:

$$\Delta T = T - T_{pi} \approx \lambda \, RF \qquad (1)$$

where the constant of proportionality, λ, is the *climate sensitivity* parameter in K (W m^{-2})$^{-1}$. It is important to note that this expression is valid when applied to global mean forcing and global mean temperature response. Since the Intergovernmental Panel on Climate Change’s (IPCC) 5th Assessment Report AR5 (see Myhre et al. 2013), the usage of *effective radiative forcing* (ERF) has become commonplace. The usefulness of RF is as a comparative measure, so that the global-average temperature change from, for example, a 1 W m^{-2} perturbation due to contrails, is similar to that resulting from 1 W m^{-2} due to aviation-induced CO_2 changes. Over time, this has found not to be the case. ERF incorporates some adjustments resulting from an RF (e.g., in cloudiness) that occur on a more rapid timescale (the mentioned effects on natural clouds occur within hours to days) than resulting surface temperature changes (which occur over periods of decades). The difference between RF and ERF for contrails and contrail cirrus has been found to be of the order 0.5 (i.e., ERF is 50% less) (Bickel et al., 2020, Lee et al., 2021).

Metric is strictly a quantitative measure for comparative purposes. So, for example, ERF is a ‘metric’. However, in the context of (in particular) non-CO_2 aviation effects, the usage of the term ‘metric’ has become shorthand and resulted in considerable confusion. The intention, and term adhered to here is ‘emission metric’, where an effect from non-CO_2 emissions is quantified as an equivalency to CO_2 emissions, or CO_2-e. The topic has been widely discussed since the introduction of the global warming potential by the IPCC’s First Assessment Report in 1990 (IPCC, 1990). There are many emission metrics available for CO_2 equivalency. Their discussion is beyond the scope of the present document but the reader is referred to, e.g., Fuglestvedt et al. (2010) and Myhre et al. (2013) for extensive overviews.

3. BASIC CHEMISTRY AND MICROPHYSICS

The formation of a new phase within a parent phase is termed nucleation. In order to build the new phase, tiny nuclei of it need to build up in the parent phase and to grow to a stable size. Nuclei that are too small are unstable and will be destroyed quickly due to the thermal motion of its constituent molecules and due to collisions with ambient molecules. However, once a nucleus is sufficiently large (a few nanometres), it will become stable and the system gains energy by further growth of the germ. Nucleation is a process that needs to overcome an initial energy barrier (i.e. the formation of a sufficiently large seed nucleus) in order to proceed spontaneously. Solid surfaces of foreign materials can help stabilizing the seed nuclei. If this happens, it is called heterogeneous nucleation. If only molecules of the nucleating substance are involved, it is called homogeneous nucleation. In the exhaust of aircraft engines nucleation processes occur in different contexts. In a first step volatile aerosol particles are created from condensable gases that are rapidly cooled once entering the ambient atmosphere and, secondly, the creation of ice particles in the contrail. A simple sketch of how particles evolve to a contrail in the exhaust of a jet engine is presented in Figure 3.1.

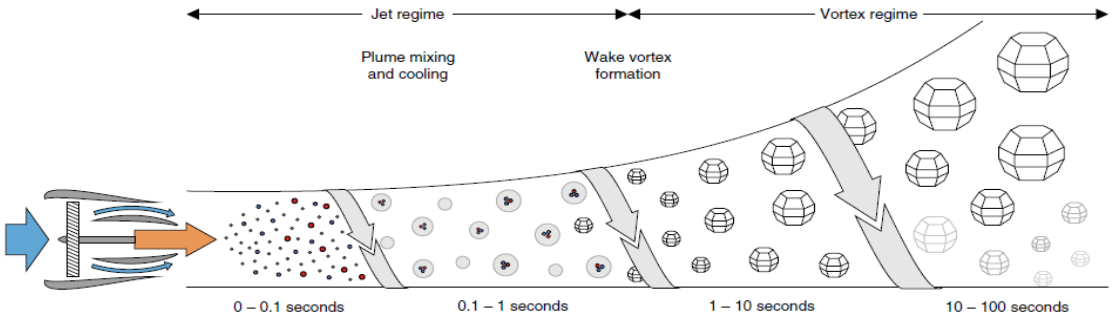

Figure 3.1 Sketch of the temporal evolution of particles (volatiles, non-volatiles, ice crystals) in the exhaust of a jet engine during the jet and vortex regimes, (Kärcher, 2018). The dynamic evolution of contrails is conveniently divided into three phases. The first one, the "jet regime" is characterized by the jet, that is formed by the gases which are emitted by the engines at high speed and temperature relative to the ambient air. The friction between the jet and the ambient air leads to mixing; the jet expands and cools quickly. After about a third of a second it is already sufficiently cold (about -40°C) for ice crystals to form and a contrail becomes visible for a distant (e.g., ground-based) observer. Simultaneously, the airstream around the wings organises itself into a pair of counter-rotating vortices which after about 20 seconds starts to dominate the contrail dynamics. This regime is accordingly termed the "vortex phase". The two vortices form two vortex tubes with the ice crystals caught inside. The vortex tubes induce each other a downward motion, which leads to adiabatic compression, warming and partial loss of ice crystals. The vortex system becomes unstable after a few minutes, which can be seen when vortex rings and waves become apparent in the young contrail. This signifies the end of the vortex phase and the beginning of the “dispersion phase” where the remaining ice crystals (if any) get influenced by the ambient atmosphere.

3.1 CHEMISTRY AND MICROPHYSICS OF PARTICLE FORMATION

The exhaust of jet engines contains water vapour and carbon dioxide from fuel combustion. However, trace amounts of particles are also present, predominantly

soot from incomplete combustion and a variety of condensable gases such as nitric acid, sulphuric acid (in presence of sulphur in fuels derived from fossil sources), and unburned hydrocarbons. These offer nucleation sites for water vapour to yield secondary particles in the rapidly cooling exhaust. In addition, the exhaust contains particles present in the ambient atmosphere that get ingested into the engine and the bypass flow. All types of particles may be important for contrail ice formation depending on their microphysical and chemical properties (see Kärcher 2018 for an overview). For contrail formation, the presence of a hydrocarbon fuel is unnecessary, as noted by the 1957 flight of a B-57 on hydrogen where it was observed "The engine burning hydrogen had produced a dense and persistent condensation trail, while the other engine operating on JP 4 left no trail." (NACA, 1957). In this case, aerosol particles from the background air and mixed into the plume serve as condensation nuclei. Note that the word "persistent" in the quotation is not synonymous to the word "persistent" as it is nowadays used to characterize contrails that exist longer than 5 to 10 minutes. The observation that the JP 4 exhaust did not produce a contrail while the hydrogen exhaust did, is consistent with the theory, as presented in section 5 below.

Volatile particles, which can grow to sufficiently large sizes to become relevant for ice formation, are predominantly formed on abundantly present ionised molecules and molecule clusters (chemi-ions) in the exhaust (Yu and Turco, 1998, Arnold et al., 1999, Kärcher and Voigt, 2017). The amount of sulphur in the fuel thereby controls in particular the size those newly nucleated particles can grow to and hence the importance of these particles for ice particle nucleation (Kärcher et al. 2000, Brock et al. 2000). The relevance for ice formation is further influenced by the hygroscopicity of the particles depending on their chemical nature. The condensable organic constituents of the particle emissions are particularly poorly characterized, and will depend on fuel properties, and also on combustor technology and engine power settings.

3.2 MICROPHYSICS OF ICE NUCLEATION

The formation of contrail ice involves two nucleation steps. First, liquid droplets form on emitted soot particles or on other types of particles (depending on the fuel). In the second step, ice germs form within the liquid droplets.

The formation of liquid drops from emitted soot particles has been studied in the laboratory by Popovicheva et al. (2004, 2008), and Demirdjian et al. (2007)[2]. The essence is that the surfaces of aircraft soot particles contain molecules with polar properties (so-called functional groups containing oxygen and OH) that attract the water dipoles by electric forces. Further, aircraft soot surfaces contain water soluble substances. Once water molecules are attached by functional groups they start to form water clusters around these active sites. More important is that aircraft soot particles obtain coatings of water-soluble material already within the engines. They are efficient sinks for ambient water molecules and their presence triggers the formation of an aqueous coating on the soot particles which gets thicker as the humidity rises within the expanding plume. A fraction of the soluble matter consists of sulphur-containing species, but it is neither the dominant fraction nor necessary for contrail formation. Contrails form even when the fuel does not contain sulphur or carbon, as already noted.

[2] See also Gierens et al., 2016: Condensation trails from biofuels/kerosene blends scoping study, ENER/C2/2013-627, chapter 1.3). https://elib.dlr.de/113112/1/Contrails-from-biofuels-scoping-study-final-report.pdf.

If the ambient temperature is several degrees (about 5K) below the contrail-formation threshold (explained below in Section 5.1), the intermediate water supersaturation gets so high in the expanding plume that the soot particles acquire a thick water coating which then freezes. As the soot core is rather hydrophobic after dissolution of the soluble surface substances into the acquired water, the freezing process does not involve the soot core; it occurs in the aqueous solution envelope without interaction with the solid surface and is thus a homogeneous freezing process. Homogeneous freezing has been described by Koop et al. (2000) as a process that depends mainly on water activity in the solution (i.e., the ratio of the saturation vapour pressures over the solution and over pure water at the same conditions), and not on the nature of the solution. Pure water droplets freeze at −38°C (supercooling limit), but solutions stay liquid down to lower temperatures and their supercooling limit depends on the water activity. A typical contrail-formation threshold for kerosene is about −40°C, that is, already below the supercooling limit for pure water. −40°C is the supercooling limit for quite dilute solutions with an activity close to unity.

The aircraft soot particles are coated with dilute solutions and thus they readily freeze at temperatures below the contrail-formation threshold. A transition to drop-in SAF raises the threshold temperature by a few tenths of a degree (because of a slightly increased EI_{H2O}/Q ratio), and it raises the maximum supersaturation attained in the expanding plume, such that is it increases the thickness of the acquired water coating, which achieves a still higher activity close to unity. Thus, up to −38°C (supercooling limit of pure water), the droplets will freeze readily. In case of alternative fuels like hydrogen, that allow condensation at much higher temperatures, initially formed droplets may not freeze if the ambient temperature exceeds −38°C. Instead the droplets may soon evaporate (like the droplets that form in the exhaust of a chimney in winter time). Whether the droplets freeze or not depends in such a case on surface properties of those solid aerosol particles from the ambient air on which the emitted water vapour condensed. However, further work is required to evaluate this area as contrail formation conditions depend on the technical realizations of the hydrogen-burning engines.

4. JET FUEL COMPOSITION AND AVIATION EMISSIONS

4.1 COMPOSITION OF DIFFERENT TYPES OF JET FUEL AND THEIR PHYSICAL PROPERTIES

The basic specification for crude oil-based fuels is ASTM D1655 (Jet A/Jet A-1, ASTM, 2022) and DefStan 91-091 (Jet A-1, Ministry of Defence, 2022), with national variants in China, Russia, and Brazil.

Jet fuels have performance specifications, meaning that their composition is not explicitly described. Instead, safe performance is guaranteed by lower or upper limits on selected chemical and thermophysical properties, or directly on few selected species mass or volume fractions within the composition.

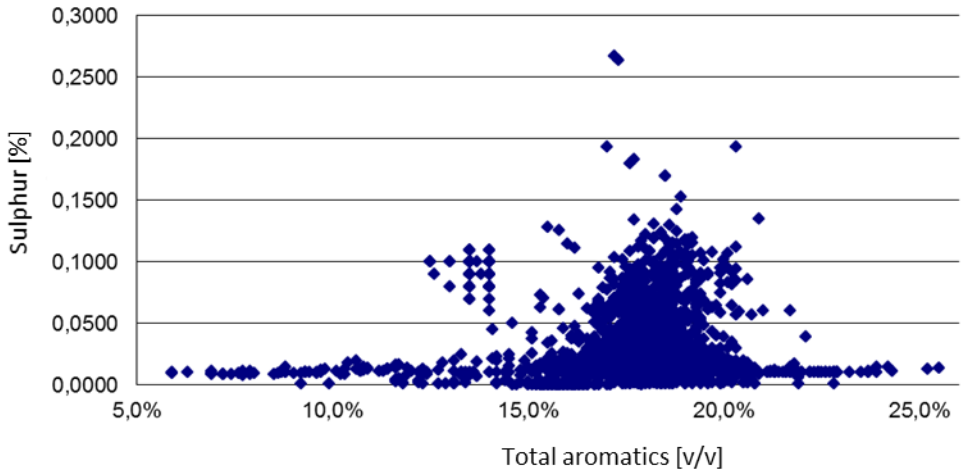

Figure 4.1 Distribution of sulphur and aromatics in Jet fuels used in Germany from Nov 2010 to Oct 2011. Each data point represents a fuel. (Zschocke, 2014)

As a consequence, the composition of jet fuel varies depending on the crude oil, processing technology, and regulatory environment. This variability is systematically captured in studies such as the PQIS (The Defense Energy Support Center, 2009) and the UK Annual Survey of Aviation Fuel Quality (Energy Institute, 2014). Specific surveys have captured the variability of jet fuel (Hadaller et al., 2006; the Metron Aviation Fuel Study in the US [altjetfuels, 2015], and the Lufthansa BurnFair Study [Zschocke, 2014]). An example (displayed in Figure 4.1) depicts the sulphur and aromatic contents of all jet fuels used in Germany from Nov 2010 to Oct 2011.

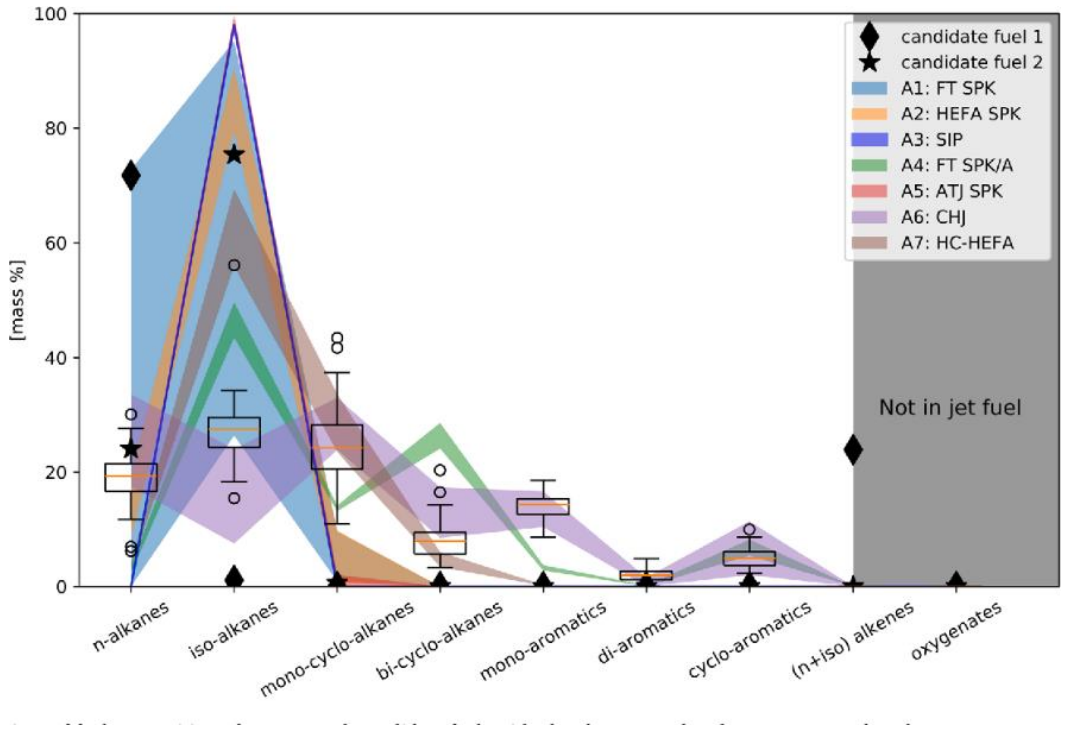

Figure 4.2 Fuel family mass fractions of ASTM D7566 approved synthetic hydrocarbons (coloured areas) and of 57 conventional fuels from the CRC World fuel survey (Hadaller et al., 2006) (bars and whiskers).

Fuels can be described at three levels of detail:

- Level 0 - global: fuel family mass fractions,
- Level 1 - detailed: mass fraction per C-number compound per family,
- Level 2 - complete: identification of mass fraction for each species in the fuel.

Figure 4.2 gives an insight into the variance in conventional jet fuels (whiskers) based on 57 samples and approved SAF present in the DLR SimFuel database as of March 2023. The approved SAF are listed in the Annexes of the ASTM D7566 standard as:

A1 Fischer-Tropsch Hydroprocessed Synthesized Paraffinic Kerosine (FT SPK),

A2 Synthesized Paraffinic Kerosine From Hydroprocessed Esters And Fatty Acids (HEFA SPK)

A3 Synthesized Iso-Paraffins From Hydroprocessed Fermented Sugars (SIP)

A4 Synthesized Kerosine With Aromatics Derived By Alkylation Of Light Aromatics From Nonpetroleum Sources (FT SPK/A)

A5 Alcohol-To-Jet Synthetic Paraffinic Kerosene (ATJ SPK)

A6 Synthesized Kerosine From Hydrothermal Conversion Of Fatty Acid Esters And Fatty Acids (CHJ)

A7 Synthesized Paraffinic Kerosine From Hydroprocessed Hydrocarbons, Esters And Fatty Acids (HC-HEFA)

As can be seen in Figure 4.2, most approved SAFs are paraffinic fuels, which have a significantly higher n/iso-alkane content compared to conventional crude-oil based fuels. Only A4: FT SPK/A and A6: CHJ currently contain aromatics.

Fuel composition with level 1 detail provides information on the mass fraction per carbon number compound per fuel family. This information is typically obtained from GCxGC analysis (Striebich et al, 2014). The graphs in Figure 4.3 show an example for selected fuels. It should be noted that individual fuels from the same production pathway can differ significantly. Jet A-1 has a high number of compounds, while FT-SPK and HEFA-SPK are purely paraffinic with a similar distribution and number of components for n- and iso-paraffins. ATJ-SPK, on the other hand, has a significantly different composition, with only a few iso-paraffins.

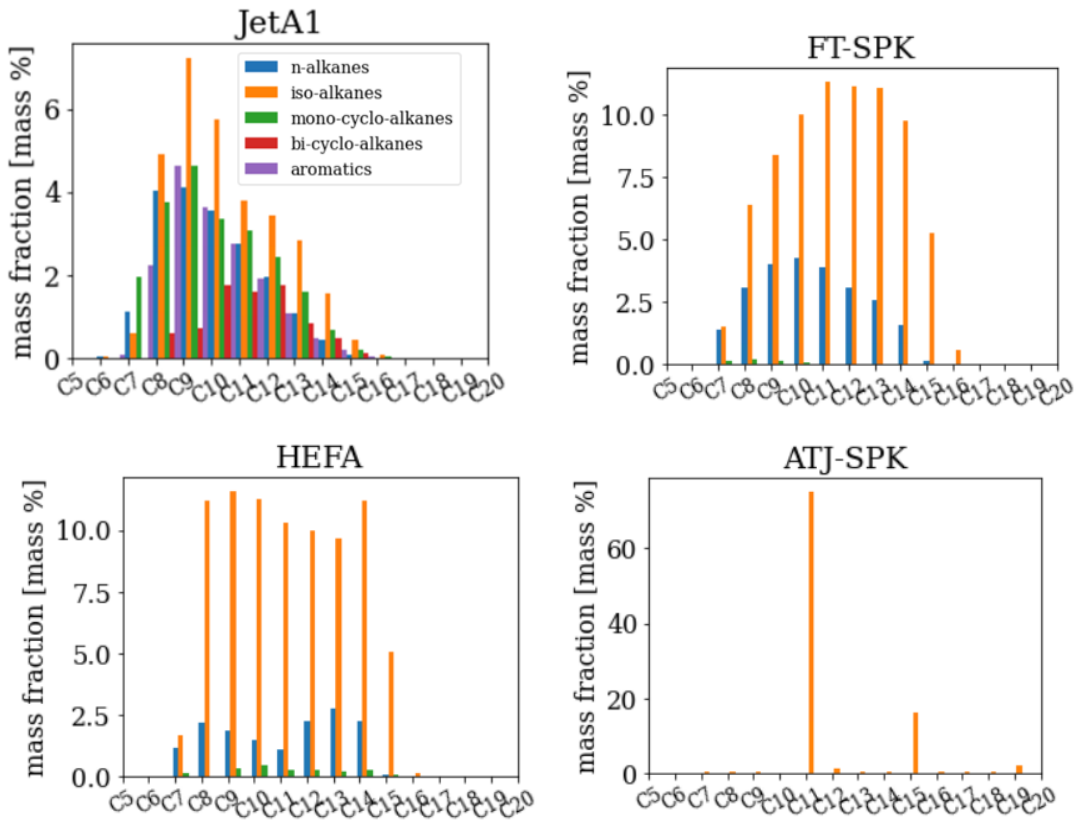

Figure 4.3 Detailed (level 1) fuel composition of conventional Jet A-1 and three SAF.

Level 2 information about the mass fraction of each molecule in the fuel can be obtained. However, this is not possible for complex mixtures of several hundred molecules. Additional information, such as the degree of branching, which can have an influence on soot as explained later, can also be obtained (see Table 4.1 for illustration).

The composition of fuel directly affects its physical properties, including viscosity, density, volatility, flash point, specific energy and others. As shown in Figure 4.4, the physical properties of HEFA fuel were compared to fuel data from the UK fuel

ITAKA HEFA fuel

Fuel specification	Min	Max	Fuel Sample
Colour			30
Acidity (mg KOH/g)	0	0.015	0.002
Aromatics IP 156 (%vol)	0	25	1.8
Sulphur (%mass)	0	0.3	0.018
Mercaptan (%mass)	0	0.003	0
IBP (degC)			148.8
10% (degC)		205	169.8
50% (degC)			198.7
90% (degC)			235.1
FBP (degC)		300	251.9
Flash point (degC)	38		41.5
Density @15degC (kg/m3)	775	840	759.6
Freezing point (degC)		-47	-59
Viscosity @-20degC (cSt)	0	8	3.885
Smoke point (mm)	5		50
Naphthalenes (%vol) if SP > 25mm		3	0
Specific Energy (MJ/kg)	42.8		44.023
Existent Gum (mg/100 ml)		7	1
MSEP	85		99

Survey data from EI - The Quality of Aviation Fuel Available in the Untied Kingdom Annual Survey 2014

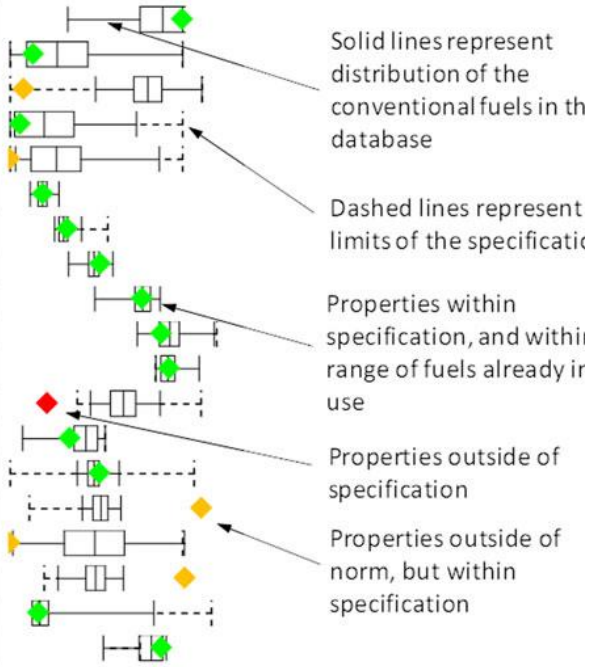

Figure 4.4 Comparison of HEFA to UK Fuel Survey from 2014 and ASTM D1655 specification limits (Blakey et al, 2022). Note: The minimum smoke point is 25 mm and the specification has no lower limit of 0 for acidity, aromatics, mercaptans, sulphur and viscosity.

survey. Note, that the HEFA is a synthetic blending component, which has to meet ASTM D7566 Annex A2 specification requirements and afterwards has to be blended before usage with conventional crude oil-based fuel. However, this plot is intended to show how synthetic fuels may vary from the range of experience and still be safe to use when blended. The impact of variability in conventional fuel composition (the range of experience) is depicted by whisker plots, with property values for selected HEFA shown as green diamonds. The properties of HEFA synthetic blending components can vary, and this variability is controlled by the ASTM D7566 Annex A2 specification requirements. A comprehensive overview of jet fuel properties is provided in Edwards (2020). The final blend containing up to 50 vol% of one single synthetic blending component has to meet the ASTM D7566 Table 1 requirements including part 2 of the extended requirement, which in particular stipulates the minimum of 8 vol% aromatics (according to ASTM D1319). This is due to the large pool of possible conventional jet fuels.

Table 4.1 Hydrocarbon species with identical generic formulae, as for example CnH2n+2 like the molecule above with 13 carbon atoms, can correspond to a single normal alkane or a very large number of iso-alkane isomers. Here two examples 2-methyl dodecane and 3,3-diisopropyl-2,4-dimethylpentane, which are characterized by very different thermophysical properties.

$C_{13}H_{28}$

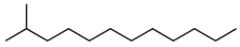

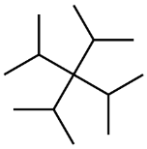

4.2 AVIATION EMISSIONS FOR JET-A AND THE IMPACT OF ENGINE TECHNOLOGY

Exhaust gases from an aircraft gas turbine burning hydrocarbon fuels consist primarily of CO_2, H_2O, with trace amounts of CO, unburned hydrocarbons (HC), particulate matter (PM), NO_x, SO_x as well as excess atmospheric oxygen and nitrogen (Lefebvre and Ballal, 2010; Chapter 9). Figure 4.5 shows the emission indices (in g per kg fuel) of the individual combustion products for a V2527-A5M engine from the ICAO emission database. While CO_2 and H_2O are the result of the completed combustion process of a hydrocarbon fuel, CO and HC emissions arise from fuel, which was not fully converted. Due to the fact that CO and HC emissions reflect unwanted losses and lower efficiency, modern engines usually meet their respective regulation limits (Owen et al., 2022). SO_x emissions stem from sulphur compounds in the fuel, which are oxidized during the combustion process. As these emissions are directly related to the fuel composition, they are regulated by sulphur limits in the fuel specification. NO_x is formed by the oxidation of nitrogen from the air. PM are unwanted combustion products, which are classified as non-volatile carbonaceous particles (nvPM) (also described as black carbon, 'BC', or 'soot'), and volatile particles (vPM). Driven by local air quality and health concerns, NO_x and nvPM regulations have become more and more stringent in recent years (see also footnote 3). As a consequence, modern engine and combustor design has focused on avoiding these emissions and meeting their regulatory limits.

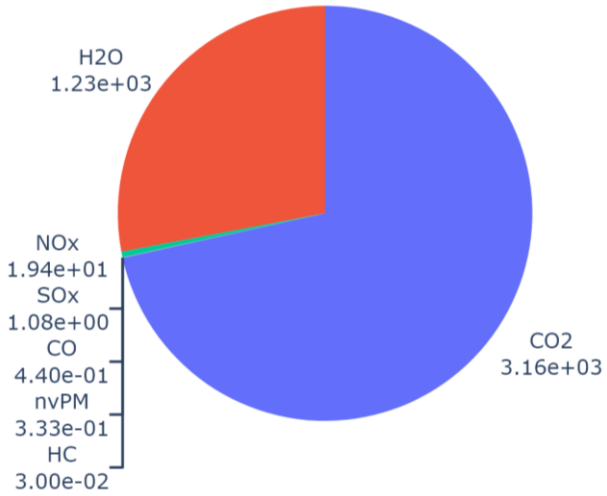

Figure 4.5 Emission Indices (EI) in g per kg fuel (calculated for a V2527-A5M engine from the ICAO emission database)

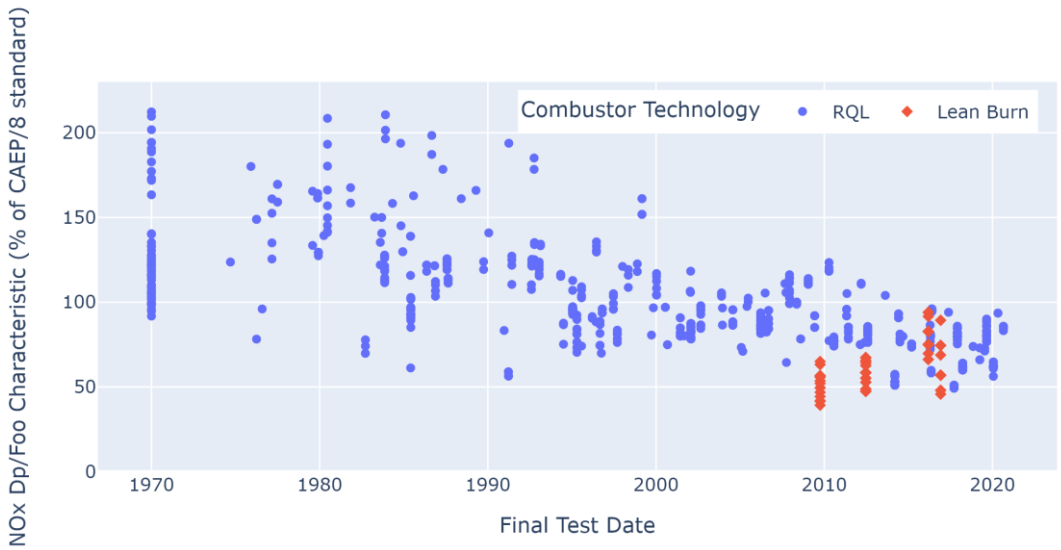

Figure 4.6 NOx emissions over time of engines (each data point), taken from the ICAO Emission database (EASA, 2023). The results are relative (in %) to the CAEP/8 standard, which is set as reference. Two combustion system architectures were selected: rich-burn quick-quench lean-burn (RQL) (blue circles) and the more recent lean-burn (red diamonds).

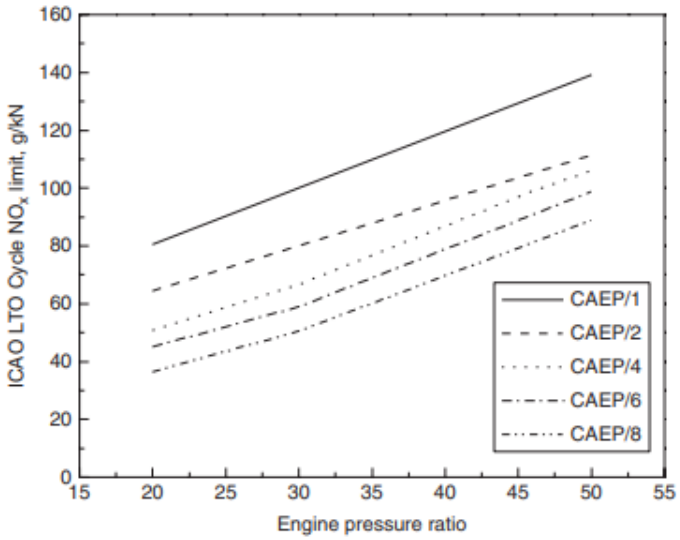

Figure 4.7 Regulatory limits (Lieuwen, et al., 2013, their Chapter 3.2) of NOx emissions on a landing-take-off cycle as function of engine pressure ratio. From the Committee on Aviation Environmental Protection (CAEP) CAEP/1 released in 1986 to CAEP/8 released in 2010.

Figure 4.6 shows the evolution of the NO_x emissions of aviation turbine engines over a period of time as recorded in the ICAO emission database, and Figure 4.7 shows the regulatory limits over time[3]. In Figure 4.6, the two main combustion technologies prevailing in modern gas turbine powered airplanes are distinguished indicating the influence of combustor technology on emissions: The Rich-burn, Quick-quench, Lean-burn (RQL) and the Lean Burn technologies. Figure 4.6 illustrates a gradual decline in NO_x emissions over the last decades. The lean-burn technology shows the lowest thrust normalized NO_x emissions (in 2010). More recently, NO_x emissions from conventional RQL engines (right side of Figure 4.6) have come down to similar levels as those achieved with lean burn technologies.

With respect to the nvPM emissions, Figure 4.8 (upper panel) shows a more distinct tendency at climb-out conditions (85% thrust), where the lean-burn technology emits orders of magnitude less particles, both in number and mass. However, at lower thrust settings, when staged lean burn engines switch to a rich burn mode, e.g. at 30% thrust in approach (Figure 4.8, lower panel), optimized RQL engines represent the lowest emission levels. It is noteworthy that current ICAO regulations are focused on operations at low altitudes in and around airports and hence on local air quality impacts. As a consequence, the monitoring of the emissions focuses on a defined landing-take-off cycle (LTO) representative of aircraft operations below 914 m (3000 ft). Consequently, as shown in Figure 4.9, thrust settings most frequently found at cruise are in the range from 40 to 65% thrust, for which only limited data from engine certification are available.

[3] CAEP/1 etc. refers to a 3-yearly cycle of ICAO's Committee on Aviation Environmental Protection, which recommends Standards and Recommended Practices (SARPs) for emissions of NOx, nvPM, CO, HCs for adoption by ICAO Council. It is "regulation" essentially, which then gets adopted in national/international (e.g. EU) regulation, since ICAO has no international legal mandate, per se.

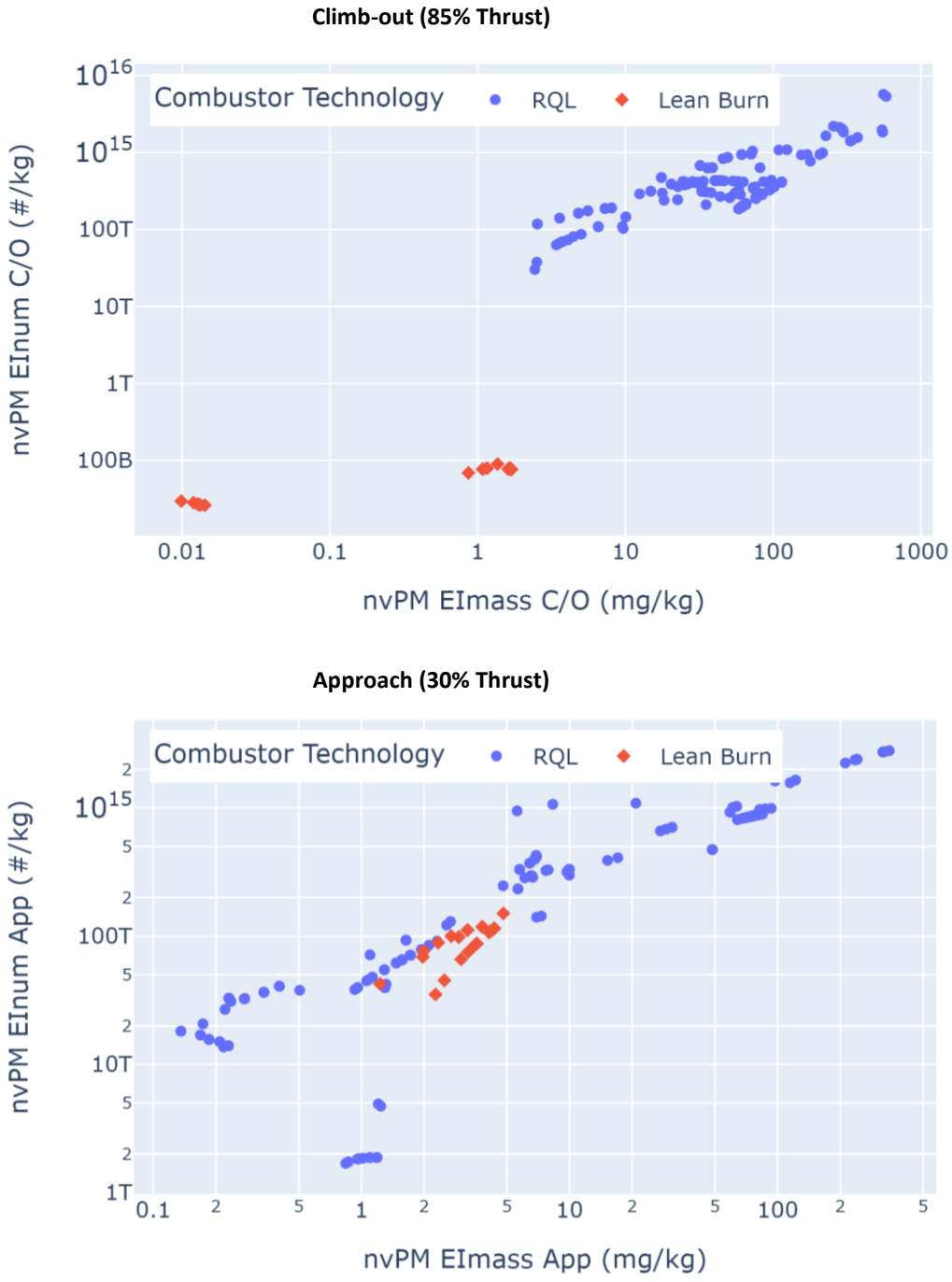

Figure 4.8 Non-volatile particle emissions of engines from the ICAO emission database (nvPM number vs. nvPM mass in logarithmic scale) for the two thrust settings climb-out and approach of the ICAO landing-take-off cycle. Data from the ICAO Emission database (EASA, 2023)

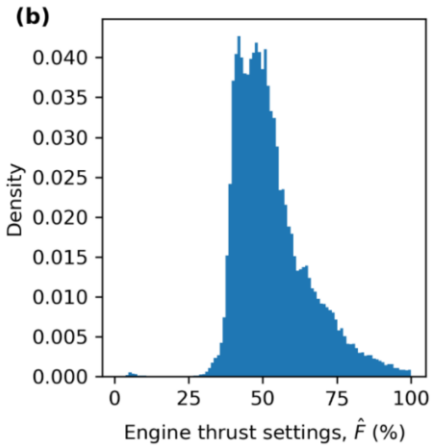

Figure 4.9 Typical range of thrust at cruise conditions (Teoh et al., 2022b).

4.3 EFFECTS OF JET FUEL COMPOSITION ON AVIATION EMISSIONS

As mentioned in Section **Error! Reference source not found.**, the fuel composition has an influence on the thermophysical and chemical properties of the fuel. Physical sub-processes like atomization, evaporation and dispersion of fuel in the combustion chamber are affected by physical properties (e.g., density, viscosity, volatility). In addition, the composition induced change in chemical properties (e.g., molecular structure, heat of combustion, chemical stability, flammability) has an effect on chemical related sub-processes such as ignition, flame speed, and chemical kinetics of fuel conversion.

As a consequence of an extreme change in fuel composition, the deterioration in fuel placement (atomization plus evaporation) could lead to a shift in the spray characteristics toward large and/or slowly evaporating fuel droplets. Or, it could lead to longer ignition times. Both conditions could potentially modify the primary zone and affect the flame stability envelope. Any such deterioration would affect safety and lead to the rejection of a fuel candidate as part of the qualification and approval process (ASTM D4054). Emissions are also sensitive to very small variations in the fuel composition, which are unavoidable when considering the large ensemble of possibilities within the fuel specification space. "Safe to fly" does not mean emissions-free. Pollutant formation chemistry is highly non-linear and very sensitive to such small changes. For instance, slightly larger droplets for the same size of the primary zone would lead to an increase in the overall time scales of the physical and chemical processes, thus to an increase in CO formation. Another important relationship between the fuel composition and a specific pollutant formation concerns soot. There is consensus within the combustion science community when it comes to the proportionality relation between the aromatics content of fuels and the formation of soot precursors.

The energy content of the fuel, i.e., the heat of combustion, has a direct impact on the fuel mass flow rate needed to reach specified or nominal temperature levels[4]. For a flight mission, this is related to take-off weight and thrust requirements, which contribute to the overall energy demand and emissions of a flight. Some emissions are proportional to the fuel mass flow rate. In this regard, the higher energy content by mass of synthetic paraffinic kerosenes (SPK) and thus

[4] The temperature level depends on many factors incl. the thrust level.

the reduced fuel consumption has a positive effect on the CO_2, H_2O and SO_x emissions. As mentioned in Section **Error! Reference source not found.**, SO_x emissions originate from sulphur compounds in the fuel. Therefore, they can be directly reduced by burning less fuel or lowering the amount of sulphur in the fuel. Besides the energy content, the hydrogen content (H content), which is usually higher for SPK fuels (Figure 4.10), has a positive effect on CO_2 emissions (due to the smaller share of carbon) (Wolters, 2020). On the contrary, the EI_{H2O}, i.e., water emission per kg fuel tends to increase proportionally to the H content of the fuel (Teoh et al. 2022). This effect tends to dominate over the positive effect of less full consumption leading to overall higher H_2O emissions for SPKs. Concerning NO_x emissions, literature results range from a slight reduction (within the uncertainty interval of the measurement devices) using SPKs in experiments and gas turbine system simulations (Wolters, 2020, chapter 4.3.1) to indifferent effects in RQL combustor rig tests (Harper et al., 2022) and emission measurements behind airplanes (e.g., Airbus A320 with V2527-A5 engines, Schripp et al. 2018), which did not show clear evidence of neither a positive nor negative effect. Carbon monoxide (CO) was also not significantly affected by the different fuel compositions.

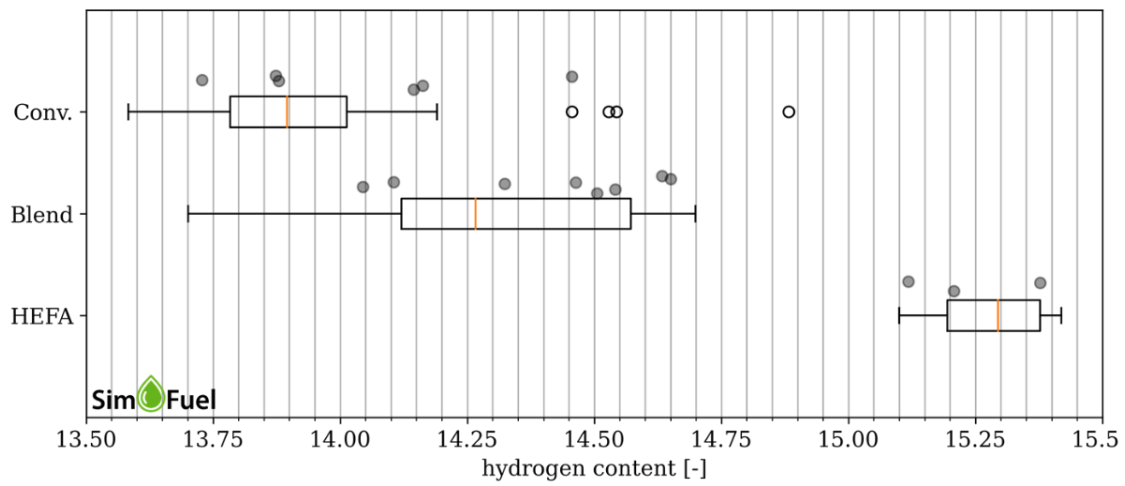

Figure 4.10 Comparison of hydrogen content (in mass percent) of fuels (dots) tested in ECLIF 1, ECLIF 2/ND-MAX campaign with distributions of fuels(whiskers) available in the DLR SimFuel database. Outliers are marked as hollow circles in the conventional fuels database. HEFA is a neat SPK fuel.

In contrast, there is strong evidence on the positive effects of SAF-SPKs or SAF blends on PM emissions. Moore et al. (2015) summarized the finding of a series of experimental campaigns (NASA APEX, AAFEX, and ACCESS) conducted by NASA and partners investigating aerosols emitted by the NASA Douglas DC-8 with CFM56-2-C1 engines. They concluded that fuel aromatic and sulphur content most affect the volatile aerosol fraction (vPM). The naphthalene content (two-ring or bi-cyclic aromatics or di-aromatics) had an effect on the non-volatile number density and volume EI as well as the black carbon mass EI. According to the authors, reducing both fuel sulphur mass and naphthalenes to near-zero levels would result in roughly a 10-fold decrease in aerosol number density emitted per kilogram of fuel burned. Brem et al. (2015) published a similar finding based on jet engine emission certification measurements. The authors pointed out that the nvPM (in mass) emission measurement correlated best with the fuel hydrogen content. Findings from ground measurements were confirmed by Moore et al. (2017), who showed that biofuel (HEFA-SPK) blending reduced the in-flight particle number and mass

emissions of an aircraft by 50% to 70%. In the following years, the evidence grew: Schripp et al. (2018) measured behind an Airbus A320 with V2527-A5 engines, and demonstrated that the particle emission indices reduced up to 50% (number) and 70% (mass) for two alternative jet fuel blends. They confirmed a better correlation of the particle emissions with the H content than with aromatics content. Teoh et al. (2022b) extended the methodology of Brem et al. (2015) for a wider range of engine thrust settings (10 % < $\hat{F}$ < 100%) and higher ΔH (up to 1.1%) using the measurements from the NASA ACCESS and ECLIF2/ ND-MAX campaigns. The resulting impact of changing hydrogen content on nvPM number emissions is depicted in Figure 4.11.

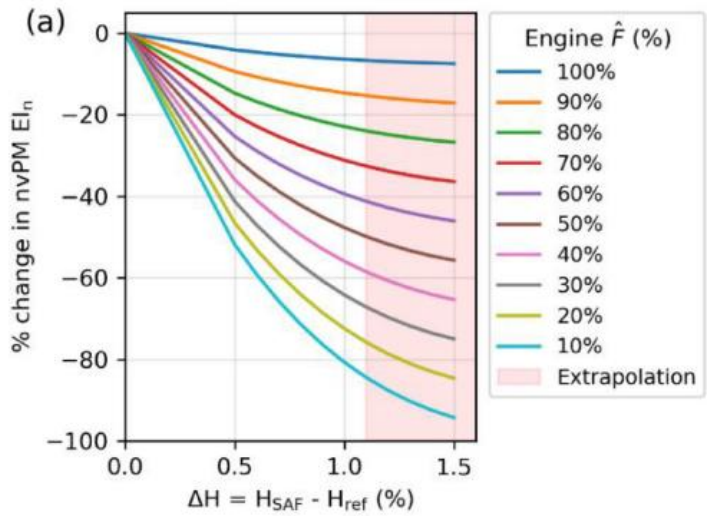

Figure 4.11 Calculated impact of changing hydrogen on nvPM number emissions for different thrust settings $\hat{F}$ (Teoh et al., 2022b).

The hydrogen content of the fuel is the primary factor that affects the impact of a fuel on nvPM number and mass emissions. Figure 4.10 compares the hydrogen content of conventional fuels (CRC world fuels survey), SAF blends, and HEFA SPK with fuels previously tested in ECLIF 1 and ECLIF 2 / ND-MAX measurement campaigns. Some Jet A-1 fuels, basically severely hydrotreated fuels, have a hydrogen content above 14.5%, while some SAF blends have a hydrogen content below the average of conventional fuels. There are two reasons for this: the choice of Jet A-1 for blending and the presence of Synthetic Aromatic Kerosene in some blends.

Figure 4.12 (upper panel) shows the hydrogen content of the CRC world survey fuels, mainly Jet A, Jet A-1, JP8, JP5, as function of the aromatic content (Hadaller et al., 2006). Figure 4-12 (lower panel) displays the hydrogen content of the same fuels vs. the di-aromatic content. The aromatic content is only weakly correlated to the H-content of the fuels.

The influence of different components of a fuel on the hydrogen content is depicted in Fig. 4-13. N-alkanes and iso-alkanes have the same and the highest hydrogen content. The influence of the carbon number is limited. Mono- and bi-cycloalkanes are closest to the hydrogen content of conventional jet fuels (median of CRC fuels: 13.9). The lowest hydrogen content is shown for aromatics, especially for di-aromatics.

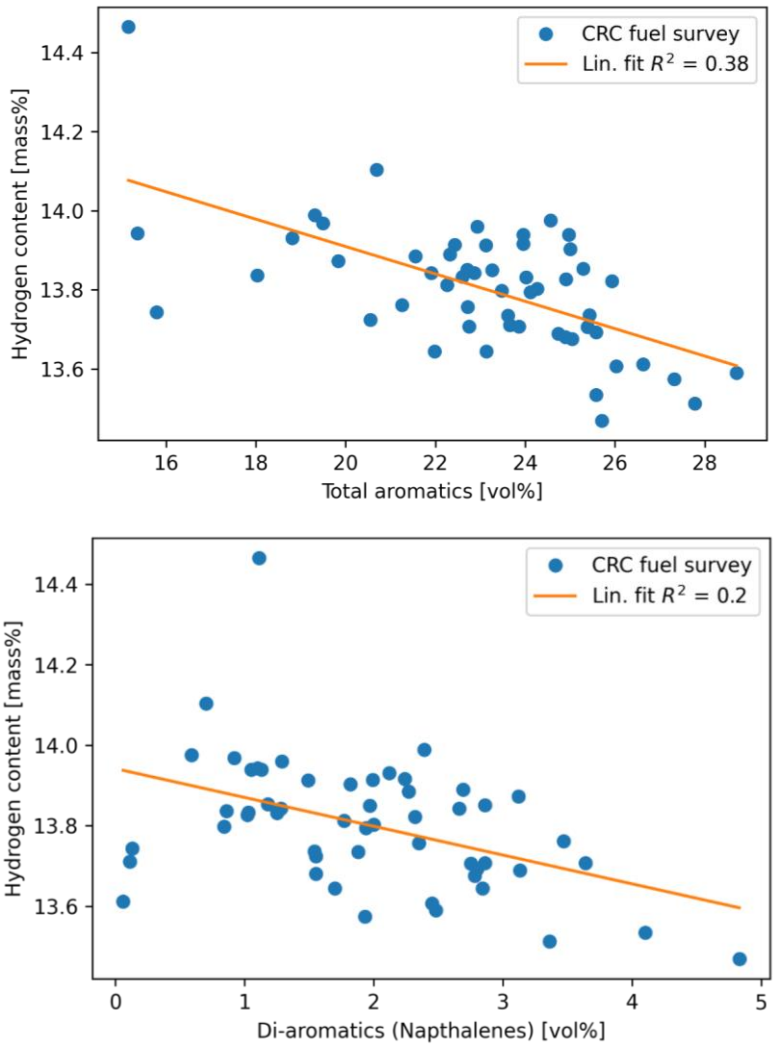

Figure 4.12 Hydrogen content as functions of the aromatics content (upper panel) and the di-aromatics content (lower panel) of fuels, CRC world fuel survey (Hadaller et al., 2006).

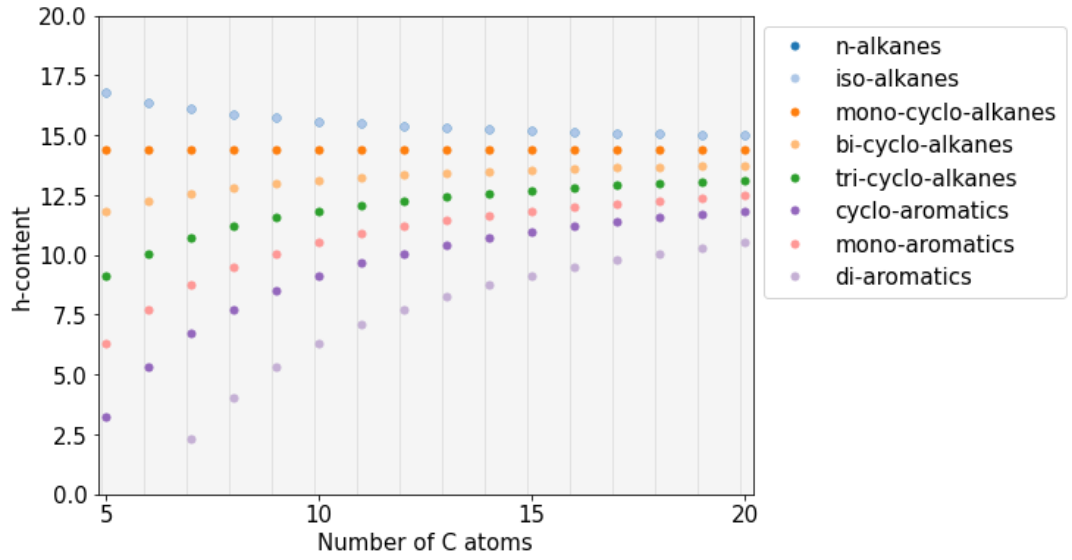

Figure 4.13 Influence of fuel family and carbon number on hydrogen content (Bauder et al., 2023). Note: n-alkanes and iso-alkanes overlap.

Table 4.2 Reproducibility of different methods to measure hydrogen content of aviation fuels (Thom, 2018). D3701 is not shown as this measurement device is not produced anymore.

ASTM	**Method**	**Reproducibility**	**Reproducibility standard deviation (based H = 14 mass %)**
D3343	Correlation	R = 0.10 %	0.5 mass % ~ 30 % nvPM EIn
D5291	LECO/Flash EACHN analyzer	H: R = X^0.5 * 0.2314	0.31 mass % ~ 19 % nvPM EIn
D7171	Low-Resolution Pulsed Nuclear Magnetic Resonance Spectroscopy	@ 40 °C R = 0.01580 (X + 5.0000)	0.11 mass % ~ 6.2 % nvPM EIn

ASTM lists four measurement techniques to determine the H content of aviation fuels. These are summarized with the reproducibility standard deviation in Table 4.2. In the frame of emission impact studies, because of the large uncertainties, ASTM D3343 and D5291 are not recommended. NMR based methods (ASTM D3701 and D7171) have considerably lower uncertainties. However, as noted by Thom (2018), ASTM D3701 has a bias and the relevant measurement device is no longer produced. This was confirmed in a DLA funded study as reported in Edwards (2020). ASTM D7171 is basically a newer version of D3701, which uses improved magnets and algorithms, and is therefore the recommended choice for H content measurements. Additionally, the H content can be inferred from GCxGC composition data. Edwards (2020) reports that ASTM D7171 and GCxGC-based measurement showed a very good agreement. Similar results have been found in the JETSCREEN project.

Traditionally, the smoke point ASTM D1322 (ASTM DO2) is used to characterize the sooting tendency of different fuels. The smoke point is the height of a flame where any increase in the flow rate would cause the flame to emit soot. This technique has several drawbacks: (a) it depends on subjective judgement, like the decision when a flame is at the smoke point, and the decision where the tip of the flame is, and (b) there are high uncertainties for fuels with a strong sooting tendency. To overcome these issues, the yield sooting index (YSI) was introduced by McEnally and Pfefferle (2007). It allows the quantification of the soot tendency of pure components and mixtures with a significantly lower level of uncertainty compared to concepts like the smoke point or the threshold sooting index. Applying the YSI, Pütz et al. (2022) recently investigated the impact of branching on sooting tendency and showed the strong variability of the sooting tendency for compounds of the same carbon number / same H content. This indicates that the isomeric variability (level 2 compositional information) should be considered in the formulation of low sooting fuels.

4.4 EFFECTS OF SULPHUR AND AROMATIC REDUCTION ON FUEL QUALITY, PHYSICOCHEMICAL FACTORS AND EMISSIONS

Aromatics and sulphur occur naturally in crude oil. Aviation fuel specifications have been developed to allow refinery production on a global basis such that no country is excluded from international travel. Reducing the aromatic fraction of the jet fuels could support the reduction in the nvPM emissions from aviation. Two refining technologies appear to be the most suitable for large scale reduction of aromatics from a jet fuel: (1) hydrotreating, which is considered the most common method, and (2) extractive distillation (Barrett and Speth, 2021; Weibel, 2018; Faber et al., 2022). Hydrotreatment is a process in which a hydrocarbon stream reacts with hydrogen in presence of a catalyst in order to reduce sulphur, nitrogen, oxygen and possibly aromatic contents, depending on severity. Extractive distillation is a refining separation process that relies on a solvent to separate polar species from a petroleum stream, commonly used to extract aromatic components in refineries (Barrett and Speth, 2021; Weibel, 2018; Faber et al., 2022). Considering the advantages of these two technologies for reducing aromatics from the jet fuel, hydrotreatment has the additional effect of removing sulphur from the fuel. On the other hand, when the fuel is processed by extractive distillation, the aromatic content could be completely separated and the amount of aromatic fraction to be returned to the product can be controlled. These two technologies are technologically mature at refinery scale and applicable where, according to literature, there is no impact on the fuel's ability to meet ASTM or Defence standards (Faber et al., 2022). However, it should also be noted that a reduction in aromatics will reduce fuel density which, based on D7566 data, could fall below the 775 kg/m^3 specification limit. This would in turn impact fuel energy content by volume and aircraft flight range where volume limited. The aviation industry is currently considering if such a situation would be viable for fully synthetic fuels in the long-term. The assessment of the implementation costs and the possible increase in CO_2 emissions due to the use of these technologies has recently been debated (Barrett and Speth, 2021; Weibel, 2018; MathPro, 2023). These reports emphasize the relevance of considering different variables for these analyses, such as type of refinery[5] (MathPro, 2023), technological availability (MathPro, 2023;

[5] There are processes in refining crude oil, which can be intensified, removed or relaxed, depending on the local demand and market. You can vary the hydrotreatment of straight run kerosene or intensify the hydrocracking of the diesel cut to produce more kerosene. Both examples have a different effect on the final jet fuel composition. While the former is rather

Barrett and Speth, 2021; Weibel, 2018). and particular fuel requirements (Barrett and Speth, 2021; Weibel, 2018).

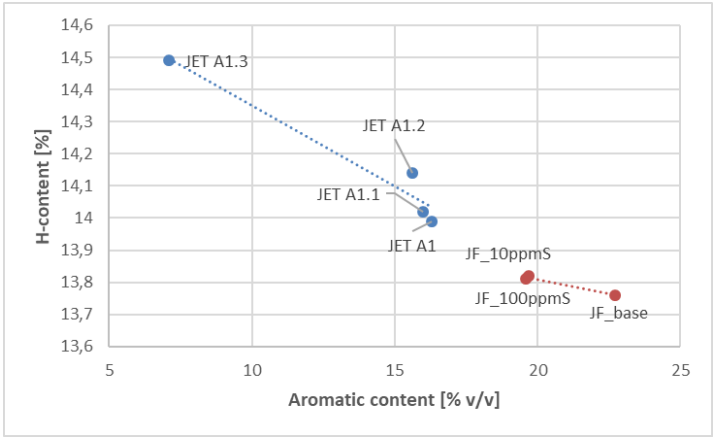

Figure 4.14 Impact of different degree of hydrotreatment on H-content of a conventional Jet A-1 (blue; JETSCREEN, 2022) and data (red) from Tucker et. al. (2011).

Figure 4.14 displays the H-content of conventional fossil jet fuels as a function of the aromatics content. The increase in the H-content was achieved by intensifying the degree of hydrotreatment of straight run kerosene. Two available datasets are considered: the detailed dataset created within the JETSCREEN (2022) project and the data presented by Tucker et. al. (2011). Additionally, several studies have been performed in the sector (EASA, 2010; Barrett et al, 2021; MathPro, 2023). No other data sets have been identified that provide such detailed information on the effect of aromatic reduction or increase in fuel hydrogen content by hydrotreating in jet fuels or by extractive distillation.

smooth and removes heteroatoms (S) and metals without modifying substantially the composition the later affects more severely the composition.
Additionally, the authors from the reference MathPro, 2023 developed a preliminary, scoping estimate of the economics and effect of hydrotreating on sulphur and aromatics for two processing schemes: Conversion refineries and Hydro-skimming refineries.

Table 4.3 Impact of hydrotreament on aromatics, sulphur, H content and on the relative change of nvPM emissions at 50% thrust. JETSCREEN Fuels and Tucker et al. (2011) fuels as in Figure 4.14

Fuel	total aromatics [% vol]	di-aromatics [% vol]	sulphur [ppm]	H-content [%mass]	Δ H-content* [%mass]	Δ nvPM EI_n** [%]
JETSCREEN A-1	16.3	1.1	300.	13.99	0.09	-10.23
JETSCREEN A-1.1	16.0	0.7	45.	14.02	0.12	-13.64
JETSCREEN A-1.2	15.6	0.1	6.2	14.14	0.24	-27.28
JETSCREEN A-1.3	7.1	0.0	6	14.49	0.59	-67.07
JF_base	22.7	2.2	2200	13.76	-0.14	15.92
JF_100ppmS	19.6	1.2	98	13.81	-0.09	10.23
JF_10ppmS	19.7	1.0	9	13.82	-0.08	9.09

* ΔH-content relative to CRC median of 13.9 %mass

** Δ nvPM EI_n calculated with the equation reported by Teoh et al. (2022) at 50% thrust

The database obtained from the JETSCREEN (2022) project and plotted in Figure 4.14 presents a group of fuels, that includes a base Jet A-1 and hydrotreated version of that fuel. The names presented in the figure have the following notation: JETSCREEN A.1 (JET A.1 in Figure 4.14[6]) represents the base fuel used, i.e., before any hydrotreatment process. JET A1.1 (mild hydrotreament), JET A1.2 (moderate hydrotreatment) and JET A-1.3 (severe hydrotreatment). The reduction in the aromatic concentration from the fuel A1 to the A1.1 was obtained mainly for a reduction in the naphthalene concentration, going from around 1.6 %v/v to less than 1.0 %v/v. To obtain fuel A1.2, more severe hydrotreatment was carried out, which removed almost all of the di-aromatics and a reduction in total aromatics concentration from 16.3 %v/v to 15.6 %v/v was achieved. In the most severely hydrotreated fuel, the A1.3, the mono-aromatic concentration of the fuel has been dropped to 7.1 %v/v and a final concentration of naphthalene of less than 0.1 %v/v was obtained. The information of the aromatic and di-aromatic content has been reported with the ASTM D1319 and ASTM D1840 methods. As previously mentioned, one of the main advantages of the hydrotreatment process is that sulphur can be simultaneously reduced. In the case of the JETSCREEN fuels, the sulphur content of the hydrotreated fuels went down from more than 100 mg/kg for the base jet fuel to less than 20 mg/kg for the highly hydrotreated fuels, A1.2 and A1.3

The impact of hydrotreatment is summarized in Table 4.3 The H-content relative to the CRC median of 13.9% mass is used to estimate the change of nvPM EI_n at a thrust level of 50% using the correlation reported in Teoh et alii (2022). The reported JETSCREEN fuels have all a higher H content with respect to the CRC median value, resulting in:

- 10% lower nvPM EI_n emissions in the case of the JETSCREEN base Jet A-1;
- an absolute reduction of 13.64% or 3.4% in addition to the base fuel reduction for the mild hydrotreatment (A-1.1);

[6] Note: The nomenclature in Figure 4.14 is not consistent with Table 4.3. Also, in Figure 4.14 the data points should have the name JETSCREEN A-1, and not Jet A-1, etc.

- an absolute reduction of 27.28% or 17.05% in addition to the base fuel reduction for the moderate hydrotreatment (A-1.2);
- an absolute reduction of 67.07% or 56.84% in addition to the base fuel reduction for the severe hydrotreatment (A-1.3).

The results of Tucker et al. (2011) show a very effective reduction in sulphur, but only a moderate increase in fuel H content of 0.56% mass. Consequently, the hydrotreatment of JF_base to JF_10ppmS resulted in a relative nvPM EI_n reduction of only 5,7%.[7]

The change in fuel composition also impacts a wider range of fuel properties. The comparison between some selected critical fuel properties is presented in Figure 4.15, which depicts how the properties of the jet fuel vary with the hydrotreating process and how they relate to specification limits (red area). The boxplots show the range of experience of conventional fuels from the CRC world fuel survey. As it can be seen, not all properties are affected the same way. Besides reducing sulphur and aromatic content, there are other positive effects, e.g., the net heat of combustion increases as the level of hydrotreating increases, which would result in lower fuel consumption by mass but higher fuel consumption by volume. However, other properties, such as flash point, can decrease to a point where it could be below ASTM specification limits, as is the case of the fuel that was severely hydrotreated, the JETSCREEN A1.3. Depending on the overall refinery process, one could think of a change of the process to produce a fuel that is better suited for additional hydrotreatment and hence would not fail in flash point after a hydrotreatment.

Lubricity (not displayed) slightly worsened from 0.62 mm (JET A1) to 0.72 mm (JET A1.3) in the BOCLE (ASTM D5001), but still is below the maximum limit of 0.85 mm. Should lubricity become a limitation, aviation approved additives are available for use.

For the fuels considered in the work of Tucker et al. (2011) plotted in Figure 4.14, the following notation was considered:

- JF_base with a concentration of 2200 ppm of sulphur (base case),
- JF_100ppmS hydrotreated to achieve 100 ppm of sulphur,
- JF_10ppmS hydrotreated to achieve a 10 ppm of sulphur.

Even if the main focus of this work was to achieve a substantial reduction in the sulphur content, a limited reduction in fuel aromatic content and increase in H content was also obtained as can be seen in Figure 4.14. The topic of the impact of reducing sulphur content has also been reviewed by QinetiQ (2010). In this paper as well as in Tucker et al. (2011), it was concluded that the desulphurization process achieved a simultaneously reduction of the aromatic concentration and naphthalene concentration, and consequently an increase, even slightly, in the hydrogen content of the jet fuel[8]. Data about the impact on hydrogen is unfortunately not reported. Other listed advantages for the jet fuel as a result of the desulphurization are: a

[7] For the study only one reactor was used and the feed flow rate was set at 162 g/hour. With a fixed hydrogen pressure of 40 bar, the desulphurisation severity could be controlled by temperature alone in the range 280 to 348 °C to achieve 0.1 to 0.001%mass sulphur.

[8] In the case of the paper by Tucker et al. (2011), the observed changes in the fuel properties following the hydrotreatment from 2200 to 10 ppm sulphur were: 13.2% reduction of aromatics and 55.0% reduction of naphthalenes. The QinetiQ report does not present values for the reduction but mentioned the expected reduction in aromatics/naphthalenes.

reduction in fuel acidity (of about 90% in Tucker et al., 2011), and a lower freezing point, a better smoke point, an almost complete mercaptan removal (more than 90% in Tucker et al., 2011), and an improvement of the thermal stability. Side effects identified with the sulphur reduction were a reduction in lubricity, increase in conductivity response and potential increase CO_2 due to the more severe conditions required.[9]

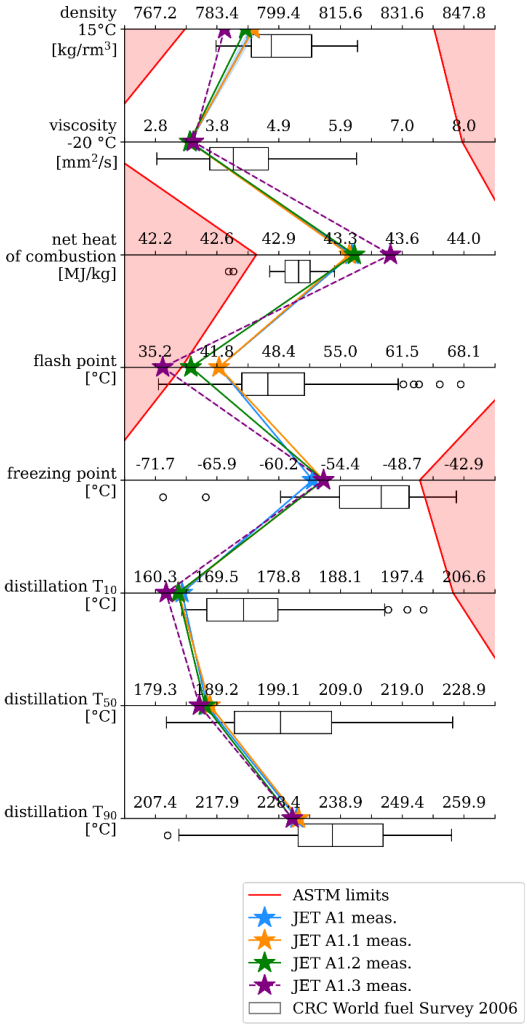

Figure 4.15 Comparison between fuel properties for the JETSCREEN (2021) fuels.

[9] Information provided by Tucker et al. (2011): The lubricity decreased due to the hydrotreatment. The Ball-on-Cylinder Lubricity Evaluator (BOCLE) test displayed a wear scar changing from 0.51 mm at 2200 ppm sulphur to 0.79 mm at 10 ppm sulphur, representing an increase of 54.9%. While still within Def Stan 91-91 limits of 0.85 mm maximum.
The water separometer index MSEP and Electrical Conductivity: MSEP and Electrical Conductivity Product MSEP rating and conductivity remained unchanged following hydrotreatment. However, on addition of 1 ppm Stadis 450 additive, the 100 ppm and 10 ppm sulphur products showed a significantly higher response (>200 pS/m) versus the base fuel. This suggests trace components in the base fuel were interacting with the Stadis additive and reducing activity. (The values are still within the range of the Electrical Conductivity in the Def Stan 91-91: 50-600.)

Regarding the aromatic reduction from hydrotreatment or extractive distillation processes, mainly di-aromatics/naphthalene has been targeted as a relevant aromatic to be removed in order to reduce the PAHs that promote soot formation (MathPro, 2023; Barrett and Speth, 2021). Recently, MIT presented the results of a project focused on the evaluation of naphthalene removal (Barrett and Speth, 2021; Weibel, 2018; Brin, 2020). The project considered both hydrotreatment and extractive distillation from the modelling perspective. The results from MIT as well as the work by Pelucchi et al. (2021) introduce the particular relevance of naphthalene reduction by hydrotreatment or/and extractive distillation to reduce particular matter formation. However, most reports lack experimental data about the impact of the processing technology on fuel hydrogen content.

5. JET FUEL COMPOSITION AND CONTRAIL FORMATION AND LIFETIME

5.1 THERMODYNAMIC CONDITIONS FOR CONTRAIL FORMATION

The thermodynamic conditions for contrail formation were derived long ago by Schmidt (1940) and Appleman (1953). Busen and Schumann later (1995) noted discrepancies between observations of contrail formation and theoretical predictions and introduced the overall propulsion efficiency factor, which made theory match the observations more closely. Schumann (1996) gave a complete and detailed derivation of the thermodynamic theory, which is named "Schmidt-Appleman theory" after its two first developers.

The principle behind contrail formation is that mixing of two airmasses that both are subsaturated (i.e. their relative humidity is below 100%) can result in a supersaturated state (i.e. the relative humidity of the mixture exceeds 100%). In the case of contrail formation, the two airmasses are the exhaust gases, which are emitted hot and with high vapour pressure, and the ambient air, which is cold and has low vapour pressure. After emission, the mixture immediately attains ambient pressure, so the mixing and contrail formation process is isobaric. Mixing more and more ambient air into the exhaust gases lets them cool down and lets the vapour pressure approach the ambient value. If during this process the vapour pressure transiently reaches values above the saturation vapour pressure, condensation sets in and liquid droplets form that instantaneously freeze in the cold ambient air. Hence, a contrail forms. A contrail does not form, if the mixture never gets supersaturated (i.e. if the vapour pressure of the mixture stays below the saturation pressure all the time).

The Schmidt-Appleman criterion is a purely thermodynamic condition (see also Figure 5.1) and contains no microphysical conditions or criteria. There are always copious particles that serve as condensation nuclei present, either in the exhaust itself, or mixed-in with the ambient air. Thus, particle availability is not assumed to be a constraint for initial contrail formation.

The mixing trajectory in a temperature (T)-partial pressure of water vapour I diagram (Schmidt-Appleman diagram) is a straight line. The formula for its slope, G, contains the relevant quantities:

$$G = \frac{de}{dT} = \frac{c_p p}{\varepsilon} \frac{EI_{H2O}}{(1-\eta)Q},$$

with $c_p \approx 1004$ J/(kg K): isobaric heat capacity of air, p: ambient pressure, ε=0.622 (ratio of molar masses of water and air), $EI_{H2O} \approx 1.24$ emission index of water vapour (i.e. about 1.24 kg water vapour are produced by burning 1 kg of kerosene), η: overall propulsion efficiency of the aircraft, and $Q \approx 43.1$ MJ/kg: lower heating value (or combustion energy) per unit mass of the fuel. Fuel properties enter this formula via EI_{H2O} and Q. Their ratio, EI_{H2O}/Q, the so-called energy-specific emission index of water vapour, is higher for alternative fuels than for kerosene, which renders contrail formation for alternatives easier than for kerosene.

Figure 5.2 shows the evolution of important contrail properties with respect to contrail age. These properties are: ice crystal number and mass concentration, crystal radius (r_{vol}) and effective radius (r_{eff}), and optical thickness. From these five quantities, four will be affected by a transition to alternative fuels with lower soot emission, namely all but the ice mass concentration, which is controlled by ambient humidity and not by aircraft and little by fuel properties. The ice crystals grow by uptake of water from the ambient atmosphere during contrail lifetime, and the contrail spreads out and expands in width and length. The inmixing of ambient air leads to dilution of the initial ice crystal number concentrations throughout contrail's lifetime. Over the contrail lifetime the contrails have higher number concentrations and smaller sizes compared to natural cirrus evolving in the same environment (Voigt et al., 2017).

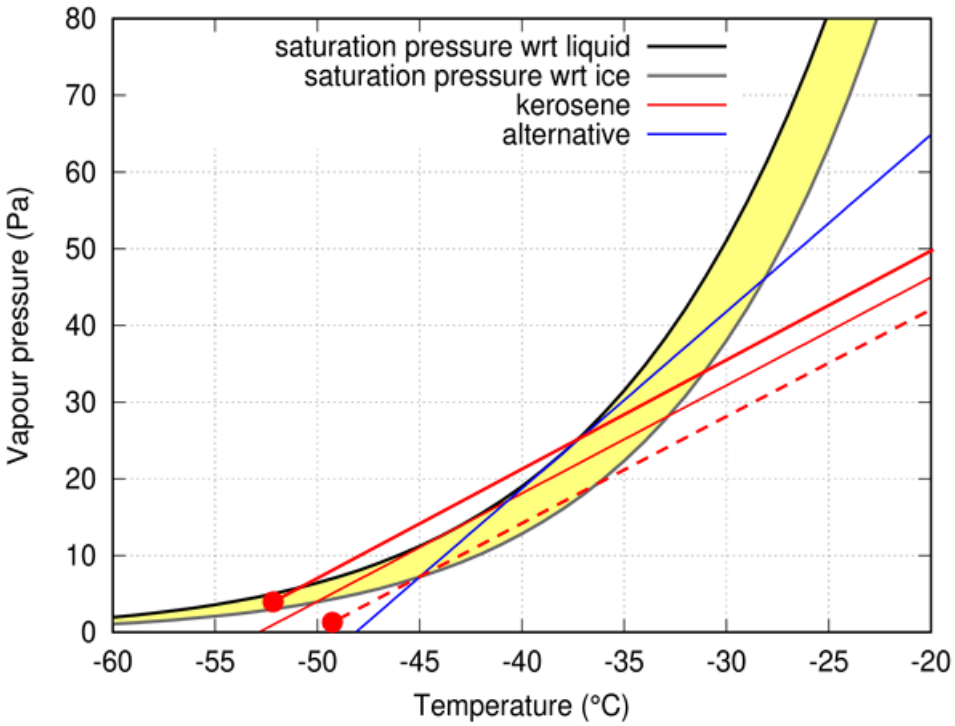

Figure 5.1 T-e (temperature vs. vapour pressure) phase diagram of water for sub-zero temperatures. The two black solid curves represent the phase boundaries between vapour and ice (lower curve) and between vapour and supercooled liquid water (upper curve). The various straight lines represent possible isobaric expansion processes of aircraft engine plumes, where plume pressure = ambient pressure. Plume expansion always starts outside the diagram at the high engine exit temperature and ends at the low temperature of the ambient air. The slope of the mixing lines depends on ambient pressure, on the emission index of water vapour, on the chemical energy of the fuel and on the overall propulsion efficiency of the aircraft. Contrail formation requires that the mixing line crosses the phase boundary between vapour and supercooled liquid water. This leads to condensation of water vapour into liquid droplets which quickly freeze at temperatures below -38°C. The two solid mixing lines (red and blue) just touch the phase boundary and thus represent threshold cases for two different fuels. Contrail persistence requires that the ambient air is supersaturated with respect to ice (the area marked yellow), that is, that the mixing line ends above the phase boundary between vapour and ice. The dash-dotted mixing line is an example for this. The dashed mixing line does not cross the phase boundary between vapour and supercooled liquid and thus represents a plume without contrail formation.

Note that the difference between the red curve (representing kerosene) and the blue curve (representing an alternative fuel with higher H/C ratio) is exaggerated in this diagram for the sake of clarity. Higher H/C ratio implies higher threshold temperature and a larger phase region where contrails can be persistent. (Figure adapted from Hofer et al., 2024).

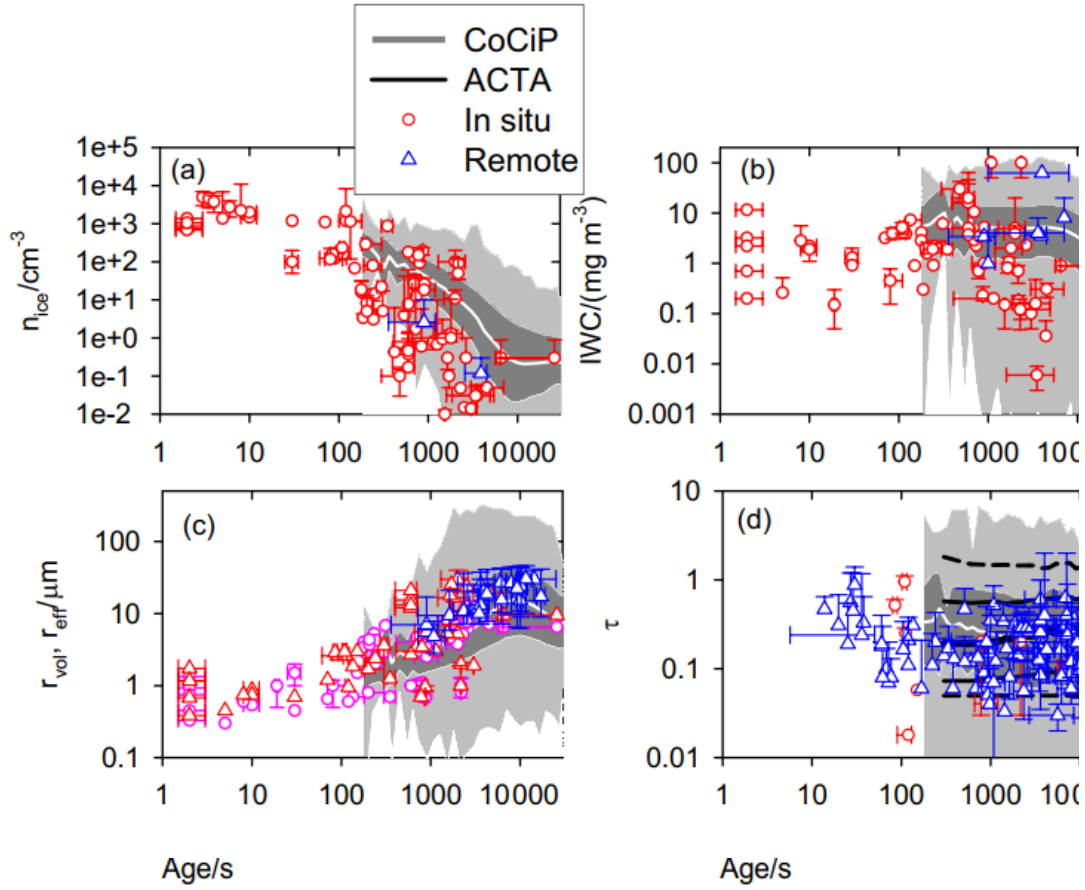

Figure 5.2 Contrail properties vs. contrail age. The figures show ice crystal number concentration (panel a), the ice mass concentration (IWC, panel b), the mean volume (purple) and effective radius (blue) of the crystals (c), and the optical thickness (d). Data are from various sources, in-situ measurements and satellite data, including tracking of contrails using satellite imagery (ACTA). The grey areas mark contrail properties as modelled by a contrail tracking model (CoCiP, Schumann 2012). The figure is adapted from Schumann et al. (2017).

5.2 IMPACT OF JET FUEL COMPOSITION ON THE FORMATION AND LIFETIME OF CONTRAILS AND CONTRAILS CIRRUS

Fuel properties enter the Schmidt-Appleman formula via EI_{H2O} and Q. Their ratio, EI_{H2O}/Q, the so-called energy-specific emission index of water vapour, is higher for alternative fuels than for kerosene, which renders contrail formation for alternatives easier than for kerosene. This means that contrails of alternative fuels can form at slightly higher temperatures and cover larger areas than contrails from kerosene. These effects are, however, weak to moderate and are constrained by the threshold temperature for supercooling of liquid pure-water droplets.

Pure water droplets do not freeze above about −38°C, but certain nuclei, solid aerosol particles, in the ambient air can initiate freezing at higher temperatures if their surface properties (in particular their crystal lattice) are similar to the crystal lattice of ice. Such nuclei represent a small fraction of the ambient aerosol. Contrails formed at temperatures above the supercooling limit for pure water droplets, e.g., from combustion of hydrogen, will probably consist of droplets from

which only a minor fraction will freeze while the majority of droplets is expected to evaporate. But, as noted earlier, this prediction has not yet been tested experimentally. This work should be done before we can assess if contrails at such high temperatures are less relevant for climate.

5.3 IMPACT OF THE FRACTION OF (POLY)AROMATIC/PARAFFINIC MOLECULES AND SULPHUR ON CONTRAIL FORMATION, AND CONTRAIL LIFETIME

There is a multitude of experimental evidence on aviation emissions, contrail formation and evolution, which are needed to investigate the related climate impact. Based on aviation turbine engine studies, using the technologies available at the time of publication (traditional RQL combustors) combustion of one kg of kerosene in aircraft gas turbines leads to the formation of 10^{14} to 10^{16} soot particles of 10 to 60 nm size and to up to 10^{17} volatile aerosol particles with sizes below 10 nm (Petzold et al., 1999; Moore et al., 2017; Brock et al. 2000). While the volatile aerosol particles have higher number concentrations, the soot particles predominantly serve as condensation nuclei for contrail formation due to their larger particle size compared to volatile aerosol (Kärcher and Yu, 2009; Kärcher, 2018, Kleine et al., 2018).

Concerning lean burn engine technologies, Moore et al. (2017b) report on take-off engine particle emission indices for in-service aircraft at Los Angeles International Airport. 275 engine take-off plumes were measured in May 2014 at 400 m downwind of the runway. They observed total and non-volatile particle number EIs in the order 10^{16} to 10^{17} kg^{-1} and 10^{14} to 10^{16} kg^{-1}, respectively. Black-carbon-equivalent particle mass EIs varied between 175 to 941 mg kg^{-1} except for the General Electric GEnx engines, which had significantly lower mass EI at 46 mg kg^{-1}. They present a data set on plume EIs, aircraft and engine specifications, and manufacturer-reported engine emissions certifications for future studies to better understand and model aircraft emissions and their impact on air quality. The data evaluation from the recent VOLCAN (VOL avec Carburants Alternatifs Nouveaux) campaign (https://www.airbus.com/en/newsroom/stories/2023-03-airbus-most-popular-aircraft-takes-to-the-skies-with-100-sustainable) on ground based and in-flight emission measurements and contrail observations (https://www.dlr.de/de/medien/videos/2023/video-projekt-volcan) from an Airbus A319 with LAEP-1A engine technologies burning kerosene and SAF is ongoing and therefore out of scope of this report on published public data.

The number of ice crystals that are formed is roughly proportional to the number of soot particles emitted as long as the emission index is in the so-called soot-rich regime, which is above ~10^{14} particles per kg fuel, see Figure 5.3. The proportionality factor depends on temperature. It is small if the ambient temperature is little below the Schmidt-Appleman threshold temperature[10] (e.g., Bräuer et al., 2021) and approaches unity (i.e., each soot particles nucleates an ice crystal) at temperature sufficiently (~5 K) below the threshold (e.g., Kärcher et al., 2015; Kleine et al., 2018; Voigt et al. 2021; Bier and Burkhardt, 2022). In the mid-latitudes this is the dominant case, but not in the tropics and subtropics where cruise levels are often close to the contrail formation threshold (Bier and Burkhardt, 2022).

Contrail formation in the soot-rich regime were measured in flight in a large number of campaigns (Busen and Schumann, 1995; Petzold et al 1997, Jensen et al., 1998; Heymsfield et al., 1998; Schröder et al., 2000; Voigt et al., 2011; Voigt et al., 2012; Moore et al., 2017; Schumann et al., 2017; Kleine et al., 2018; Voigt et al., 2021).

[10] See also Section 5.1

In addition, satellite observations were used to investigate contrail optical properties and climate impact (e.g., Minnis et al., 1998; Vázquez-Navarro et al., 2015; Wang et al., 2023). A compilation of results from in-situ measurements and satellite observations is given by Schumann et al., (2017), see Figure 5.2.

The engine particle emissions change from burning alternative fuels relative to petroleum-based fuels is driven by variations in the amount of fuel aromatic and sulphur species (Schripp et al., 2018). For instance, the Fischer-Tropsch fuels and the hydro-processed esters and fatty acids (HEFA) fuels contain no aromatic compounds and nearly no sulphur (Moore et al., 2015). Blending regular JP-8 with sustainable aviation fuels leads to a significant decrease in the emitted particles with increasing alternative fuel content. An increasing content of aromatics in regular Jet A-1 fuel leads to increased particle emissions of a jet gas turbine (Brem et al., 2015). Experiments with a T63 turboshaft engine showed a reduction of particle emissions when changing from regular kerosene to a mainly paraffinic fuel (Cain et al., 2013). A significant particle emissions reduction was observed on a turbofan engine for kerosene blended with an aromatic-free Fischer-Tropsch fuel (Timko et al., 2010). Hence, soot emissions and microphysical properties are altered by the changes in fuel composition, particularly by the types and fractions of aromatic species. Alternative jet fuels with lower aromatic contents not only produce fewer soot particle emissions, the produced soot particles are also smaller (Lobo et al., 2015; Moore et al., 2017; Schripp et al., 2022) and have different morphologies as determined by electron microscopy (Liati et al., 2015). This has an impact on their ice-forming ability.

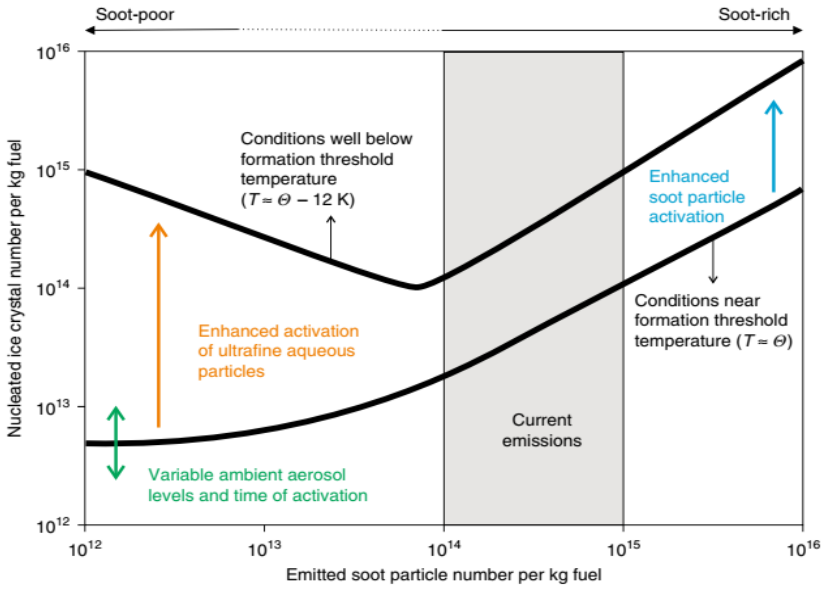

Figure 5.3 Dependence of the number of ice crystals formed in contrail initiation on the number of emitted soot particles per kg of fuel. The current emission level belongs to the "soot-rich" regime where the ice number is proportional to the soot number concentration. This proportionality ceases in the "soot-poor" regime. Other particles than soot, e.g. co-emitted volatile particles or ambient particles entrained into the exhaust plume start to contribute to ice formation in the soot-poor regime. At temperatures well below the Schmidt-Appleman threshold temperature, decreasing soot emission in the soot-poor regime can even lead to increasing numbers of ice crystals. Figure from Kärcher (2018).

Recently, modelling studies on the chemical reaction kinetics of complex fuels (Kathrotia et al., 2021a, b) also highlight the influence of the naphthalene content for soot precursor chemistry even beyond established correlations such as the hydrogen content. Finally, compared to ground-based measurements, the emissions from jet engines at cruise altitudes are affected by numerous parameters under real operational conditions.

Moore et al. (2017) investigated the effect of two Jet A-1 fuels with different aromatic and sulphur contents and a 50% HEFA biofuel blend on engines particle emissions by probing the exhaust from the NASA DC-8 CFM56-2-C1 turbofan engines in cruise (Figure 5.4). Engine's non-volatile particle emissions increase with increasing thrust setting or increasing fuel flow. Non-volatile soot particles (in black carbon equivalent mass) are reduced for the 50% HEFA biofuel derived from the camelina plant compared to conventional Jet A-1. The emission of soot particles is reduced as the HEFA blend had a lower aromatic and naphthalene content and aromatics and in particular naphthalene are efficient soot precursors. The soot particles emitted from the SAF blends are also slightly smaller compared to the soot particles from Jet A-1 emissions, see Figure 5.4.

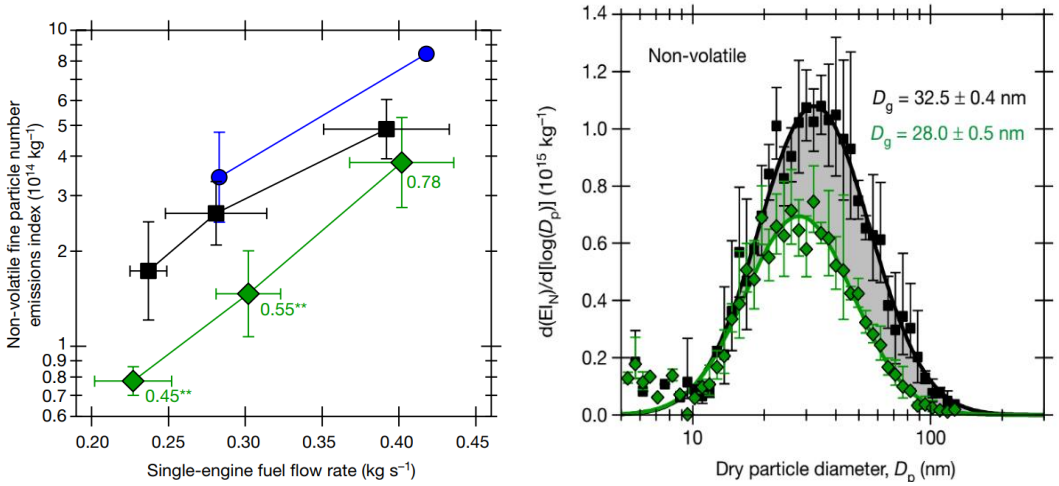

Figure 5.4 Left panel: Summary of particle emission indices of two Jet A-1 fuels with different aromatic and sulphur contents (blue and black) and of a 50% HEFA biofuel blend (green) at different thrust settings and cruise conditions at altitudes of 9,140 to 10,970 m. Right panel: Size distributions of emitted non-volatile particles at high-thrust cruise conditions. Black squares and green diamonds show data for the medium-sulphur-content Jet A-1 fuel and the 50:50 biofuel blend, respectively. Solid lines are log-normal fits and the shaded area represents the difference between the two fitted curves. (Figures from Moore et al., 2017).

Voigt et al. (2021) investigated the effect of different fuels on contrail ice crystals. They performed in-flight measurements of the emissions and contrails from sustainable aviation fuels blends with different aromatic contents. SAF1 and SAF2 for the blending were produced from camelina plant (HEFA). The semisynthetic jet fuel (SSF1) was produced by the Fischer-Tropsch process. Different Jet A-1 fuels were used for the experiment and the Jet A-1 fuels were blended with the SAF to yield the desired aromatic/H-content variations of the SAF blends. The emissions from an A320 with IAE V2575 engines were probed by the DLR Falcon. The microphysical properties of the contrails, which had formed in ice supersaturated conditions, were measured at a contrail age of 2 minutes. A 20 to 50 % reduction of the soot particle emission index was measured for the for low aromatic fuels blends compared to Jet A-1. This transfers into a reduction in ice crystal number concentrations in contrails (Figure 5.5). A larger reduction in ice crystal numbers can be explained by the lower sulphur content of the specific fuels, which reduces the activation of the soot particles. The reduction in soot particle emissions depends on many parameters, e.g., the fuel's aromatic or hydrogen content but also on the sulphur content of the SAF and the kerosene fuels. Sustainable aviation fuels with a high hydrogen and low aromatic and naphthalene content lead to reduced non-volatile soot particle emissions and to a reduction in ice number concentrations in contrails.

The soot and ice particle reductions in contrails correlate with the fuel's aromatic content. Bi-cyclic aromatics such as naphthalene have been demonstrated to be even more efficient soot precursors due to their stronger molecular bonding of the cyclic aromatic ring structures (Figure 5.5). Even for near zero naphthalene content, there still is a significant emission of soot particles indicating that mono-aromatics and to a lesser degree paraffinic components also contribute to soot particle formation. A common description of the fuels aromatic or paraffinic

content is given indirectly by the hydrogen content (cf. Figure 4.12) or the hydrogen to carbon ratio of the fuel. The hydrogen content alone is not able to cover all the fine structure details of the fuel's hydrocarbon molecules, which is required to directly relate the fuel composition to soot particle emissions (cf. Section **Error! Reference source not found.**). The combustion process itself of different engines has an influence on the soot particle emissions (cf. Section **Error! Reference source not found.**). Currently, ongoing ground and flight experiments investigate the effect of 100% SAF on emissions and contrail formation in combination with the use of different combustor technologies in combination with the use of different combustion modes.[11]

[11] (https://www.dlr.de/content/en/articles/news/2023/01/20230309_emissions-and-contrail-study-with-100-percent-sustainable-aviation-fuel.html).

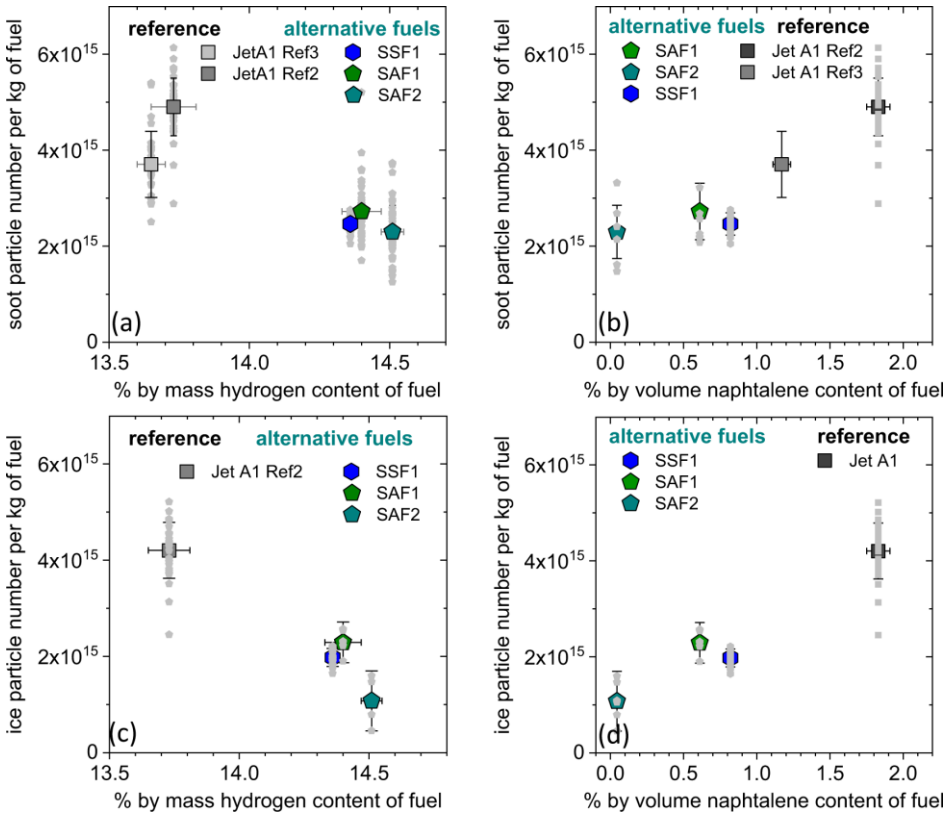

Figure 5.5 Non-volatile (i.e., soot) and apparent ice particle emissions per kg of fuel at cruise conditions for the reference Jet A-1 fuels and for the low-aromatic sustainable aviation fuel blends. (a) and (b): Non-volatile particle emissions per kg of fuel for the reference Jet A-1 fuels (dark grey and black symbols), and for the low-aromatic fuel blends: the Fischer-Tropsch-based semisynthetic fuel blend SSF1 (blue), and the HEFA-based sustainable aviation fuel blends SAF1 (green) and SAF2 (cyan). (c) and (d): Same for apparent ice emission indices. Soot and apparent ice emissions are shown with respect to hydrogen content and bi-cyclic naphthalene content of the fuels. Arithmetic mean soot and ice particle emissions indices (±1 arithmetic standard deviation) are given by the coloured symbols: Grey symbols are individual data points from exhaust and contrail crossings. High hydrogen and low naphthalene sustainable aviation fuel blends reduce soot number emission indices and apparent ice number emission indices in contrails (Voigt et al., 2021).

Figure 5.6 suggests that the reduction in the number of emitted soot particle by low-aromatic fuels compared to the kerosene case leads to a reduction in ice crystal number concentrations in contrails. About 80% of the soot particles are activated into ice in ice supersaturated conditions. The ubiquitous smaller volatile aerosol particles play a minor role for ice activation in the high soot regime of emissions from engines with traditional RQL combustion technologies. However, in addition to its lower naphthalene content, the SAF2 blend had a significantly lower sulphur content, originating from the use of a severely hydrotreated Jet A-1 as blending component. For SAF2, the ice activation on soot is reduced, which might be an indication for the increasing importance of sulphur for soot activation into ice in the low soot regime.

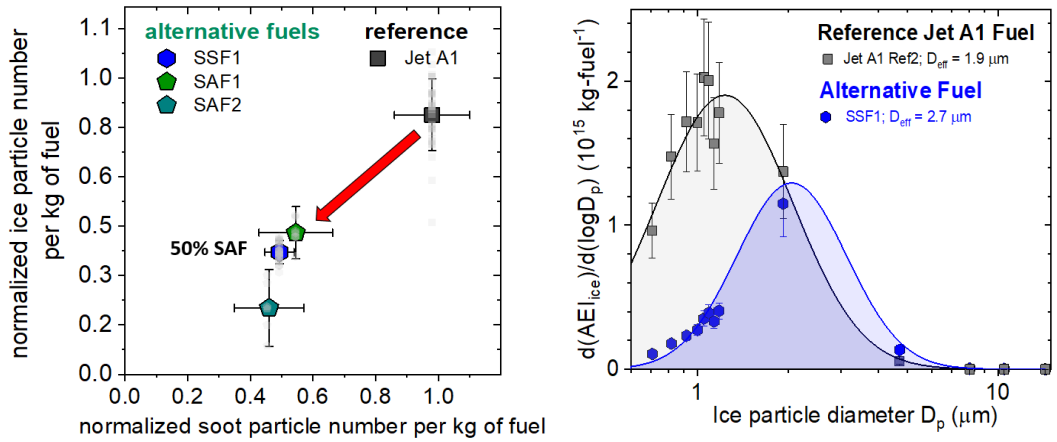

Figure 5.6 Left panel: Correlation between soot particle and apparent ice emission indices for reference Jet A-1 fuel, and for the low-aromatic sustainable aviation fuel blends. Arithmetic mean soot and ice particle emissions indices normalized to the fuel flow for the reference Jet A-1 fuel (black), for the semisynthetic fuel blend SSF1 (blue), and for the HEFA-based sustainable aviation fuel blends SAF1 (green) and SAF2 (cyan). The whiskers denote ±1 arithmetic standard deviation; grey symbols are individual data points. Burning low-aromatic aviation fuels results in reduced soot and ice number concentrations in contrails.

Right panel: Ice particle size distribution in 1 min old contrails formed at similar ambient conditions when burning the Jet A-1 (black) and synthetic Fischer-Tropsch based fuel blend (SSF1, blue) with low aromatic content. Less ice crystals are produced by the SSF1 fuel compared to the Jet A-1 fuel. The ice crystals of the SSF1 fuel are larger as the available water vapour is shared by less ice crystals, therefore the 1 min old SSF1 contrail has slightly larger ice crystal sizes compared to the contrail from Jet A-1. Both panels from Voigt et al. (2021).

Combustion of hydrocarbon, sulphur-containing fuels leads to the formation of charged molecular clusters, so-called chemi-ions, with a large emission index of the order 10^{17} per kg fuel (Arnold et al., 2000). They facilitate the formation of volatile aerosol particles, not only from inorganic constituents but primarily from condensable hydrocarbons. Hence, non-sulphuric volatile aerosol is present in aircraft plumes with similarly high numbers of the order 10^{17} kg^{-1} (Schumann et al., 2002). In addition, fuel sulphur is an important source of particles (sulphuric acid solution droplets) in the exhaust with comparably large numbers. Those volatile particles are initially small with sizes of a few nanometres and do not serve as condensation nuclei as long as there is sufficient soot (particle sizes 20 nm up to 60 nm). However, in the "soot-poor" regime (less than 10^{14} per kg fuel, Kärcher and Yu, 2009; Kärcher, 2016, 2018), the volatile aerosol together with aerosol from the ambient air can substantially contribute to droplet nucleation potentially even leading to an increase in the number of ice crystals formed with decreasing soot emission at low temperatures significantly below the Schmidt-Appleman threshold temperature. Recent measurements (not yet published) indicate that using 100% HEFA-Synthetic Paraffinic Kerosene brings the emissions of nvPM down to the lower end of the soot rich regime of conventional RQL combustors. The use of new low-soot-emission combustor technologies with lean burn combustors leads to even lower nvPM emissions facilitating for the first time the investigation of particle and ice formation processes in the soot-poor regime experimentally. The data

evaluation of those experiments is currently ongoing[12] and results are expected to be published in the near future.

5.4 HOW DOES THE INITIAL CONTRAIL FORMATION PROCESS IMPACT THE LATER EVOLUTION OF THE CONTRAILS?

The effect of details of contrail formation on mainly soot particles and of vortex processing (cf. caption of Figure 3.1) of the fresh ice crystals on later contrail properties has recently been studied by Bier and Burkhardt (2022). Their results are interesting with respect to the question as to how the reduced soot emission using SAF affects the contrail climate impact. Their new model version regards both the effects of the temperature on soot activation (i.e., how much the ambient temperature is below the threshold for contrail formation at the given relative humidity) as well as the later partial sublimation of the ice in the sinking vortex pair. This is the first time that both effects have been studied together in a global model.

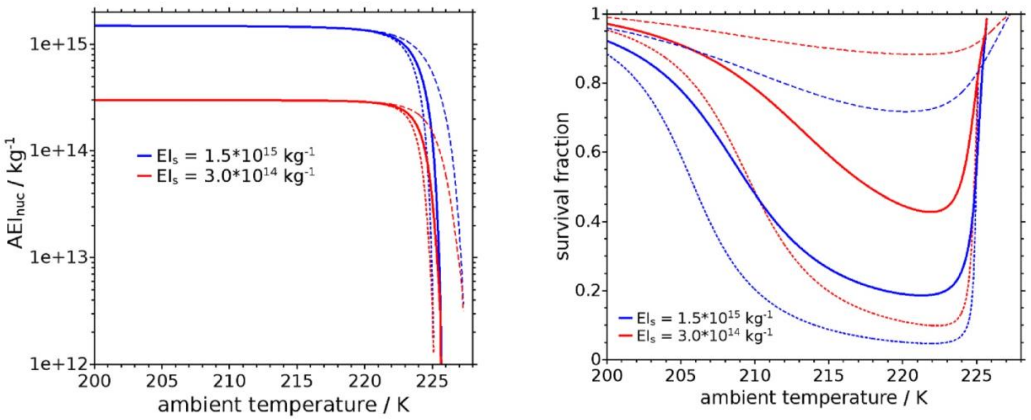

Figure 5.7 Left: Number of nucleated ice crystals from 1.5 $\times 10^{15}$ kg^{-1} soot emission (blue) and 3 $\times 10^{14}$ kg^{-1} soot emission (red) at 110 (dotted), 120 (solid), and 140% (dashed) relative humidity over ice and at a threshold temperature of about 225 K for these RHi values. The figure shows that practically all soot particles form an ice crystal 5 K below the threshold.

Right: The survival fraction of freshly formed ice crystals in the vortex varies with initial number of ice crystals, the ambient temperature and, in particular, the ambient supersaturation. Note that relative humidity of 140% occurs much more rarely in the atmosphere than relative humidity of 110%. In fact, the probability distribution of degrees of supersaturation (i.e. relative humidity minus 100%) is exponential with a mean value of about 15%. (Figures from Bier and Burkhardt, 2022).

According to these results, an 80% reduction of the soot number does not imply an 80% reduction of the number of ice crystals after the vortex regime. The reduction depends on temperature and relative humidity. The reduction is close to zero close to the contrail formation limit, but grows with decreasing temperature. The effect

[12] https://www.airbus.com/en/newsroom/stories/2023-03-airbus-most-popular-aircraft-takes-to-the-skies-with-100-sustainable

increases with supersaturation, as Figures 5.7 and 5.8 show. The curves are nonlinear due to the complex interplay of the diverse processes.

Compared to natural cirrus clouds, contrails have much larger ice crystal number densities but smaller crystals. The ice water mass of both kinds of ice clouds is similar in similar environments because most of the ice mass of a contrail, when it is, say, 10 minutes old, originates from ambient humidity. The initially emitted water vapour is only a tiny fraction of the contrail ice mass. Although the vortex-processing of the ice lowers the ice number density, a contrail has still much larger ice number density then natural cirrus when it starts to disperse within its parent ice supersaturated region. The vortex-phase leads to a vertical extension of the young contrail of a typically 200 - 400 m. The ambient wind changes with altitude both in speed and direction (vertical wind shear) so that the upper parts of a contrail are shifted by the wind differently from the lower parts; this leads to the horizontal spreading of contrails, which proceeds at an average rate of about 5 km/h (Freudenthaler et al., 1995).

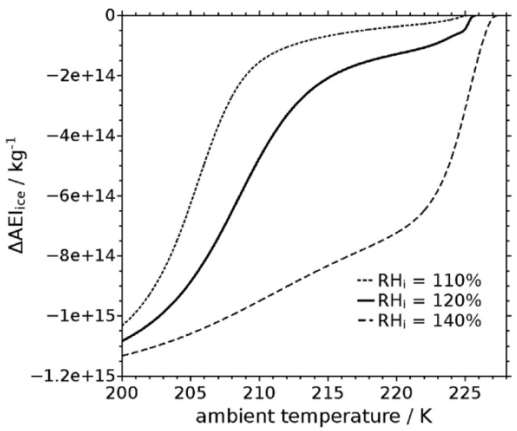

Figure 5.8 The absolute reduction of ice crystals remaining after the vortex phase when the number concentration of emitted soot particles is reduced by 80%, depends sensitively on temperature and supersaturation. The contrail formation threshold for these calculations was about 225 K. (Bier and Burkhardt, 2022)

As long as the spreading occurs within the parent ice-supersaturated region (ISSR), the contrail ice crystals that are situated at the contrail edges and surfaces (that is, in direct contact with fresh supersaturated air) grow until they are sufficiently heavy to fall down through the atmosphere. In contrast, ice crystals in the inner contrail zones (the "core"), quickly consume the water vapour in excess of saturation and then stay relatively small in an ice saturated environment and cease to grow. Thus, a persistent contrail has two populations of ice: a core with high number density of small crystals and a fall streak with low number density of large ice crystals (Unterstrasser et al., 2016a, b). Of course, the falling crystals disappear, and other crystals closer to the core come in contact to fresh supersaturated air, and so on, until all contrail ice crystals are so large that they sediment. This is (see below) the microphysical pathway to contrail termination (Bier et al., 2017).

Application of SAF leads to lower soot number densities compared to kerosene use. If these are still in the soot-rich regime, that is, higher than about 10^{14} soot particles per kg of fuel, then the initial number density of ice crystals will be lower as well, and even if the vortex action leads to a larger ice crystal loss for SAF than for

kerosene contrails, the young SAF contrail will in most cases consist of less but larger ice crystals than the young kerosene contrail in otherwise equal situations. The ice mass of both contrails will be similar, as explained above. This has two consequences which both are beneficial for climate:

- SAF contrails are optically thinner than kerosene contrails under equal circumstances. The optical thickness is a measure for the interaction (scattering and absorption) of matter with radiation. The main interaction process between radiation and ice is scattering, which increases with the total surface of the available ice crystals. Having similar ice mass (or volume), a kerosene contrail with larger number density offers more surface for scattering than a SAF contrail. Thus, SAF contrails impede the flow of radiation less than a comparable kerosene contrail, which implies a lower individual radiative forcing.
- SAF contrail ice crystals are larger than kerosene contrail crystals. Thus, they attain earlier a considerable fall speed than ice crystals from kerosene combustion. This leads to a shorter lifetime, if the contrail resides within ice supersaturated air and follows the microphysical pathway to termination, as described above. A shorter lifetime implies a lower radiative effect integrated over the contrail lifetime.

Note that these considerations are valid only in the soot-rich regime. In the soot-poor regime, the number of formed ice crystals can increase with decreasing soot number emission index, in particular at temperatures far below (~10 K) the Schmidt-Appleman limit. In such a case, optical thickness and lifetime of contrails may increase with decreasing soot emission.

5.5 WHEN DO CONTRAILS BECOME LONG-LIVED?

Ice crystals exchange water molecules with their immediate environment. Equilibrium conditions, that is, equal water fluxes from the crystals into the air and from the air onto the crystals, define the state called "saturation". Ice crystals sublimate (and shrink) under sub-saturated conditions. They give more water molecules to the air than what they get back. Under such conditions a contrail will dissipate after a while, which depends on the degree of sub-saturation. Contrails can survive one or two hours in slight sub-saturation (e.g. relative humidity of 90%) (Li et al., 2023), but they are short lived and vanish within seconds if the relative humidity is very low, say 10%.

Thus, contrail persistence is thus only possible in an ice supersaturated environment, i.e., the relative humidity with respect to ice is 100% or higher. Such parts of the atmosphere are termed "ice supersaturated regions" (ISSR).

Relative humidity comes in two "flavours", relative humidity with respect to ice, where the exchange of water molecules between ice crystals and the air is considered, and relative humidity with respect to liquid water, where the exchange of water molecules between liquid droplets and the air is considered. The latter is the relevant quantity for formation of water clouds: As soon as saturation with respect to liquid water is reached and just slightly surpassed (by a fraction of one percent), droplets condense and a water cloud is formed. The atmospheric aerosol serves as the necessary condensation nuclei. In contrast, ice crystal formation does not commence as soon as ice saturation is reached. The formation of the ice crystal lattice is more complicated than the formation of relatively unordered water. Thus, natural ice formation typically commences only at large supersaturation of more than 45%.

Contrail ice forms in two steps, droplet condensation followed by freezing, an example of Ostwald's phase rule. Because droplets are formed first, water saturation is needed while the plume expands and this is the Schmidt-Appleman condition. The droplets freeze once the temperature falls below the supercooling limit of –38°C and the fate of the resulting ice crystals then depends on the ambient relative humidity with respect to ice. As stated, contrails are persistent in ISSRs, where the crystals grow until they get sufficiently heavy to fall through the air. Once they fall into sub-saturated air, they start to sublimate.

Ice supersaturation conditions are met on 10-15% of the flight trajectories in cruise, mainly on flight levels just below the tropopause. Ice supersaturation is rare in the lowermost stratosphere where only about 2% of aircraft trajectories are in ISSRs (Gierens et al., 1999; Petzold et al., 2020).

In ISSRs, average supersaturation values are of the order 15%, which usually is not sufficient for natural formation of cirrus clouds, but sufficient for carrying persistent contrails. Aircraft tracks in ISSRs are on average 150 km long, but with a large variability in length. Specimens with more than 3000 km extension have been detected as well (Gierens and Spichtinger, 2000). The average vertical extension is a few 100 m, but again, quite thick ISSRs occur occasionally (Spichtinger et al., 2002). ISSRs are often stacked upon each other with shallower or thicker sub-saturated layers in between (Gierens et al., 2020). ISSRs are frequent in the tropics, but mainly at altitudes above current flight levels. They are also relatively frequent in the mid-latitudes, in particular, in a 30 hPa thick layer beneath the tropopause. They occur in certain dynamical regimes more often than in others (Gierens and Brinkop, 2012; Irvine et al., 2012; Irvine et al., 2014; Wilhelm et al., 2022). ISSRs related to the synoptic air flow can exist for more than 24 hours (Spichtinger et al., 2005).

A review on ice supersaturation can be found as an article in a book on Atmospheric Physics (Gierens et al., 2012).

5.6 WHAT OTHER PARAMETERS MAY AFFECT THE FORMATION AND LIFETIME OF CONTRAILS?

The lifetime and the total radiative effect of a persistent contrail depend strongly on the current meteorological conditions and are thus rather variable (Wilhelm et al., 2021). The ambient conditions are in fact the dominant ones. Two contrails from different drop-in fuels in the same meteorological conditions may differ less than two contrails from equal fuel in different weather situations. An immediate meteorological influence is the vertical wind shear (direction and speed change of the horizontal wind with altitude), which leads to different transport of the upper and lower end of a young contrail, i.e., about 5 min, with a vertical extension of about 200 - 400 m at the beginning of the dispersion phase (Unterstrasser et al., 2014) and thus to the contrail's lateral widening (Schumann et al., 2017). The ice crystals grow in the supersaturated environment. After 2 min, about one fourth of the contrails ice water content stems from the engine (Voigt et al., 2021). Later the contrail's water mass is mostly composed of atmospheric water; the emitted water is merely a small fraction.

Many numerical simulations of contrails in the dispersion phase are described in the literature, studying the effects of many influential quantities, e.g. temperature, relative humidity, wind shear, vertical wind, stratification stability (i.e., temperature profile or lapse rate and related quantities), turbulence, radiation, nearby cirrus clouds or even clouds mixed with the contrail (e.g., Unterstrasser and Gierens, 2010a, b; Unterstrasser et al., 2016a, b; Lewellen, 2014; Lewellen et al.,

2014; Schumann et al., 2017). Observation of persistent contrails during their lifetime requires geostationary satellite data (e.g., Vázquez-Navarro et al., 2015, Wang et al., 2023).

Contrail termination implies sublimation of their ice content. This is achieved through two mechanisms: falling of ice crystals into sub-saturated layers (microphysical pathway), and subsidence (settling) of the airmass that contains the contrail (synoptic pathway). The generally beneficial effect of using alternative fuels (bigger and thus heavier ice crystals) is reduced under the synoptic pathway (Bier et al., 2017). In such cases ice is forced down together with the ambient air by the prevailing synoptic conditions, which leads to adiabatic heating and thus sublimation of the ice crystals, independent of their size (all crystals disappear). But, if the synoptic situation allows long-living contrails, ice crystal falling becomes important and then the heavier ice crystals of contrails from alternative fuels fall faster, yielding a reduction of contrail lifetime and integrated radiative impact.

Contrail evolution follows the microphysical path in large long-living ISSRs, which are related to large-scale weather patterns (high- and low-pressure areas and the associated air flows). ISSRs can exist for more than 24 h (Spichtinger et al., 2005a) and if the wind does not transport the contrails out of their parent ISSR, contrails can achieve ages of many hours. Shorter-living ISSRs can be the result of smaller-scale atmospheric phenomena (e.g., waves; Spichtinger et al., 2005b), and rather lead to the synoptic path, that is, contrails disappear because they are forced downward by the air flow. To date, there are not enough data to decide whether the microphysical or the synoptic path predominates. The only study of this topic, i.e., Bier et al. (2017), considered only 8 randomly selected cases, of which three were microphysically controlled and two dynamically controlled. The remaining cases could not be classified unequivocally.

Contrail "lifetimes" vary from a few seconds (Busen and Schumann, 1995; Sussmann and Gierens, 1999) up to many hours (Minnis et al., 1998; Vázquez-Navarro et al., 2015; Schumann et al., 2017; Wang et al., 2023). Statistical modelling of contrail lifetimes by applying tracking data from satellite images resulted in an average lifetime of 3.7±2.8 h, with lifetimes below 5 h in 80% and lifetimes exceeding 10 h in 5% of all tracked cases (Gierens and Vázquez-Navarro, 2018).

5.7 WHAT IS THE RELATIVE IMPORTANCE OF JET FUEL COMPOSITION IN COMPARISON TO OTHER FACTORS/PARAMETERS THAT MAY AFFECT THE FORMATION AND LIFETIME OF CONTRAILS?

The importance of fuel composition relative to other factors depends on the time horizon that is considered. For a single contrail (that is, a time horizon up to a few hours), the current weather situation and its further development certainly dominates contrail properties and lifetimes. Two contrails produced by the same aircraft/engine combination and the same fuel, but in different weather situations, can differ more than two contrails produced using different fuels, but in the same weather (i.e., atmospheric conditions). The overwhelming weather influence of the meteorological situation (see Wilhelm et al., 2021) is best illustrated by the huge variability in the local imbalance in the radiative flux[13] of individual contrails. The local imbalances in the radiative flux easily cover a range of ±100 W/m^2.

On climatological time horizons (several years) the weather influences average out, and the climatologically, i.e., global and multi-annual mean radiative forcing is of

[13]Note that Wilhelm et al., 2021 denote local imbalance in the radiative flux "iRF" (instantaneous radiative forcing).

the order 50 mW/m². This level is affected by the types of aircraft flown and the kind of fuel used, as shown by the climate model studies of contrails from alternative fuels, like those of Bock and Burkhardt (2019) and Bier and Burkhardt (2022).

5.8 IMPACT OF JET FUEL CHEMICAL COMPOSITION ON THE CRITICAL PARAMETERS DENSITY, VOLATILITY, ENERGY CONTENT

Studies like burnFAIR (Zschocke, 2014), the JETSCREEN project (JETSCREEN, 2021), and the NJFCP project (Kosir et al., 2020) demonstrated that SAF can offer advantages as lower sulphur emissions (depending SAF blend sulphur content) and PM emissions (depending on SAF blend H content), reduced CO_2 emissions (depending on feedstock and production process), lowered jet engine maintenance costs (depending on fuel H content as well as fuel thermal stability), lower fuel burn (specific energy and energy density, potentially thermal stability) as well as other operational benefits as increased maximum take-off weight (energy density). The maximization of these benefits is of interest and would provide environmental and economic benefits.

On the other hand, aviation safety has to be ensured by all means. Aviation safety is built upon redundancy and the verification of critical system operations. Currently, Jet A/A-1 is the primary energy carrier used in commercial aircraft. The fuel not only propels the aircraft but also performs other essential functions beyond chemical heat release as illustrated by Figure 5.9. Jet fuel interacts with various aircraft functions and operations, and approved alternative fuels must operate as coolants, work seamlessly with pumps and seals, remain stable in long-term storage, and be safe under severe operability conditions.

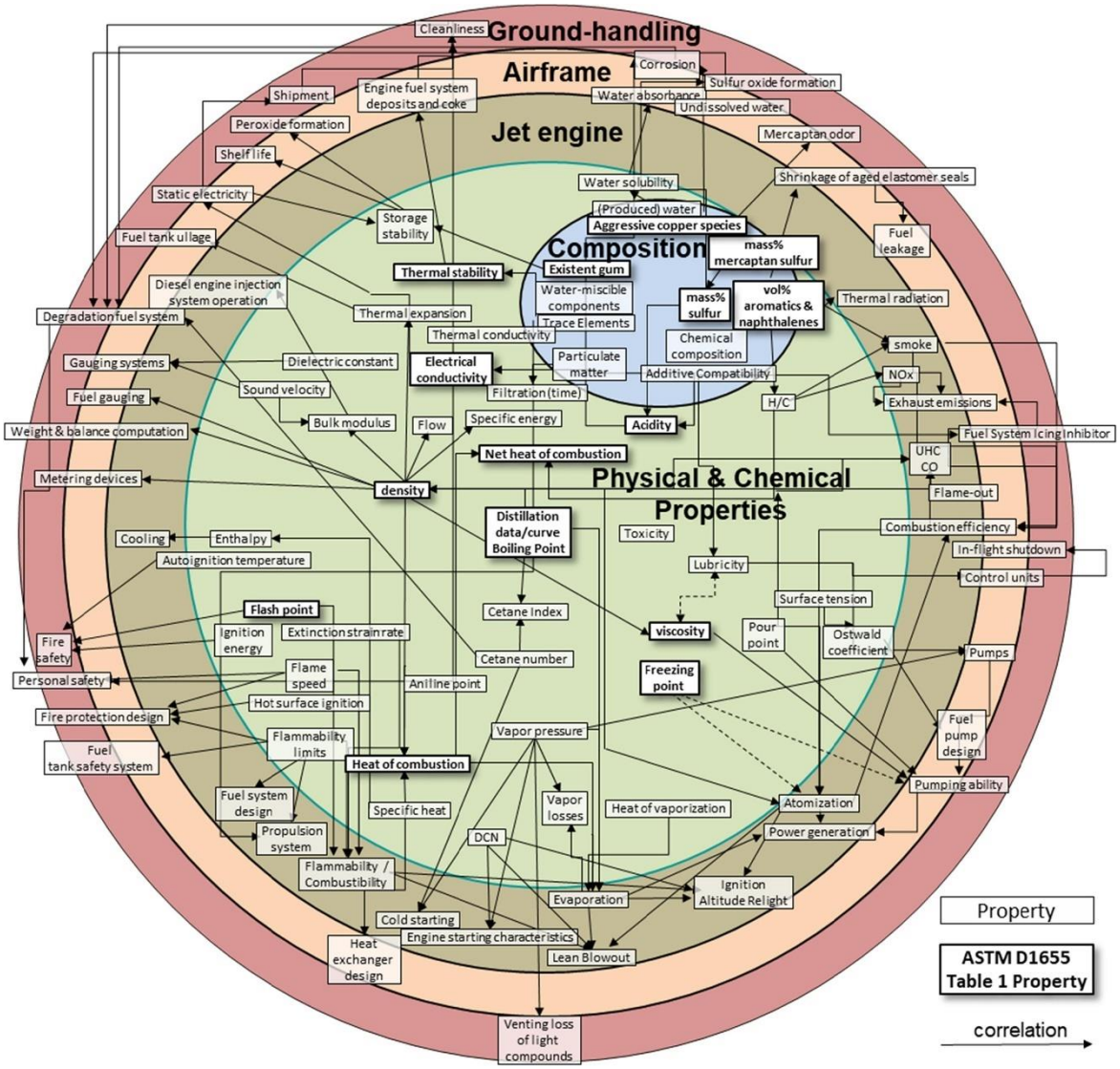

Figure 5.9 Overview of interdisciplinary and interdependency of the properties tested during the ASTM D4054 process. Properties (boxes) are grouped by discipline (circles). An arrow indicates the relationship between properties. ASTM D1655 Table 1 properties are shadowed and boxed with thicker lines (Heyne et al, 2022).

In short, to optimize a jet fuel, the value and performance have to be maximized while ensuring operability and safety. Such an optimization can be performed in two means:

a) Blending strategies,

b) Fuel formulation.

Ad (a): Commercial blending strategies focus on meeting fuel specification requirements to ensue operability, safety as well as maintaining customer supply / economic viability. As a result, a range of kerosene components might be used for the blending and safety margins towards specification limits are high. The H content

of resulting SAF blends is usually only slightly higher than the one of conventional jet fuels on the market, and sometimes even below, causing increased PM emissions (Zschocke, 2014). During ECLIF II/ND-MAX, blending was performed in a targeted manner and above-average H content. Jet A-1 was selected as base for blending with a HEFA-SPK. As a result, the SAF2 fuel (blended with the above-average H content, ultra-low sulphur Jet A-1) showed significantly lower PM emissions and ice crystal formation as compared to the SAF 1 blend with an average Jet A-1 (Voigt et al., 2021).

Ad (b): The optimization of the fuel formulation depends on the fuel production pathway and applied processing technology. Based on the information presented, if the optimisation target is to minimise PM emissions, the ASTM D7566 lower aromatic limit of 8% mass, as well as the lower density limit of 775 kg/m^3 becomes the constraining factor. However, flash point, low temperature viscosity, and the distillation slope limits (T90-T10, T50-T10) can also become major constraining factors. The latter can be resolved by applying additional upgrading, which might impact product yield and/or economic viability. However, limited information is available on holistic fuel optimisation that considers operational safety / technical suitability, economic viability as well as impact on environment and climate. Additional degrees of freedom arise with the upcoming modification of ASTM D7566 to allow 100% drop-in SAF formulations. The above does not consider the influence of aviation turbine engine design which may also be significant relative to fuel effects.

5.9 WHAT IS THE IMPACT ON (EFFECTIVE) RADIATIVE FORCING?

Contrails interact with radiation and thus affect the balance of radiation flows into and out of the atmosphere. Two wavelength bands are important for the radiation balance, the visible radiation (about 400 nm to 4 µm) from the sun and the thermal infrared radiation (wavelengths exceeding 4 µm) from the Earth. Contrails, like all clouds, interact with both kinds of radiation. Scattering of solar radiation back to space reduces the energy flow into the Earth-atmosphere system and trapping of outgoing thermal infrared radiation reduces the energy loss of the system. The solar effect works during daytime only, while the infrared effect works day and night. Overall, i.e., in the mean over time and globe, the infrared effect is stronger than the solar effect and the Earth-atmosphere system gains energy, which eventually leads to heating.

As mentioned above, transition to low-aromatic aviation fuels is expected to lead to optically thinner contrails (as long as we stay in the soot-rich regime[14]). Optically thinner contrails imply less scattering of sunlight but also lower absorption and reemission of infrared radiation. Thus, both cooling and warming contributions of SAF contrails are smaller than in their kerosene counterparts.

The solar radiative effect of contrails consists essentially of the change in the albedo (backscattering ability) of a scene with and without contrail. For contrails, one can estimate that to first order the albedo change is proportional to the optical thickness of the contrail, which in turn is inversely proportional to the average crystal radius (combine equations on p. 1089 of Meerkötter et al., 1999). Thus, larger SAF crystals lead to a smaller albedo change.

The infrared effect of contrails is essentially the difference between the total irradiance of the ground and lower atmosphere (without a contrail) and the total

[14] We don't know what happens if ice crystal number densities increase with further decrease of soot number densities in the soot-poor regime.

irradiance of the contrail. The total irradiance is proportional to the temperature of the radiating body raised to 4th power (Stefan-Boltzmann law), that is the difference is proportional to $\sigma(T_{contrail}^4 - T_{background}^4)$, where σ is the Stefan-Boltzmann constant[15]. The proportionality factor is the so-called emissivity, which describes the deviation of a radiating body from a blackbody. For a contrail which is mostly optically thin, the emissivity is again inversely proportional to crystal size (combine equations on p. 1090 of Meerkötter et al., 1999). Thus, also the infrared effect of SAF contrail is reduced compared to kerosene contrails.

A good example of the spatial distribution of contrail radiative effects over the globe is given in Figure 5.10. It shows a couple of noteworthy things. At any time, modelled persistent contrails cover only a minor part of the globe. The figure shows with a grey background the local night and with a white background local day. The boundary between day and night in such a map is called the terminator. There are cooling (blue) and warming (red) contrails, and the cooling contrails are found closer to the terminator in the sunlit part of the map. This means, that cooling contrails occur during the day and often close to sunrise or sunset when the sun is shining from the horizon. In this situation, scattering of sunlight away from the Earth into space is most effective (cf. Meerkötter et al., 1999). During the night, contrails are always warming. However, contrails whose lifetime is a couple of hours and extends over sunrise or sunset, may undergo a change from cooling to heating or vice versa. Thus, the whole contrail lifetime needs to be considered in the evaluation of its overall radiative effect. This is not an easy task, in particular if it has to be done for many contrails and for many points in time. One possibility is then to use relatively simple formulae (e.g. Corti and Peter, 2009; Schumann et al., 2012; Wolf et al., 2023) that are based on statistical regression using results from detailed radiative transfer models. Regression formulae provide statistical expectation values, that is, values that are correct on average, but not necessarily for a concrete situation.

[15] $\sigma = 5.670 \times 10^{-8}$ W m^{-2} K^{-4}

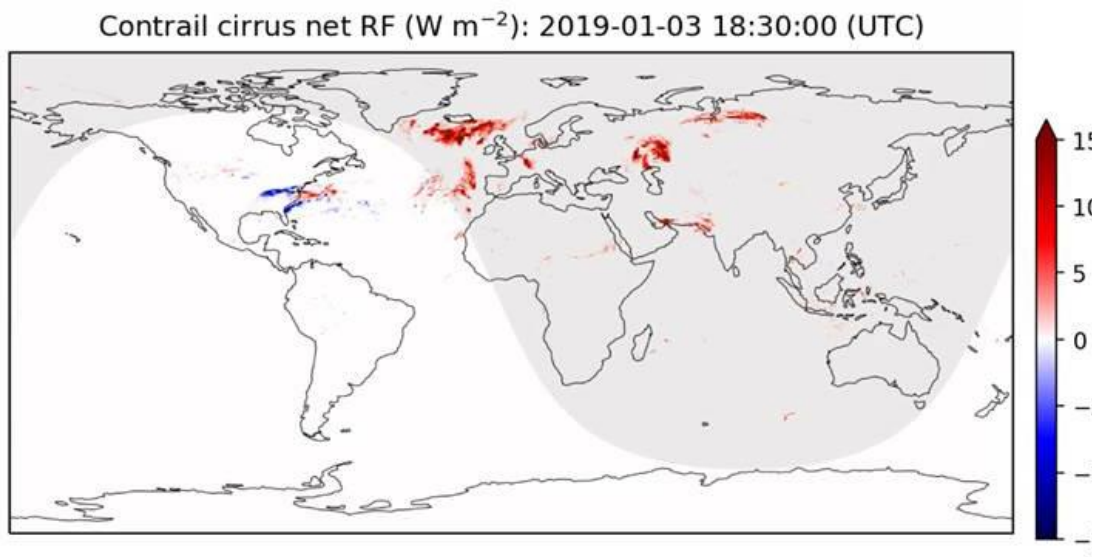

Figure 5.10 Snapshot of warming (red) and cooling (blue) contrails from air traffic on 3 Jan 2019 at 18:30 UT calculated with the contrail model used in Teoh et al. (2022b). (Pers. comm. Teoh and Stettler, Imperial College, London, UK.9

A transition to low-aromatic aviation fuels (but still in the soot-rich regime) reduces both solar (cooling) and infrared (warming) effects of contrails and thus the net-effect on radiation as well. This benefit adds to the shorter lifetime of SAF-induced contrails due to the higher fall speed of its larger ice crystals (as long as contrail termination follows the microphysical pathway, see above). As a consequence, the contrail detectability and detectable coverage decrease, the fraction of optically thicker contrails and thus its coverage gets smaller. In total, SAF-induced contrails have a smaller radiative impact than kerosene-induced contrails.

As mentioned above (see also Section 5.3) a reduced number of emitted soot particles results in a lower number of initial ice particles in contrails. In simulations with global climate models a reduced number of initial ice particles results in a smaller radiative forcing. The change in the radiative benefit non-linearly depends on the initial number of initial ice particles (Burkhardt et al., 2018; Bock and Burkhardt, 2019; Teoh et al., 2022). Figure 5.11 shows that in the modelling exercise of Burkhardt et al. (2018) an initial (after the vortex phase) reduction of ice crystals by 80% is needed to reduce the contrail RF by 50%, i.e., the relative reduction in radiative forcing is smaller than the relative reduction in the initial number of ice particles.

The effect of a reduction in soot particles due to blending with sustainable aviation fuels on contrail formation, lifetime and climate impact has been parameterised and investigated by Teoh et al. (2022a). They used a trajectory-based contrail model (Schumann et al., 2012; Schumann et al., 2017) with engine emissions on a flight by flight basis and calculated the formation, evolution and the radiative forcing of contrails based on weather information from the European Centre for Medium- Range Weather Forecasts ECMWF over a five years period from 2015 to 2019 over the Northern Atlantic flight corridor.

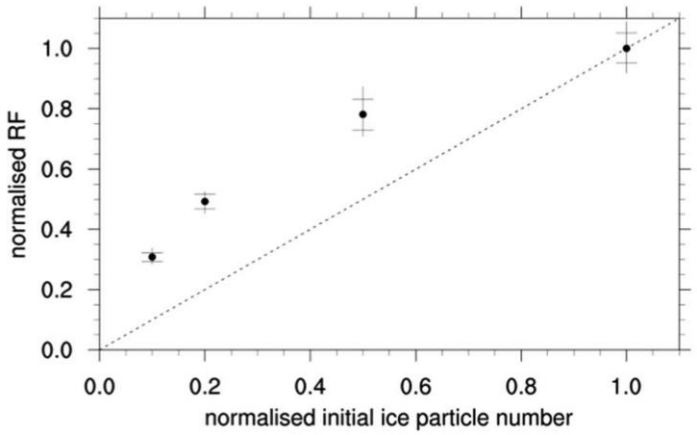

Figure 5.11 RF-reduction vs. reduction of initial (after the vortex phase) ice crystal number in the global average according to simulations by Burkhardt et al. (2018).

Based on the hydrogen content of fuels they derived a SAF blending ratio and calculated the resulting reduction in soot particle emissions (Figure 5.12). The correlation of the fuel's hydrogen content with the soot particle emissions (Figure 4.6) was evaluated with observations on the ground and in flight (Moore et al., 2017; Schripp et al., 2020; Voigt et al., 2021). The higher water vapour emissions resulting from the higher hydrogen content leads to a higher potential occurrence of contrails by up to 5% for 100% SAF as pointed out in Section 5.1. An increase in the H content in the SAF blending ratio also leads to a non-linear reduction in soot particle emissions, with a higher reduction (larger slope) for up to 50 % SAF blends, as confirmed by measurements (Schripp et al., 2020), and a decrease in soot particle reduction for larger blending ratios. The reduction in soot particles leads to a reduction in ice particle numbers in contrails and in their optical depths of the ice crystals. Slightly larger ice crystal sizes (Voigt et al., 2021) lead to larger sedimentation rates, which explains the lower contrail lifetime. The combined effects result in a reduction of the contrail cover. For 100 % SAF-SPK, a maximum reduction of 52% in soot particle emissions was derived. Voigt et al. (2021) suggest that this would reduce radiative forcing from contrails. However, more studies are needed to evaluate relation between the fuel hydrogen content and the soot particle emission indices in particular at higher SAF blending ratios.[16]

[16] In addition to the fuel's hydrogen content, other parameters can have an impact on contrail formation, e.g., the fuel's sulphur content and the engine type and thrust setting.

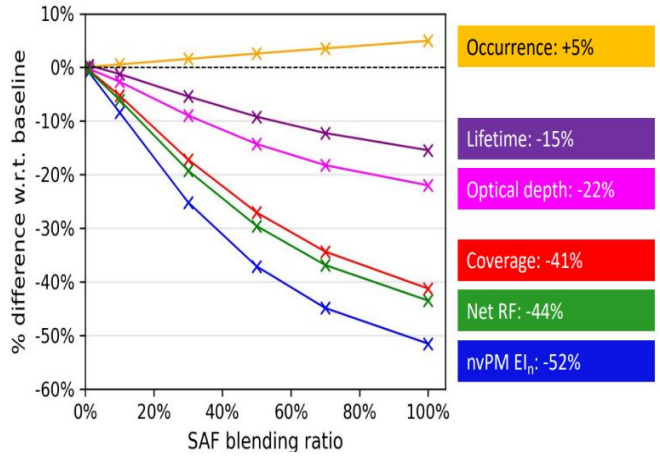

Figure 5.12 Relative difference in non-volatile particle number emissions, in contrail ice crystal number and optical depth, contrail lifetime, contrail coverage and in radiative forcing from contrails for increasing SAF blending ratios with respect to the reference Jet A-1 case with 13.8% aromatics (from Teoh et al., 2021b). The effect of enhanced potential contrail occurrence is of minor importance and masked by the strong reduction in contrail cover and radiative forcing (from Teoh et al., 2022b).

6. UNCERTAINTIES AND LIMITATIONS

6.1 PRESENT-DAY UNCERTAINTIES IN THE CONTRAIL CIRRUS RF AND ERF TERMS

The present-day (2018) ERF of 57 mW m^{-2} (17 – 98 mW m^{-2} 5-95% confidence interval) for contrail cirrus represents the forcing in that particular year, as a result of 2018's air traffic and represents the most recent assessment that accounts for a range of available models and calculations, normalized in terms of traffic and details of calculation (Lee et al., 2021). The uncertainty range spans from nearly double the assessed mean ERF to less than half. This, and other non-CO_2 uncertainties, when combined, dominate the total non-CO_2 forcing, and are a factor of approximately 8 larger than that of CO_2. Of this, the contrail cirrus uncertainty (relative to CO_2) dominates and is slightly larger. It is important to recognize that this uncertainty assessment is built upon recent historical (2018) emissions, for which the underlying fuel was virtually all fossil fuel, rather than low-aromatic SAF.

The composite normalized RF given in Lee et al. (2021) was from the results of three models; those of Bock and Burkhardt (2016), Chen and Gettelman (2013)[17] and Schumann et al. (2015). Finally, the results were adjusted to give an ERF by applying a factor of 0.46, the mean of three model results for an 'efficacy' estimation (an adjustment to λ in equation (1) on page 4). However, it should be noted that this ERF adjustment was for fast feedbacks in the climate system only, and is therefore not a complete description of 'efficacy'. This efficacy accounted for linear contrails only. The results of the updated Chen and Gettelman (2013) modelling performed specifically for the Lee et al. (2021) assessment exercise were not adjusted in this way, since they were already considered to be an ERF, with fast feedbacks inherent in the global model used. All the details of the adjustments can be found in the Supplementary Information of Lee et al. (2021), documentation and accompanying spreadsheet.

The uncertainties calculated for the contrail cirrus model results presented by Lee et al. (2021) are rather different to the other ERFs, as shown in Figure 1.1, which illustrates all the ERFs associated with aviation. Since only three models are/were currently available, the uncertainties were not statistical in nature, in the same way as, e.g., the "net NO_x" results are. Rather, they are an underlying assumed uncertainty of ±70%, essentially based on expert judgement of how the models treat processes, or omit known processes. The processes fall into two groups: those connected with the upper tropospheric water budget and the contrail cirrus scheme itself, and those associated with the change in radiative transfer due to the presence of contrail cirrus (see Lee et al., 2021 for details).

Lastly, the ERF adjustment of 0.46 will have large uncertainties. It was not possible to quantify these and combine them with the other underlying uncertainties in a meaningful mathematical way, thus the likely overall uncertainties of the overall contrail + contrail cirrus term given by Lee et al. (2021) are likely to be an *underestimate*, that is, if we could consider all sources of uncertainty, the "error bar" for contrails would be larger than it currently is in Figure 1.1 (see p. **Error! Bookmark not defined.**).

It is important to comment also on our current overall understanding on contrail + contrail cirrus ERF, which is assessed by Lee et al., 2021 using an IPCC methodology,

[17] As detailed by Lee et al. (2021), the Chen and Gettelman (2013) results were recalculated with smaller ice initial crystal diameters, to bring in line with updated measurements.

to be "low". Moreover, it is the result of only three models. More recent work by, e.g., Bier and Burkhardt (2019, 2022) highlight that further processes need to be considered in global modelling, such as ice crystal loss during the vortex phase which controls ice crystal numbers in young contrails. Incorporating wake vortex losses reduced a prior RF estimate of these authors by 22%. (Such a percentage reduction would not necessarily apply to the assessed overall results of Lee et al., 2021 but it would be reasonable to suggest that it would reduce the mean ERF, since none of the models used considered this extra physical loss process.) Clearly, the magnitude of RF or ERF for present day traffic and fuels is not “settled” and subject to change with improvements to the modelling.

Against the backdrop of inherent uncertainty over the size of the contrail cirrus ERF, some efforts have been made to assess the potential effect of reduced aromatics in future ‘sustainable’ aviation fuels.

As noted above, ERF appears to by a relatively good proxy for the expected equilibrium temperature change according to equation (1) on page 4 for many different types of climate forcings in terms of fast feedbacks.[18] However, it appears that this is not the case for contrail cirrus. Rather recently, Bickel (2023) provided a first estimate for the efficacy of contrail cirrus, which accounts for longer-term feedbacks in the climate system. While in Lee et al. (2021) the ratio of the ERF from contrail cirrus to the ERF from aircraft-induced CO_2 is about 1.5, the corresponding ratio of the expected equilibrium temperature changes is only 0.6 according to Bickel (2023). This would mean that the climate change arising from contrail cirrus is substantially smaller than previously assumed, if the Bickel's (2023) results are confirmed.

6.2 GLOBAL MODELLING OF SAF EFFECTS ON CONTRAIL CIRRUS

To date, not a great deal of work has been done on modelling the effects of SAF usage on contrail cirrus and its forcing at the global scale, the notable exceptions being those of the DLR and MIT modelling groups (Burkhardt et al., 2018; Bier and Burkhardt, 2019; Bier and Burkhardt, 2022; Caiazzo et al., 2017). More recently, Teoh et al. (2022b) have recommended to target SAF to the most warming contrails to maximize the potential benefits.

The basis of the above modelling efforts is the premise that aromatic compounds are largely responsible for soot formation in the combustor of an aircraft engine, and that reducing such compounds in the fuel results in lower soot number emissions and that lower soot numbers result in fewer ice crystals, which reduces the radiative forcing of persistent contrails. The evidence that aromatic compounds in the fuel are mostly responsible for soot in the exhaust is largely empirical, i.e., from observations (see Section 5.3) but not exclusively so (Richter et al., 2021; Brem et al., 2015), and the actual chemical kinetics of the soot formation mechanism is only poorly understood. Nonetheless, the observational evidence for this step is good, although precisely which compounds in the fuel form soot still requires further work. There are numerous observations of SAF reducing soot number emissions from aircraft engines at the ground (see Moore et al., 2015 for a summary) and a few at altitude (e.g., Moore et al., 2017; Voigt et al., 2021).

Less well characterized is the effect of lowering soot number (from either combustion technology, or SAF usage) on ice crystal number although the

[18] ERF is definitely a better proxy than RF.

measurements of Voigt et al. (2021) provide the first observational evidence for this.

The effects of lowered soot number concentration emissions have been incorporated into the assumptions of global models (e.g. Burkhardt et al., 2018) such that the RF is recalculated, based on the assumed lowered soot number concentrations reducing initial ice crystal numbers, which were prescribed at 0.5, 0.2, and 0.1 of the present-day values to study the effect on modelled RF. The results are reproduced in Figure 5.11, which shows a non-linear reduction in normalized RF for normalized reductions in ice crystal number, such that an 50% reduction in ice crystal number results in a reduced forcing by approximately 20% and a reduction in ice crystal number of 80% results in an approximately 50% reduction in forcing. Similarly, in a study of future emissions and fuel composition changes, Bock and Burkhardt (2019) assume that for a 2050 scenario (their case C2050-T50M, see their Table 1), where soot emissions are reduced by 50% (from an assumed SAF uptake), the water vapour emission index and propulsion efficiency increases (affecting the contrail threshold formation conditions), and the initial ice crystal number concentration is assumed to reduce by 50% (as a result of the 50% reduction in soot number concentrations). These changes imply an approximately 14% reduction in RF for a 50% reduction in implied soot emissions, using the 2050 baseline and the N_{ice}/water EI/propulsive efficiency modified scenarios (Bock and Burkhardt, 2019).

Bier and Burkhardt (2019) progressed their global contrail/contrail cirrus modelling by additionally considering the link between soot number concentrations and N_{ice} in an offline study, using the parameterization of Kärcher et al. (2015) to study ice nucleation (RF estimates were not provided). Bier and Burkhardt (2019) point out that the Kärcher et al. (2015) parameterization does not consider the formation of ice crystals on ultrafine aqueous particles (Kärcher and Yu, 2009; Kärcher, 2018) and that this needs to be considered in low-soot scenarios.

Bier and Burkhardt (2022) combine the approach of Burkhardt et al. (2018) and Bock and Burkhardt (2019) to study, amongst other things, the effect of soot number concentrations in ice crystal number. Assuming present-day soot number emissions of 1.5×10^{15} kg fuel^{-1}, they found that an 80% reduction of soot number emissions leads to a decrease in RF of 41% compared to 50% as in Burkhardt et al. (2018); this was attributed to an increase in the ice crystal survival fraction for decreased ice nucleation using a new parameterization of vortex phases losses of ice crystals. It can be tacitly assumed that the caveats highlighted by Bier and Burkhardt (2019) regarding the lack of inclusion of ultrafine particles at low soot number emissions are still applicable.

The other major modelling initiative of contrail cirrus has been undertaken by MIT (Caiazzo et al., 2017) who estimated contrail forcing over North America. Using assumed emission indices for ice nuclei (EI_{IN}, 10^{15} kg fuel^{-1}) and revised water vapour emission indices assumed for biofuels, and a parameterized radiative forcing model (Schumann et al., 2012), Caiazzo et al. (2017) found that an increase of the water vapour emission index resulted in an 8% increase in contrail occurrence over North America, and the assumed reduction in EI_{IN} of 75% resulted in net changes in contrail RF (induced by switching to biofuels) that ranged from −4% to +18% among a range (5 types) of assumed ice crystal habits (shapes). These results are in contrast to those of Burkhardt et al. (2018), Bier and Burkhardt (2022) and seem to arise from consequential changes to optical depth and the balance of SW to LW forcing. Clearly, the inconsistency between the DLR and MIT results requires more study and analysis.

Teoh et al. (2022b) use the COCIP model (Schumann, 2012) to study the targeted use of SAF in the North Atlantic. They provide a useful comparison of studies in their Supplementary Information (see Table 6.1). Based on a fuel hydrogen content-based soot emission relationship (Fig. 4.11), they find a higher sensitivity and reduction potential of the radiative forcing from contrail ice crystals for lower blending ratios compared to the relative effect of changes in higher blending ratios for a 5 years period in the North Atlantic region (Fig 5.12).

Clearly, the studies are not comparable in the sense of global mean contrail RFs, since different years and domains were studied. Nonetheless, the disparities in the results show that there are significant uncertainties involved. Moreover, none of the studies consider the role of ultrafine aqueous particles (Kärcher and Yu, 2009; Kärcher, 2018 and references therein) shown in Figure 5.3.

6.3 ASSESSING THE POTENTIAL BENEFITS OF A REDUCTION IN CONTRAILS VERSUS ANY INCREASE IN CO_2 EMISSIONS

A key consideration in any prospective reduction in the RF of persistent contrails is determining whether there is any 'trade' with an increased usage of fuel, or energy, that might have consequences for CO_2 emissions from fossil fuel sources. Because of the complexity of such a comparison, this is usually assessed with a 'emissions equivalent metric', widely denoted as a "CO_2e". Emission metrics can be given in absolute terms (e.g., a physical unit of response per kg emission) or in relative terms by normalizing to a reference gas, usually CO_2. Myhre et al. (2013) summarize their purpose and usage as follows: "Metrics do not define goals and policy—they are tools that enable evaluation and implementation of multi-component policies (i.e., which emissions to abate). The most appropriate metric will depend on which aspects of climate change are most important to a particular application, and different climate policy goals may lead to different conclusions about what is the most suitable metric with which to implement that policy…"

Table 6.1 Comparison of the change in the simulated contrail properties from Teoh et al. (2022b, "This study" relative to existing studies. The percentage change in contrail properties from all the studies reported below arise from the use of SAF and/or assumption of a lower nvPM EI_n to approximate the effects of SAF.

	This study	Caiazzo et al.[18]	Burkhardt et al.[19]	Bock & Burkhardt[20]	Schumann et al.[21]
Study domain	North Atlantic	USA	Global	Global (2050)	Global
nvPM EI_n	-52%	-75%	N/A	N/A	-50%
Dist. forming persistent contrails	+5%	+8%	N/A	N/A	N/A
Contrail ice particle number	-55%	-75%	-80%	-50%	N/A
Contrail ice crystal size	+26%	+58%	N/A	N/A	N/A
$\tau_{contrail}$	-22%	-29%	-49%	-30%	-21%
Contrail cirrus coverage	-41%	N/A	-41%	-15%	-23%
Contrail net RF	-44%	(-4, +18)%*	-50%	-14%	-39%

* The reported values from Caiazzo et al.[18] likely represent the mean contrail net RF', instead of the annual mean

Arguably, the most widely used and well-known CO_2e metric is the Global Warming Potential (GWP) calculated over a particular time horizon (TH). This is essentially the integrated radiative forcing response to (commonly) a pulse release of x kg of a climate forcer over y years divided by the integrated radiative forcing from the same pulse emission of x kg CO_2 over y years. Alternatively, the analogue temperature response – the Global Temperature change Potential (GTP; Shine et al., 2005) extends the usage of the radiative response of pulse emissions to their temperature effect, via some simplified climate model response. There are many derivative natural science CO_2e metrics such as the GWP-"star" (GWP*; Allen et al., 2016), the integrated Global Temperature change Potential (iGTP; Peters et al., 2011), the Average Temperature Response (ATR; Marais et al., 2008) and econometric CO_2e metrics that seek to take a natural science metric a step further to account for monetary valuation over time, e.g., the Global Damage Potential (GDP; Kandlikar, 1995). A detailed comparison and breakdown of such metrics is beyond the scope of this report, and the reader is referred to Fuglestvedt et al. (2010) and Myhre et al. (2013) for comprehensive overviews. The core issue for aviation non-CO_2 forcers is that they represent "short lived climate forcers" (SLCFs), and their usage in CO_2e metrics is highly debated, since the original metrics of GWP, and other natural science derivative metrics, were envisaged for use with other long-lived greenhouse gases under, e.g., the Kyoto "basket".

Two relevant circumstances are envisaged in terms of a change in fuel composition that might require CO_2e assessment in the context of changing liquid hydrocarbon fuel type for aviation:

- Firstly, a reduction in the aromatic content of fossil kerosene at source in the refinery.
- Secondly, the deployment of SAF selectively in postulated contrail avoidance.

The climate response to reduced-aromatic content fossil kerosene

The first circumstance is a targeted mitigation of persistent contrails. The core issue is that in actively removing a fraction of the aromatic content, extra energy over the counterfactual is likely to be expended to do this. For a 50% reduction in naphthalene content, Faber et al. (2022) estimated this to be approximately 97 kg CO_2 per tonne of kerosene. This amounts to a 3% increase in associated CO_2 emissions. In evaluating such a "trade-off", there are a number of considerations to be made. Firstly, the associated uncertainties of the global ERF term of contrails/contrail cirrus – these will propagate into the metric term. Values of CO_2e for contrails were given by Lee et al. (2021) for a range of metrics and time horizons; no uncertainties were given for the metric values, but these were included in the discussion of Fuglestvedt et al. (2023). So, for example, the Global Warming Potential with a time horizon of 100 years (GWP100[19]) for contrail/contrail cirrus was determined to be 0.63 by Lee et al. (2021), the underlying uncertainties in the ERF (these, potentially underestimated, see above) are 0.19 to 1.08 (this ignores any uncertainties on the CO_2 ERF but these are 8 × smaller than those of the contrail/contrail cirrus ERF term). If it is assumed that a 50% reduction in naphthalene translates to a 50% reduction in soot, and it is assumed that this translates to a reduction in N_{ice} of 50%, then based on the modelling calculations of Burkhardt et al. (2018) (and acknowledging the uncertainties of this assessment, as outlined above in Section 6.2), then a 20% reduction in contrail RF might be expected for a 2% increase in CO_2. This assumes that the refinery process is powered by fossil-fuel energy. The percentage changes are for context: they cannot be used

[19] Although as outlined, CO_2e metrics for short-lived climate forcers are the subject of much debate, the GWP100 is the metric/TH universally used in present climate policy.

in themselves as an indicator of benefit – such an evaluation of potential benefit/disbenefit can only be undertaken with CO_2e metrics, or an alternative methodology that uses a climate response such as e.g., RF or temperature. Such a comparison has not been undertaken.

Clearly, from the assumptions and inherent uncertainties that have been outlined above for a potential assessment process of CO_2e (via whatever metric, a subject of discussion itself), a "favourable" climate outcome through the use of reduced aromatic content of fossil kerosene cannot be assumed.

Selective deployment of SAF for contrail avoidance

For this circumstance, there are similar, but additional constraints. In contrail avoidance, there is the potential for increased fuel burn, and, hence, increased CO_2 emissions should a mission profile be flown that is a deviation from the optimal for the stage of flight. An increase is not necessarily a given, but given the overall aim of air traffic management and pilots' priority to minimize fuel usage where possible, this is a likely outcome for some unknown portion of the time. The key point is that in contrail avoidance, this must be evaluated in the potential practice of it. If such a CO_2 increase is projected, this must be weighed against the postulated reduction in contrail forcing, and the above uncertainties over contrail forcing, choice of CO_2e metric and TH apply. In addition, since choices would be made on an individual flight basis, the projected forcing of the individual contrail should be made, not a global average. This places additional constraints on the evaluation.

Teoh et al. (2022b) have suggested that if SAF is a scarce resource, then its usage should be made in circumstances of maximum benefit, i.e., a co-benefit (over the reduction in fossil CO_2) of reducing contrails. Here the premise is that contrails could and should be avoided: however, this is a complex evaluation that is time and location-specific (Sausen et al., 2023; Shine and Lee, 2021). It cannot be assumed that the SAF usage results in zero CO_2 (fossil equivalent) emissions, since this is highly feedstock-dependent process and induced land-use change-specific (Hutchings et al., 2023; Becken et al., 2023). So, such a proposal requires a complex evaluation, on mission-by mission basis. Much of the data required for this are either unavailable (e.g., adequate real-time/validated ice-supersaturation forecasts; individual contrail forcing events) or are highly uncertain.

7. FUTURE IMPLICATIONS AND CHALLENGES

7.1 IMPACT OF FUEL REGULATIONS, E.G., REQUIREMENTS FOR THE AROMATIC CONTENT AND THEIR DIFFERENT CHEMICAL STRUCTURE

The specifications of aviation fuels, specifically ASTM D1655, ASTM D7566, and DefStan D91-091, form the principal regulatory framework for fuel quality. These specifications have been developed to ensure a safe and reliable fuel use, as aviation safety has to be guaranteed by all means. In general, aviation safety is built upon redundancy and the verification of critical system operations. Unlike other components on the plane that have redundant counterparts, the fuel lacks redundancy. Currently, Jet A/A-1 is the primary energy source used in commercial aircraft. In addition to its role in propelling the aircraft, it serves various essential functions beyond the mere release of chemical heat. Jet fuel interacts with various aircraft functions and operations, so that approved alternative fuels must operate as coolants, work seamlessly with pumps and seals, remain stable in long-term storage, and be safe under severe operability conditions.

In fact, both ASTM D1655 and DefStan D91-091 only impose restrictions on the maximum levels of aromatics and naphthalenes in fuel, without any specified lower limit on aromatic content. However, the lower aromatic content is predominantly regulated by the secondary effect of the fuel minimum density specification. The motivation behind the maximum limits and the Smoke Point measurements is to limit smoke production and the formation of carbon or soot deposition. ASTM D7566 Table 1 specifies the upper limits for the blended SAF together with the lower limit of 8%vol (using ASTM D1319, IP 156, ASTM D8305). This lower limit is set in place "to ensure that shrinkage of aged elastomer seals and associated fuel leakage is prevented" (ASTM D7566.) This 8%vol minimum limit is based on current experience and research is ongoing to identify the actual need for aromatics. World fuels surveys show that there is a certain amount of conventional Jet A-1 with aromatic content below 8% on the market. In general, this does not cause any issues as aircraft refuel with higher aromatic fuel at the next airport. Challenges may arise only when there is prolonged operation on a single fuel type with low aromatic content, as exemplified by a lubricity incident that occurred in New Zealand in the early 2000s. A recently launched world fuels survey aims at bringing more clarity concerning the quantity and characteristics of jet fuel on the market. Regarding SAF, the inclusion of reporting obligations within the RefuelEU Aviation regulation (RefuelEU, 2023) will facilitate the monitoring and provide deeper insights into the origin, quantity, and characteristics of SAF purchased by airlines.

Recently, some efforts are being made to integrate non-CO_2 climate impacts into the EU ETS (Niklaß et al., 2019). In a first step, the European Commission decided for the Monitoring, reporting and verification (MRV) of EU ETS emissions. Industrial installations and aircraft operators falling under the EU ETS are obligated to develop an approved monitoring plan to track and report their annual emissions. In this context, it has been suggested to reduce the propensity of the fuels to generate soot. The report at hand shows that the sooting propensity of a fuel strongly correlates with the H-content. Furthermore, it indicates potential benefits from lowering the maximum sulphur and aromatic limits. Considering the disproportionate impact of di-aromatics / naphthalene on soot emissions, it may be necessary to prioritize reducing their respective limits. Additionally, it might be recommended to establish a lower threshold for H content in order to manage PM emissions. Thus, concerning MRV (Monitoring Reporting Verification) activities, there is a need to enhance the test methods for fuel hydrogen content (preferably

ASTM D7171) and sooting propensity, either by improving existing methods or by restricting them to high-accuracy techniques.

With non-CO_2 impacts potentially being included in EU ETS, there might be a shift of the refineries to produce low aromatic / low sulphur fuels. Note that this would require additional energy for the refineries (cf. Section 6.3), potentially increase CO_2, and might affect supply. A prerequisite to such an action would be that an optimal aromatic content range can be identified based on a detailed impact assessment. Subsequently, it would be possible to align the aromatic limits for both conventional jet fuels and SAF blends, necessitating the implementation of a lower aromatic limit for conventional fuels.

Furthermore, it is crucial to perform empirical investigations to assess the impact of different technologies, such as severe hydrotreatment and extractive distillation, on reducing aromatic content. These studies should consider various factors, including composition, sooting propensity, additional energy requirements, and economic considerations. It is necessary to comprehend the techno-economic consequences of lowering the aromatic limits, along with identifying the most appropriate technological solution (see Section ¤). Additionally, there is a need for further research to explore the effects of increased levels of isomerization on sooting propensity. Given that severe hydrotreatment may pose challenges related to cold flow properties, it is imperative to incorporate isomerization as well. In summary, it is crucial to undertake research that investigates the consequences of reducing the aromatic content to 8%vol, while ensuring the operational safety of fuels, especially in legacy aircraft. The preservation of safety remains the foremost and uncompromising prerequisite.

7.2 IMPACT ON TECHNICAL REQUIREMENTS, E.G. AROMATIC IMPACT ON SEALS AND ELASTOMERS; SULPHUR IMPACT ON LUBRICATION

In the years from 2008 to 2010 a series of studies (like the EASA SULPHUR or the US PARTNER program) have been performed on low aromatic / low sulphur fuels. Low aromatic/low sulphur fuels have been reported to have the following potentially deleterious effects (Miller et al., 2010):

- Poor lubricity, which can cause pump failure
- Elastomer compatibility issues, potentially causing leakages
- Poor electrical conductivity, risk of static charge build-up.

Lubricity as well as poor electrical conductivity can be improved with additives. However, older technology elastomer (e.g., nitrile rubber) compatibility might remain of an issue for low sulphur/ultra-low aromatic fuels. Newer fluoroelastomers could avoid this problem provided the operational range of temperature can be covered. However, open questions remain on understanding of the effect a reduction of aromatics will have on a variety of aged elastomers.

Recent research in the JETSCREEN (2021) program showed that further work needs to be done to determine the impact of ultra-low sulphur/aromatic fuels on fuel system gauging accuracy and volume-limited flight range. This is difficult as the systems vary from aircraft to aircraft.

7.3 INTERACTION WITH CLIMATE-OPTIMIZED FLIGHT TRAJECTORIES

The combination of climate-friendly flight routing and the targeted use of SAF has been investigated in a recent study by Teoh et al. (2022a). As long as there is a limited availability of SAF, it might be advantageous to use the SAF in flights with strongly warming contrail circumstances. In addition to the lower CO_2 footprint of SAF from the life cycle analysis, this could augment the effect of the reduced climate impact from reduced soot emissions and reduced contrail cover, should the (poorly understood) effect of ultrafine aerosol particles not result in an increase at low temperatures, well below contrail threshold conditions – a condition modelled but not yet observed. In their numerical study, Teoh et al (2022a) investigate the contrail and CO_2 effect of a 1% SAF blending evenly distributed around the fleet or distributed in a 50% blend to the flights with strongly warming contrails (Figure 7.1). They claim that the total climate benefit from CO_2 and contrails can be strongly enhanced, when SAF is used in a targeted way dedicated to strongly warming contrail regions. Their study does not treat the effect of SAF on UAPs. Hence the combination of measures such as climate-friendly air traffic routing and SAF could enhance the climate gain if ultrafine aerosol particles are shown to be unimportant. However, before this strategy can become effective, considerable challenges have to be overcome (see also Shine and Lee, 2021):

- Operational weather forecasts have to much better predict water vapour at cruise altitude for a better prediction of ice supersaturated regions, where contrails would be strongly warming during their lifetime (Gierens et al., 2020).
- It is necessary to show in demonstration for real flight traffic that persistent contrail can be avoided by operational flight guidance, see Sausen et al. (2023) for a first attempt.
- Procedures for planning and guiding aircraft along climate-friendly trajectories have to be established (Molloy, 2022).

More basic than the challenges outlined above, is the low confidence (Lee et al., 2021) in the size of the overall effects of contrail cirrus on climate, as outlined in Section 6.2, reinforced by recent work that indicates the smaller climate sensitivity of contrail cirrus than that of CO_2.

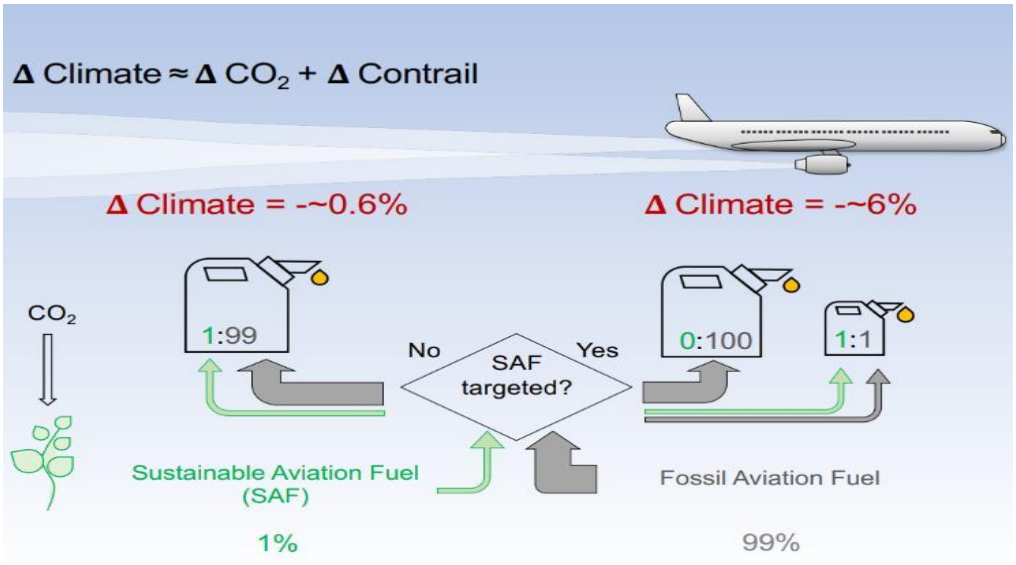

Figure 7.1 Contrail and CO_2 effect of a 1% SAF blending evenly distributed around the fleet or distributed in a 50% blend to the flights with strongly warming contrails. The total climate benefit from CO_2 and contrails can be enhanced by a factor of up to 10, when SAF is burned in strongly warming contrail regions (from Teoh et al., 2022a).

8. FUTURE RESEARCH OPPORTUNITIES

To support the future development of refineries and regulations, more evidence on the impact of different conventional jet fuel sulphur and aromatic reduction technologies (hydrotreatment, extractive distillation in conversion and hydroskimming type of refineries) is required. The impact of the processing technology on fuel composition and sooting propensity has to be evaluated especially for ultra-low sulphur / aromatic conventional fuels. Furthermore, while proven for SAF blends (Voigt et al. 2021), the effectiveness of conventional fuel sulphur/aromatic reduction (increased H content) on reducing contrail induced climate impacts should be quantified experimentally.

Further research is needed to understand if the lower aromatics limit (8% for SAF blends) can be reduced. Furthermore, it should be assessed if aromatic compounds can be replaced by cyclo-alkanes or lower sooting fuel components, while warranting the drop-in capability of the fuels.

The emissions from engines with Lean Burn combustors and the resulting impact on contrail formation should be investigated for both, kerosene and SAF. Thereby, the non-volatile and total particle number as well as the ice crystal number in contrails need to be measured. Data in the engine emission database suggest a strong reduction in non-volatile particulate matter in the lean burn mode tested in the typical LTO cycle. Theoretical considerations by Kärcher (2018) suggest that in the low soot regime in the absence of soot, co-emitted volatile or semi-volatile particles might take over and act as nuclei for ice crystals in contrails. More work is required to explore contrail formation in the low soot regime on kerosene and SAF.

As long as the production of SAF is low, conventional kerosene can be hydrotreated or hydrocracked with hydrogen in a high-pressure environment to enhance the fuel's hydrogen content and to reduce aromatics and sulphur. This affects the fuel composition in terms of mono- and polycyclic aromatics and paraffins and therefore also soot particle emissions. Hydrotreatment and hydrocracking increases the fuel's hydrogen content which might be beneficial for soot particle formation. In particular, reducing the naphthalene content has little effect on the fuel's bulk properties (i.e. reduced risk of being outside specifications requirements after hydrotreatment) but a strong impact on soot emissions reductions and ice crystal concentration reduction (Voigt et al. 2021). As the treatment and the production processes of the hydrotreated or hydrocracked fuels are different than the production of biofuels and synthetic fuels, the exact change in fuel composition and molecular structure is not known. Ground and flight tests as well as modelling are required to assess the resulting impact on particle emissions and the effects on contrails. The impact assessment also requires to consider the enhanced energy consumption for the hydrogen production for the hydrotreatment.

In the future, hydrogen as a fuel might gain importance for aviation, either in the form of direct hydrogen combustion or in fuel cells or hybrid-electric propulsion systems. Burning hydrogen has the great advantage that it does not release any CO_2 emissions in contrast to burning hydrocarbon fuels. Hence the use of hydrogen supports the decarbonization of the aviation sector. However, research is needed to investigate the impact of hydrogen on the non-CO_2 effects. So far only preliminary studies on the non-CO_2 effects of hydrogen powered aircraft exist, e.g., Marquart et al. (2001), Ström and Gierens (2002) and Marquart et al. (2005).

Hydrogen combustion happens in a hot flame, which mainly produces water vapour. And as soon as nitrogen from the air is involved, that would lead to the formation

of NO_x, which is dependent on the flame temperature. Also, as a pure hydrogen fuel does not contain hydrocarbons or sulphur, the formation of soot particles and volatile sulphate aerosol will be reduced to near zero. So, contrail formation takes place in the "soot-poor" regime. Inmixing of ambient aerosol will probably lead to ice particle formation possibly at lower number concentrations compared to kerosene, the ice crystals then grow to larger sizes, sediment faster, have a lower lifetime and thereby eventually a smaller climate impact. Still, other semi-volatile aerosol particles could be emitted at high number concentrations and lubrication oil particles may condense and could act as ice nuclei. Also, ions will form in the hot combustion flame promoting ion-induced particle nucleation again potentially acting as ice nuclei. Finally, unknown and unexplored processes could occur in the hydrogen combustion process, leading to particle formation and impacting contrail formation. In summary, these processes are largely unknown and have to be investigated in order to allow for the recommendation of hydrogen combustion. As the interaction between the gases and the particles is highly complex and in non-equilibrium, observations on ground and at cruise altitudes are required to evaluate contrail formation processes and their climate impact.

Fuel cells also do not emit CO_2 and are therefore advantageous for the climate (Gierens, 2021). Fuel cell emissions consist of a saturated water / water vapour mixture at a given temperature significantly colder than the hot exhaust from combustors. Also, for fuel cells, particle emissions are unknown but cannot be excluded. The water from a fuel cell exhaust will be sprayed in the atmosphere at the fuel cell outlet and could form larger droplets. In addition, the colder temperature of the saturated water-vapour mix lead to very high water-supersaturation and can enable the spontaneous nucleation of droplets out of the gas phase, a process which does not occur naturally in the atmosphere. The spontaneous nucleation could enable high ice particle number concentrations at low temperatures and humid conditions, the occurrence frequency of these conditions remain to be investigated. All these processes interact and are poorly understood and neither constrained by theory nor observations. Large and comprehensive research efforts are required to investigate these phenomena in order to assess the climate impact from hydrogen combustion or fuel cells.

9. CONCLUSIONS

- Aviation contributes via CO_2 and non-CO_2 effects to climate change. Contrails (linear contrails and contrail cirrus) are part of the non-CO_2 effects and may contribute significantly to the current aviation effective radiative forcing (ERF). Unfortunately, the uncertainties regarding the radiative forcings and effective radiative forcings of the non-CO_2 effects are much larger than those of CO_2 effects, and the uncertainties due to contrails and contrail cirrus dominate the total uncertainty of all aviation sources. This situation becomes aggravated (i.e., the uncertainty becomes larger) when going down the cause-effect chain from radiative forcing to the actual climate impacts, that is for instance, the contribution to global warming (i.e., the 'efficacy' of contrail cirrus).
- The formation of contrails (short-lived ones and persistent ones) follows the thermodynamic theory of Schmidt and Appleman. The formation is a result of isobaric mixing of two airmasses, the hot and humid exhaust gases from the engines and the ambient air. Such a mixing can transiently lead to supersaturated conditions with respect to water, which then leads to condensation of droplets and, if the ambient atmosphere is sufficiently cold, to freezing, and, hence, to contrail formation. Aerosol particles, which serve as condensation nuclei, are always present in the atmosphere and the exhaust, and thus aerosols are not explicitly mentioned in the Schmidt-Appleman theory. Their presence is assumed as given.
- Contrail persistence requires the ambient air to be in ice supersaturated state, or nearly so. Ice supersaturation is frequent in the upper troposphere close to the tropopause. It is a condition where the exchange of water molecules between the crystal surfaces and the ambient air has a net direction onto the crystals, which thereby grow. For reference, we mention that the formation of natural cirrus clouds (i.e. ice clouds) needs quite substantial ice supersaturation (several 10%).
- While the Schmidt-Appleman criterion only decides whether a contrail is formed in a given situation or not, it says nothing about contrail microphysical and optical properties. The most important properties of a persistent contrail are the concentration of ice crystals after the so-called vortex phase and the lifetime and growth of its areal coverage. The concentration of ice crystals depends on the number emission index of soot (in the soot-rich regime) and of volatile particulate emissions (in the soot-poor regime) and thus the type of fuel. It depends furthermore on how many of the soot particles (in the soot-rich regime) get activated (i.e. act as droplet condensation nuclei), which in turn depends on the ambient conditions of temperature and water vapour partial pressure (or, equivalently, relative humidity) and the contrail factor G, that is in turn, the ambient pressure together with the fuel's energy specific emission index and the overall propulsion efficiency. It depends further on the downward distance the pair of wing vortex tubes, in which the ice crystals are initially caught, sink up to their dissolution (vortex phase), since this downward motion causes heating and partial sublimation of the ice crystals. The horizontal spreading of a contrail depends on vertical shear of the horizontal winds. The lifetime depends on the general synoptic weather situation. That is, fuel and its properties (e.g. chemical composition, aromatic content) has an almost direct effect on the number concentration of ice crystals, but only a quite indirect effect on a contrail's lifetime.
- Radiative properties of persistent contrails depend primarily on day or night-time conditions (balance of SW vs LW) and in addition, crystal size, shape, and

number density, which in turn depend inter alia on the fuel type and composition. For current levels of soot emissions, the number density of soot particles first determines the initial number of ice crystals. The latter gets then modified by adiabatic compression, heating, and partial sublimation in the vortex tubes behind an aircraft. The more ice crystals survive, the smaller they are, and vice versa. For a given ice mass, larger crystals imply smaller optical thickness (less interaction with radiation) and higher crystal fall speeds (thus a shorter lifetime in microphysically controlled situations[20]), thus less contribution to the overall radiative forcing (RF) and effective radiative forcing (ERF).

- Both ground test and in-flight experiments have shown that fuels with reduced aromatics and naphthalene contents emit fewer soot particles. As long as this still happens in the so-called "soot rich" regime, this implies lower initial droplet and ice crystal number density and thus leads to contrails with less but larger ice crystals. If soot emissions are reduced down into the so-called "soot-poor" regime, volatile exhaust particles and ambient particles can start to contribute to droplet and ice formation.[21]
- There is a trade-off between the reduced contrail ERF and the additional energy necessary resulting in greater LCA CO_2 emissions for production of SAF which has lower aromatic and naphthalene content. (This is critical, if SAF is conventionally produced). Whether this is beneficial or not depends on the state of knowledge of contrail forcing (known with only low confidence), the increased CO_2, and the CO_2e metric and time-horizon used to perform the 'trade off' calculation.
- Most global modelling of contrail climate impacts so far has been performed for standard kerosene-based contrails. Only a few studies on SAF-based contrails are currently available in the literature. It must be noted, that these studies do not explicitly represent engines, the fuels and the combustion processes. Not even the soot emission is explicitly treated. Instead, an initial ice crystal number concentration is assumed, and the transition from kerosene to SAF is simply treated as a reduction by a chosen factor of the initial ice crystal number concentration, in agreement to the results of the measurement campaigns. Essentially, these models show that lowered initial ice crystal number leads to lower radiative forcing and the statement, that low-aromatic fuel would lower the contrail climate impact is merely a plausible interpretation of these modelling results but not a firm proof. To strengthen the plausibility requires a better understanding which compounds in the fuel cause the soot, and how the soot formation actually proceeds.
- Aviation safety has to be ensured by all means. Currently, an 8%vol minimum of aromatics in blended SAF fuels is in place in order to prevent shrinkage of elastomer seals. This limit is based on current experience. There are further issues with low aromatic/low sulphur fuel linked to poor lubricity and poor electrical conductivity.
- Experiments show that the propensity of a fuel to form soot is correlated primarily with its H-content.
- Targeted use of SAF for the mitigation of contrail climate effects, perhaps in combination with climate-friendly routing needs a more complete understanding of the contrail formation of such fuels, reliable prediction of ice supersaturated regions, a statistically robust demonstration (i.e. many flight experiments) that persistent contrails can indeed by avoided in actual flight

[20] See Section 5.6 for details.
[21] This regime is so far experimentally not widely explored and no published results are currently available.

practice and, last but not least, the establishment of rules and regulations for such a practice in the daily business.

Can consequences for the fuel industry be drawn?

This report makes clear that selectively reducing some fuel constituents that lead to the formation of soot in the exhaust leads to lower number concentrations of ice crystals in the contrail, at least initially, as long as the resulting emission index for the number of soot particles remains in the soot-rich regime, that is, as long as more than 10^{14} soot particles are emitted for each kg fuel burnt. Then, the initial reduction of ice crystals numbers is proportional to the reduction of soot particle number. However, the final reduction of ice crystal number after the vortex phase is lower and the eventual climate benefit for a single case depends on factors such as ambient temperature and contrail dissipation mechanism. Thus, to estimate how much a reduction of, say, fuel aromatics, benefits climate, either in terms of RF or ERF is not a simple calculation. Too many processes are involved, starting with the uncertainty at the very beginning, namely the soot formation itself. The effect of an aromatics reduction by x% on $EI_{n,soot}$ cannot be calculated simply, since it depends on the combustion process and other factors. The quoted measurements show lower soot numbers for lower aromatics, but in a complicated way. Then, the processing of initial ice crystals in wing vortices depends in a complicated way on a number of factors, including aircraft size, speed, ice size distribution, air temperature, etc. The later fate of the contrail depends primarily on the meteorological situation. Thus, even in the simpler and better-known soot-rich regime there are still difficult problems to be overcome that require better theories (soot formation), measurements (to confirm the theories) and global modelling of contrails to catch the tremendous meteorological variability that affects contrail evolution and their individual radiative effect. Even this latter effect depends not only on N_{ice} but also size distribution and crystal habit (shape), which may be changed with SAF/low aromatic fuel usage.

The uncertainties and difficulties are even larger in the soot-poor regime, for which only preliminary measurement results exist so far. Theory predicts that ice crystal numbers can even rise with decreasing soot emissions, since this allows ultrafine aqueous particles in the exhaust and ambient aerosol to take over the role of condensation nuclei from the soot particles. The radiative consequences of such a strong soot reduction is not known so far, since corresponding simulations with global models do not exist. Further measurements need to be made and the results incorporated in such models before they can be used for such a purpose. Ideally global models of several independent groups should be used, in order to get an estimate of the uncertainty of the results.

10. LIST OF ACRONYMS

AAFEX	NASA Measurement Campaign
ACCESS	NASA Measurement Campaign
ACTA	Automatic Contrail Tracking Algorithm
APEX	NASA Measurement Campaign
ASTM	original meaning: American Society for Testing and Materials; actually an international organisation
ATJ	Alcohol-To-Jet
ATR	Average Temperature Response
BOCLE	Ball-on-Cylinder Lubricity Evaluator
CAEP	ICAO Committee on Aviation Environmental Protection
CHJ	Synthesized Kerosine from Hydrothermal Conversion of Fatty Acid Esters and Fatty Acids
CoCiP	Contrail-Cirrus Prediction model
CRC	Coordinating Research Council
DefStan	Defence Standard
EI	Emission Index, EI_X: Emission index of species X
ECLIF1/2	Measurement campaigns
ERF	Effective Radiative Forcing
ETS	Emission Trading System
FT	Fischer-Tropsch
GCxGC	Comprehensive Two-Dimensional Gas Chromatography
GDP	Global Damage Potential
GTP	Global Temperature change Potential, also iGTP: integrated GTP
GWP	Global Warming Potential, also GWP*, a derivative of GWP
HEFA	Hydroprocessed Esters and Fatty Acids
ICAO	International Civil Aviation Organisation
IPCC	Intergovernmental Panel on Climate Change
ISSR	Ice SuperSaturated Region

LCA	Life-Cycle Analysis
LTO	Landing Take-Off (cycle)
MSEP	Micro-Separometer
MRV	Monitoring Reporting Verification
ND-MAX	Measurement campaign (NASA/DLR Multidisciplinary Airborne Experiment)
NMR	Nuclear Magnetic Resonance
nvPM	non-volatile Particulate Matter, vPM: volatile PM
PAH	Polycyclic Aromatic Hydrocarbons
PM	Particulate Matter
RF	Radiative Forcing
RQL	Rich-Quench-Lean (special kind of combustion)
SAF	Sustainable Aviation Fuel
SIP	Synthesized Iso-Paraffins
SLCF	Short-Lived Climate Forcers
SPK	Synthesized Paraffinic Kerosene
SPK/A	Synthesized Kerosine with Aromatics
VOC	Volatile Organic Compounds
YSI	Yield Sooting Index

11. REFERENCES

Allen M., J. Fuglestvedt J., K.P. Shine, A. Reisinger, R.T. Pierrehumbert, and P.M. Forster, 2016: New use of global warming potentials to compare cumulative and short-lived climate pollutants. *Nature Climate Change 6*, 773–776. https://doi.org/10.1038/nclimate2998.

Altjetfuels, 2015: Federal Aviation Administration National Alternative Jet Fuels Test Database. Available at: https://altjetfuels.illinois.edu/

Appleman, H., 1953: The formation of exhaust condensation trails by jet aircraft. *Bull. Amer. Meteorol. Soc. 34*, 14-20.

Arnold, F., J. Curtius, B. Sierau, V. Bürger, R. Busen, and U. Schumann, 1999: Detection of Massive Negative Chemiions in the Exhaust Plume of a Jet Aircraft in Flight. *Geophys. Res. Lett. 26*, 1577–1580. https://doi.org/10.1029/1999GL900304.

Arnold, F., A. Kiendler, V. Wiedemer, S. Aberle, and T. Stilp, 2000: Chemiion concentration measurements in jet engine exhaust at the ground: Implications for ion chemistry and aerosol formation in the wake of a jet aircraft. *Geophys. Res. L. 27,* 1723-1726.

Arrowsmith S., D.S. Lee, B. Owen, J. Faber, L. van Wijngaarden, O. Boucher, A. Celikel, R. Deransy, J. Fuglestvedt, J. Laukia, M. Tronstad Lund, R. Sausen, M. Schaefer, A. Skowron, S. Stromatas, and A. Watt, 2020: Updated analysis of the non-CO_2 climate impacts of aviation and potential policy measures pursuant to EU Emissions Trading System Directive Article 30(4). EASA Report to the European Commission. https://www.easa.europa.eu/en/downloads/120860/en.

ASTM, 2022: D1655-22a, Standard Specification for Aviation Turbine Fuels. West Conshohocken, PA: ASTM International.

ASTM D02 Committee. Test Method for Smoke Point of Kerosene and Aviation Turbine Fuel. West Conshohocken, PA: ASTM International. https://doi.org/10.1520/D1322-22.

Barrett, R.H. and R. Speth, 2021: Federal Aviation Administration; ASCENT Project 039: Naphthalene Removal Assessment Project; Final-Report. https://s3.wp.wsu.edu/uploads/sites/2479/2022/10/ASCENT-Project-039-Final-Report.pdf.

Bauder, U., C. Hall, and B. Rauch, 2023: DLR SimFuel Plattform. https://simfuel.dlr.de/, accessed: 06 March 2023.

Becken S., B. Mackey, and D.S. Lee, 2023: Implications of preferential access to land and clean energy for Sustainable Aviation Fuels. *Science of the Total Environment 866*, 163883. https://doi.org/10.1016/j.scitotenv.2023.163883.

Bickel, M., M. Ponater, L. Bock, U. Burkhardt, and S. Reineke, 2020: Estimating the Effective Radiative Forcing of Contrail Cirrus. *J. Climate, 33*, 1991-2005.

Bickel, M., 2023: Climate Impact of Contrail Cirrus. PhD thesis, Fakultät für Physik, Ludwig-Maximilians-Universität München, Germany. DLR Forschungsbericht 2023-14, 135p, ISSN 1434-8454, ISRN DLR-FB-2023-14, DOI: 10.57676/mzmg-r403.

Bier, A., U. Burkhardt, and L. Bock, 2017: Synoptic control of contrail cirrus lifecycles and their modification due to reduced soot number emissions. *J. Geophys. Res. 122*, 11584–11603. doi: 10.1002/2017JD027011.

Bier, A. and U. Burkhardt, 2019: Variability in contrail ice nucleation and its dependence on soot number emissions. *J. Geophys. Res. 124*, 3384-3400. doi: 10.1029/2018JD029155.

Bier, A., and U. Burkhardt, 2022: Impact of parametrizing microphysical processes in the jet and vortex phase on contrail cirrus properties and radiative forcing. *J. Geophys. Res. 127*, 1-29. doi: 10.1029/2022JD036677.

Blakey, S., B. Rauch, A. Oldani, and T. Lee, 2022: Advanced Fuel Property Data Platform: Overview and Potential Applications. In: *Front. Energy Res. 10*, 771325. DOI: 10.3389/fenrg.2022.771325.

Bock, L. and U., Burkhardt, 2016: Reassessing properties and radiative forcing of contrail cirrus using a climate model. *J. Geophys. Res. 121*, 9717-9736. doi: 10.1002/2016JD025112.

Bock, L. and U. Burkhardt, 2019: Contrail cirrus radiative forcing for future air traffic. *Atmos. Chem. Phys. 19*,
8163-8174. doi: 10.5194/acp-19-8163-2019.

Bräuer, T., C. Voigt, D. Sauer, S. Kaufmann, V. Hahn, M. Scheibe, H. Schlager, G.S Diskin, J.B. Nowak, J.P. DiGangi, F. Huber, R.H. Moore, and B.E. Anderson, 2021: Airborne Measurements of Contrail Ice Properties—Dependence on Temperature and Humidity. *Geophys. Res. Lett. 48*, e2020GL092166 doi: 10.1029/2020GL092166.

Bräuer, T., C. Voigt, D. Sauer, S. Kaufmann, V. Hahn, M. Scheibe, H. Schlager, F. Huber, P. Le Clercq, R.H.
Moore, and B.E. Anderson, 2021: Reduced ice number concentrations in contrails from low-aromatic biofuel
blends. *Atmos. Chem. Phys. 21*, 16817–16826. doi: 10.5194/acp-21-16817-2021, 2021.

Brem, B.T., L. Durdina, F. Siegeris, P. Beyerle, K. Bruderer, T. Rindlisbacher, S. Rocci-Denis, M.G. Andac, J. Zelina, O. Penanhoat, and J. Wang, 2015: Effects of Fuel Aromatic Content on Nonvolatile Particulate Emissions of an In-Production Aircraft Gas Turbine. *Environ. Sci. Technol. 49*, 13149-13157.

Brink, L. ,2020: Modeling the impact of fuel composition on aircraft engine NOx, CO and soot emissions [S.M. thesis,Massachusetts Institute of Technology]; 2021. DSpace@MIT. https://hdl.handle.net/1721.1/129181.

Brock, C. A., F. Schröder, B. Kärcher, A. Petzold, R. Busen, and M. Fiebig, 2000: Ultrafine Particle Size Distributions Measured in Aircraft Exhaust Plumes. *J. Geophys. Res. 105 (D21)*, 26555–26568. https://doi.org/doi:10.1029/2000JD900360.

Burkhardt, U., L. Bock, and A. Bier, 2018: Mitigating the contrail cirrus climate impact by reducing aircraft soot number emissions. *npj Climate and Atmospheric Science 37*, 1-7. doi: 10.1038/s41612-018-0046-4.

Busen, R., and U. Schumann, 1995: Visible contrail formation from fuels with different sulfur contents. *Geophys. Res. L. 22*, 1357-1360.

Caiazzo, F., A. Agarwal, R.L. Seth, and S.R.H. Barrett, 2017: Impact of biofuels on contrail warming: *Environ. Res. Lett. 12*, 114013. DOI 10.1088/1748-9326/aa893b.

Cain, J., M.J. DeWitt, D. Blunck, E. Corporan, R. Striebich, D. Anneken, C. Klingshirn, W.M. Roquemore, R. Vander Wal, 2013: Characterization of Gaseous and Particulate Emissions from a Turboshaft Engine Burning Conventional, Alternative, and Surrogate Fuels. *Energy Fuels 27*, 2290-2302.

Chauvigné, A., O. Jourdan, A. Schwarzenboeck, C. Gourbeyre, J.-F. Gayet, C. Voigt, H. Schlager, S. Kaufmann, S. Borrmann, S. Molleker, A. Minikin, T. Jurkat, and U. Schumann, 2018: Statistical analysis of contrail to cirrus evolution during the Contrail and Cirrus Experiment (CONCERT). *Atmos. Chem. Phys. 18*, 9803-9822. doi: 10.5194/acp-18-9803-2018, 2018.

Chen, C.C. and A. Gettelman, 2013: Simulated radiative forcing from contrails and contrail cirrus. *Atmos. Chem.*
Phys. 13, 12525–12536. doi: 10.5194/acp-13-12525-2013.

Corporan, E., T. Edwards, L. Shafer, M.J. DeWitt, C. Klingshirn, S. Zabarnick, Z. West, R. Striebich, L. Graham, and J. Klein, 2011: Chemical, Thermal Stability, Seal Swell, and Emissions Studies of Alternative Jet Fuels. *Energy Fuels 25*, 955-966.

Corti, T. and T. Peter, 2009: A simple model for cloud radiative forcing. *Atmos. Chem. Phys. 9*, 5751-5758. doi: 10.5194/acp-9-5751-2009.

Demirdjian, B., et al., 2007: Heterogeneities in the microstructure and composition of aircraft engine combustor soot: Impact on the water uptake. *J. Atmos. Chem. 56*, 83-103. doi: 10.1007/s10874-006-9043-9.

Energy Institute; QinetiQ ,2014: The Quality of Aviation Fuel Available in the United Kingdom Annual Survey 2014. London: Energy Institute.

EASA. 2010: Reduction of sulphur limits in aviation fuel standards (SULPHUR). Authors: M. Miller, P. Brook, and C. Eyers. Contract number R.2008.C11.

EASA, 2023: ICAO Aircraft Engine Emissions Databank 02/2023. https://www.easa.europa.eu/en/domains/environment/icao-aircraft-engine-emissions-databank. Published 02/2023. Accessed 06 March 2023.

Faber J., J. Király, D.S. Lee, B. Owen, and A. O'Leary, 2022: Potential for reducing aviation non-CO_2 emissions through cleaner jet fuel. CE-Delft, 22.210410.022. https://cedelft.eu/publications/potential-for-reducing-aviation-non-co2-emissions-through-cleaner-jet-fuel/.

Forster, P., T. Storelvmo, K.Armour, W. Collins, J.-L. Dufresne, D. Frame, D.J. Lunt,T. Mauritsen, M.D. Palmer, M. Watanabe, M. Wild, and H. Zhang, 2021: The Earth's Energy Budget, Climate Feedbacks, and Climate Sensitivity. In Climate Change 2021: The Physical Science Basis. Contribution of Working Group I to the Sixth Assessment Report of the Intergovernmental Panel on Climate Change [Masson-Delmotte,V., P. Zhai, A. Pirani, S.L. Connors, C. Péan, S. Berger, N. Caud, Y. Chen, L. Goldfarb, M.I. Gomis, M. Huang, K. Leitzell, E. Lonnoy, J.B.R. Matthews, T.K. Maycock, T. Waterfield, O. Yelekçi, R. Yu, and B. Zhou (eds.)]. Cambridge University Press, Cambridge, United Kingdom and New York, NY, USA, pp. 923–1054, doi:10.1017/9781009157896.009.

Freudenthaler, V., F. Homburg, and H. Jäger, 1995: Contrail observations by ground-based scanning lidar: cross-sectional growth. *Geophys. Res. L. 22*, 3501-3504.

Fuglestvedt, J.S., K.P. Shine, T. Berntsen, J. Cook, D.S. Lee, A. Stenke, R.B. Skeie, G.J.M. Velders, and I.A. Waitz, 2010: Transport impacts on atmosphere and climate: Metrics. *Atmos. Environ. 44*, 4648–4677. doi: 10.1016/j.atmosenv.2009.04.044.

Fuglestvedt, J., M.T. Lund, S. Kallbekken, B.H. Samset, and D.S. Lee, 2023: A "greenhouse gas balance" for aviation in line with the Paris Agreement. WIREs Clim. Change. e839. https://doi.org/10.1002/wcc.839.

Gayet, J.-F., V. Shcherbakov, C. Voigt, U. Schumann, D. Schäuble, P. Jessberger, A. Petzold, A. Minikin, H. Schlager, O. Dubovik, and T. Lapyonok, 2012: The evolution of microphysical and optical properties of an A380 contrail in the vortex phase. *Atmos. Chem. Phys. 12*, 6629-6643. doi: 10.5194/acp-12-6629-2012, 2012.

Gierens, K., U. Schumann, M. Helten, H.G.J. Smit, and A. Marenco, 1999: A distribution law for relative humidity in the upper troposphere and lower stratosphere derived from three years of MOZAIC measurements. *Ann. Geophys. 17*, 1218-1226.

Gierens, K. and P. Spichtinger, 2000: On the size distribution of ice-supersaturated regions in the upper troposphere and lowermost stratosphere. *Ann. Geophys. 18,* 499-504.

Gierens, K. and S. Brinkop, 2012: Dynamical characteristics of ice supersaturated regions. *Atmos. Chem. Phys. 12*, 11933-11942.

Gierens, K., P. Spichtinger, and U. Schumann, 2012: Ice supersaturation. In: Atmospheric Physics. Background - Methods - Trends. U. Schumann (Ed.). Springer, Heidelberg, Germany. Ch. 9, pp. 135-150.

Gierens, K., et al., 2016: Condensation trails from biofuels/kerosene blends scoping study, ENER/C2/2013-627, chapter 1.3.

Gierens, K., S. Matthes, and S. Rohs, 2020: How Well Can Persistent Contrails Be Predicted? *Aerospace 7*, 169. doi:10.3390/aerospace7120169.

Gierens, K., 2021: Theory of Contrail Formation for Fuel Cells. *Aerospace 8*, 164. doi:10.3390/aerospace8060164.

Hadaller, O.J. and J.M. Johnson, 2006. World Fuel Sampling Program. Final Report. CRC Report No. 647. COORDINATING RESEARCH COUNCIL, INC.

Harper, J., E. Durand, P. Bowen, D. Pugh, M. Johnson, and A. Crayford, 2022:. Influence of alternative fuel properties and combustor operating conditions on the nvPM and gaseous emissions produced by a small-scale RQL combustor. *Fuel 315*, 123045. DOI: 10.1016/j.fuel.2021.123045.

Heyne, J., B. Rauch, P. Le Clercq, and M. Colket, 2021: Sustainable aviation fuel prescreening tools and procedures. *Fuel* 290, 120004. DOI: 10.1016/j.fuel.2020.120004.

Heymsfield, A., R.P. Lawson, and G.W. Sachse, 1998: Growth of ice crystals in a precipitating contrail. *Geophys. Res. Lett. 25*, 1335–1338. doi: 10.1029/98GL00189.

Hofer, S., K. Gierens, and S. Rohs, 2024: Contrail formation and persistence conditions for alternative fuels. *Meteorol. Z, in press.*

Hutchings G., A. Almena, W. David, G. Gratton, D.S. Lee, M.M. Maroto-Valer, M. McManus, A. Morton, M. Muskett, N. Kumar, J. Pickett, M. Pourkashanian, M. Rosseinsky, and A.W. Rutherford, 2023: Net zero aviation fuels – resource requirements and environmental impacts. Policy briefing. February 2023 DES8040, ISBN: 978-1-78252-632-2, The Royal Society, London.

ICAO, 2021: Annex 16 "International standards and recommended practices, Environmental protection", Volume II "Aircraft engine emissions", 4thEdition.

IPCC, 1990: Climate Change — The IPCC Scientific Assessment. J.T. Houghton, G.J. Jenkins, and J.J. Ephraums (editors). Cambridge University Press, Cambridge, 365 p.
https://www.ipcc.ch/site/assets/uploads/2018/03/ipcc_far_wg_I_full_report.pdf

Irvine, E. A., B. J. Hoskins, and K. P. Shine, 2012: The dependence of contrail formation on the weather pattern and altitude in the North Atlantic. *Geophys. Res. Lett. 39*, L12802, doi:10.1029/2012GL051909.

Irvine, E. A., B. J. Hoskins, and K. P. Shine, 2014: A Lagrangian analysis of ice-supersaturated air over the North Atlantic. *J. Geophys. Res. Atmos. 119*, 90–100, doi:10.1002/2013JD020251.

Jensen, E.J., O.B. Toon, S. Kinne, G.W. Sachse, B.E. Anderson, K.R. Chan, C.H. Twohy, B.W. Gandrud, A.J. Heymsfield, and R.C. Miake-Lye., 1998: Environmental conditions required for contrail formation and persistence. *J. Geophys. Res. 103*, 3293-3308.

JETSCREEN, 2021: JET Fuel SCREENing and Optimization. H2020 Grant agreement ID: 723525, https://cordis.europa.eu/project/id/723525.

Kandlikar, M., 1995: The relative role of trace gas emissions in greenhouse abatement policies. *Energy Policy 23*, 879–883.

Kärcher, B., R.P. Turco, F. Yu, M.Y. Danilin, D.K. Weisenstein, R.C. Miake-Lye, and R. Busen, 2000: New Particle Formation in Aircraft Exhaust Plumes. *J. Aerosol Science 31*, 170–71. https://doi.org/10.1016/S0021-8502(00)90177-0.

Kärcher, B., 2016: The importance of contrail ice formation for mitigating the climate impact of aviation. *J. Geophys. Res. 121*, 3497–3505. doi: 10.1002/2015JD024696

Kärcher, B., 2018: Formation and radiative forcing of contrail cirrus. *Nat. Commun. 9*, 1824. doi: 10.1038/s41467-018-04068-0.

Kärcher, B., and F. Yu, 2009: Role of aircraft soot emissions in contrail formation. *Geophys. Res. L. 36,* L01804. doi: 10.1029/2008GL036694.

Kärcher, B., U. Burkhardt, A. Bier, L. Bock, and I.J. Ford, 2015: The microphysical pathway to contrail formation. *J. Geophys. Res. Atmos. 120*, doi: 10.1002/2015JD023491.

Kärcher, B. and C. Voigt, 2017: Susceptibility of contrail ice crystal numbers to aircraft soot particle emissions. *Geophys. Res. L. 44*, 8037-8036. doi: 10.1002/2017GL074949.

Kärcher, B., J. Kleine, D. Sauer, and C. Voigt, 2018: Contrail formation: Analysis of sublimation mechanisms. *Geophys. Res. Lett.*, doi: 10.1029/2018GL079391.

Kathrotia, T., P. Oßwald, C. Naumann, S. Richter, and M. Köhler, 2012: Combustion kinetics of alternative jet fuels, Part-II: Reaction model for fuel surrogate. *Fuel 302*, 120736. doi: /10.1016/j.fuel.2021.120736.

Kathrotia, T., P. Oßwald, J. Zinsmeister, T. Methling, and M. Köhler, 2021: Combustion kinetics of alternative jet fuels, Part-III: Fuel modeling and surrogate strategy. *Fuel 302*, 120737. doi: /10.1016/j.fuel.2021.120737.

Kaufmann, S., C. Voigt, R. Heller, T. Jurkat-Witschas, M. Krämer, C. Rolf, M. Zöger, A. Giez, B. Buchholz, V. Ebert, T. Thornberry, and U. Schumann, 2018: Intercomparison of mid-latitude tropospheric and lower stratospheric water vapor measurements and comparison to ECMWF humidity data. *Atmos. Chem. Phys.*, doi: 10.5194/acp-18-16729-2018.

Kleine, J., C. Voigt, D. Sauer, H. Schlager, M. Scheibe, T. Jurkat-Witschas, S. Kaufmann, B. Kärcher, and B.E. Anderson, 2018: In situ observations of ice particle losses in a young persistent contrail. *Geophys. Res. Lett. 45*, 13553-13561. doi: 10.1029/2018GL079390.

Kosir, S., R. Stachler, J. Heyne, and F. Hauck, 2020: High-performance jet fuel optimization and uncertainty analysis. *Fuel* 281, 118718. DOI: 10.1016/j.fuel.2020.118718.

Lee, D.S., D.W. Fahey, P.M. Forster, P.J. Newton, R.C.N. Wit, L.L. Lim, B. Owen, and R. Sausen, 2009: Aviation and global climate change in the 21st century. *Atmos. Environ. 43*, 3520–3537.

Lee, D.S., D.W. Fahey, A. Skowron, M.R. Allen, U. Burkhardt, Q. Chen, S.J. Doherty, S. Freeman, P.M. Forster, J. Fuglestvedt, A. Gettelman, A. R.R. DeLeon, L.L. Lim, M.T. Lund, T.J. Millar, B. Owen, J.E. Penner, G. Pitari, M.J. Prather, R. Sausen, and L.J. Wilcox, 2021: The contribution of global aviation to anthropogenic climate forcing for 2000 to 2018. *Atmos. Environ. 244*, 1-29. DOI: 10.1016/j.atmosenv.2020.117834.

Lefebvre, A.H. and D.R. Ballal, 2010: Gas Turbine Combustion: Alternative Fuels and Emissions. 3rd: CRC Press. http://www.crcnetbase.com/doi/10.1201/9781420086058.

Lewellen, D.C., 2014: Persistent Contrails and Contrail Cirrus. Part II: Full Lifetime Behavior. *J. Atmos. Sci. 71*, 4420-4438. doi: 10.1175/JAS-D-13-0317.1

Lewellen, D. C., O. Meza, and W. W. Huebsch, 2014: Persistent contrails and contrail cirrus. Part I: Large-eddy simulations from inception to demise. *J. Atmos. Sci. 71*, 4399–4419. doi: 10.1175/JAS-D-13-0316.1

Li, Y., C. Mahnke, S. Rohs, U. Bundke, N. Spelten, G. Dekoutsidis, S. Groß, C. Voigt, U. Schumann, A. Petzold, and M. Krämer, 2023: Upper-tropospheric slightly ice-subsaturated regions: frequency of occurrence and statistical evidence for the

appearance of contrail cirrus. *Atmos. Chem. Phys. 23*, 2251–2271. doi: 10.5194/acp-23-2251-2023.

Liati, A., D. Schreiber, P.A. Alpert, Y. Liao, B.T. Brem, P.C. Arroyo et al., 2019: Aircraft soot from conventional fuels and biofuels during ground idle and climb-out conditions: Electron microscopy and X-ray micro-spectroscopy. *Environ. Pollut. 247*, 658–67. doi: /10.1016/j.envpol.2019.01.078.

Lieuwen, T.C. and V. Yang, 2013: Gas Turbine Emissions. New York, UNITED STATES: Cambridge University Press.

Lobo, P., S. Christie, B. Khandelwal, S.G. Blakey, D.W. Raper, 2015: Evaluation of Non-volatile Particulate Matter Emission Characteristics of an Aircraft Auxiliary Power Unit with Varying Alternative Jet Fuel Blend Ratios. *Energy Fuels 29*, 7705–11. doi: /10.1021/acs.energyfuels.5b01758.

Marais, K., S.P. Lukachko, M. Jun, A. Mahashabde, and I.A. Waitz, 2008: Assessing the impact of aviation on climate. *Meteorol. Z. 17*, 157–172, DOI: 10.1127/0941-2948/2008/0274.

Marquart, S., R. Sausen, M. Ponater, and V. Grewe, 2001: Estimate of the climate impact of cryoplanes. *Aerospace Science and Technology 5*, 73-84.

Marquart, S., M. Ponater, L. Ström, and K. Gierens, 2005: An upgraded estimate of the radiative forcing of cryoplane contrails. *Meteorol. Z. 14*, 573-582.

MathPro 2023: Techno-economic assessment of process routes for naphthalenes control in petroleum jet fuel. Consultant Report. https://theicct.org/publication/naphthalene-control-jet-fuel-mar23/.

McEnally C. and L. Pfefferle, 2007: L. Improved sooting tendency measurements for aromatic hydrocarbons and their implications for naphthalene formation pathways. *Combustion and Flame 148*, :210–222. https://doi.org/10.1016/j.combustflame.2006.11.003.

Meerkötter, R., U. Schumann, D.R. Doelling, P. Minnis, T. Nakajima, and Y. Tsushima, 1999: Radiative forcing by contrails. *Ann. Geophys. 17*, 1080-1094.

Miller, M., P. Brook, and C. Evers, 2010: Reduction of sulphur limits in aviation fuel standards (SULPHUR). contract number R.2008.C11. Ed. by EASA.

Ministry of Defence ,2022: Defence Standard 91-091, Turbine Fuel, Aviation Kerosine Type, Jet A-1, NATO Code: F-35; Joint Service. AVTUR (14).

Minnis, P., D.F. Young, L. Nguyen, D.P. Garber, W.L. Smith Jr., and R. Palikonda., 1998: Transformation of contrails into cirrus clouds during SUCCESS. *Geophys. Res. L. 25*, 1157-1160.

Molloy, J.; R. Teoh, S. Harty, G. Koudis, U. Schumann, I. Poll, and M.E.J. Stettler, 2022: Design Principles for a Contrail-Minimizing Trial in the North Atlantic. Aerospace9, 375. https://doi.org/10.3390/aerospace9070375.

Moore, R. H., M. Shook, A. Beyersdorf, C. Corr, S. Herndon, W.B. Knighton, R. Miake-Lye, K.L. Thornhill, E.L. Winstead, Z.H. Yu, L.D. Ziemba, and B.E. Anderson, 2015: Influence of Jet Fuel Composition on Aircraft Engine Emissions: A Synthesis of

Aerosol Emissions Data from the NASA APEX, AAFEX, and ACCESS Missions. *Energy Fuels 29*, 2591-2600.

Moore, R.H., et al., 2017: Biofuel blending reduces particle emissions from aircraft engines at cruise conditions. *Nature 543,* 411-415. doi: 10.1038/nature21420.

Moore, R.H., et al., 2017b: SCIENTIFIC DATA | 4:170198 | DOI: 10.1038/sdata.2017.198

Myhre, G., D. Shindell, F.-M. Bréon, W. Collins, J. Fuglestvedt, J. Huang, D. Koch, J.-F. Lamarque, D. Lee, B. Mendoza, T. Nakajima, A. Robock, G. Stephens, T. Takemura, and H. Zhang, 2013: Anthropogenic and Natural Radiative Forcing. In: Climate Change 2013: The Physical Science Basis. Contribution of Working Group I to the Fifth Assessment Report of the Intergovernmental Panel on Climate Change [Stocker, T.F., D. Qin, G.-K. Plattner, M. Tignor, S.K. Allen, J. Boschung, A. Nauels, Y. Xia, V. Bex, and P.M. Midgley (eds.)]. Cambridge University Press, Cambridge, United Kingdom and New York, NY, USA.

NACA, 1957: National Advisory Committee on Aeronautics, https://history.nasa.gov/SP-4404/ch6-4.htm.

Niklaß, M., K. Dahlmann, V. Grewe, S. Maertens, M. Plohr, J. Schellhaase, J. Schwieger, U. Brodmann, C. Kurzböck, M. Repmann, N. Schweitzer, and M. v. Unger, 2019: Integration of Non-CO2 Effects of Aviation in the EU ETS and under CORSIA. Project report. Umweltbundesamt (German Environmental Office). 242 S.

Owen, B., J.G. Anet, N. Bertier, S. Christie, M. Cremaschi, S. Dellaert, et al., 2022: Review: Particulate Matter Emissions from Aircraft. *Atmosphere 13*, 1230. DOI: 10.3390/atmos13081230.

Pelucchi, M., P. Oßwald, W. Pejpichestakul, A. Frassoldati, and M. Mehl, 2021: On the combustion and sooting behavior of standard and hydro-treated jet fuels: An experimental and modeling study on the compositional effects. *Proc. Combust. Inst. 38*, 523– 532.

Peters, G., B. Aamaas, T. Berntsen, and J. Fuglestvedt, 2011: The integrated global temperature change potential (iGTP) and relationships between emission metrics. *Environ. Res. Lett. 6*, 044021.

Petzold, A., R. Busen, R., F.P. Schröder, R. Baumann, M Kuhn, J. Ström, D.E. Hagen, P.D. Whitefield, D. Baumgardner, F. Arnold, S. Borrmann, and U. Schumann, 1997: Nearfield measurements on contrail properties from fuels with different sulfur content. *J. Geophys. Res. 102*, 29867–29880. doi: 10.1029/97JD02209.

Petzold, A., A. Döpelheuer, C.A. Brock, and F. Schröder, 1999: In-Situ Observations and Model Calculations of Black Carbon Emission by Aircraft at Cruise Altitude. *J. Geophys. Res. 104 (D18)*, 22171-22181.

Petzold, A., P. Neis, M. Rütimann, S. Rohs, F. Berkes, H.G.J. Smit, M. Krämer, N. Spelten, P. Spichtinger, P. Nedelec, and A. Wahner, 2020: Ice-supersaturated air masses in the northern mid-latitudes from regular in situ observations by passenger aircraft: vertical distribution, seasonality and tropospheric fingerprint. *Atmos. Chem. Phys. 20,* 8157-8179. doi: 10.5194/acp-20-8157-2020

Ponater, M., S. Marquart, R. Sausen, and U. Schumann, 2005: On contrail climate sensitivity. *Geophys. Res. Lett. 32*, L10706, doi:10.1029/2005GL022580, 1-5.

Popovicheva, O.B., N.M. Persiantseva, E.E. Lukhovitskaya, N.K. Shonija, N.A. Zubareva, B. Demirdjian, D. Ferry, and J. Suzanne, 2004: Aircraft engine soot as contrail nuclei. *Geophys. Res. L. 31,* L11104. doi: 10.1029/2003GL018888.

Popovicheva, O.B., et al., 2008: Water interaction with hydrophobic and hydrophilic soot particles. *Phys. Chem. Chem. Phys. 10,* 2332-2344.

Prather, M., R. Sausen, A.S. Grossman, J.M. Haywood, D. Rind, and B.H. Subbaraya, 1999: Potential climate change from aviation. In J.E. Penner, D.H. Lister, D.J. Griggs, D.J. Dokken and M. McFarland (eds.): Aviation and the Global Atmosphere. A Special Report of IPCC Working Groups I and III. Cambridge University Press, Cambridge, UK, 185-215.

Pregger, T., and many others, 2020: Future Fuels- Analyses of the Future Prospects of Renewable Synthetic Fuels. *Energies 13*, 138.

Pütz, F., C. Hall, B. Rauch, Bastian, and A. Huber, 2022: Reinforcement Learning for the Identification of Isomers with a Strong Sooting Tendency. In: 17th International Conference on Stability Handling and Use of Liquid Fuels, IASH 2022. 17th International Conference on Stability, Handling and Use of Liquid Fuels (IASH2022), 11.-15.09.2022, Dresden, Germany.

QinetiQ,2010: QinetiQ/09/01835 Issue 1.1 Reduction in Sulphur Limits in Aviation Fuel Standards (Sulphur). https://www.easa.europa.eu/en/document-library/research-reports/easa2008c11

Rap, A., P.M. Forster, J.M. Haywood, A. Jones, and O Boucher, 2010: Estimating the climate impact of linear contrails using the UK Met Office climate model. *Geophys. Res. Lett. 37*, L20703. doi: 10.1029/2010GL045161.

Richter S., T. Kathrotia, C. Naumann, S. Scheuermann, and U. Riedel, 2021: Investigation of the sooting propensity of aviation fuel mixtures. CEAS Aeronaut J 12, 115–123. https://doi.org/10.1007/s13272-020-00482-7.

Sausen, R., I. Isaksen, V. Grewe, D. Hauglustaine, D.S. Lee, G. Myhre, M.O. Köhler, G. Pitari, U. Schumann, F. Stordal, and C. Zerefos, 2005: Aviation radiative forcing in 2000: An update on IPCC (1999). *Meteorol. Z. 14*, 555-561.

Sausen, R., S. Hofer, K. Gierens, L. Bugliaro, R. Ehrmanntraut, I. Sitova, K. Walczak, A. Burridge-Diesing, M. Bowman, and N. Miller, 2023: Can we successfully avoid persistent contrails by small altitude adjustments of flights in the real world? *Meteorol. Z.*, in press.

Schmidt, E., 1941: Die Entstehung von Eisnebel aus den Auspuffgasen von Flugmotoren. *Schriften der deutschen Akademie der Luftfahrtforschung Vol. 44,* 1-15.

Schripp, T., et al., 2022: Aircraft engine particulate matter emissions from sustainable aviation fuels: Results from ground-based measurements during the NASA/DLR campaign ECLIF2/ND-MAX. Fuel 325. doi: /10.1016/j.fuel.2022.124764, 2022.

Schröder, F.P., B. Kärcher, C. Duroure, J. Ström, A. Petzold, J.-F. Gayet, B. Strauss, P. Wendling, and S. Borrmann, 2000: The transition of contrails into cirrus clouds. *J. Atmos. Sci. 57*, 464–480.

Schumann, U., 1996: On conditions for contrail formation from aircraft exhausts. *Meteorol. Z. 5*, 4–23.

Schumann, U., F. Arnold, R. Busen, J. Curtius, B. Kärcher, A. Kiendler, A. Petzold, H. Schlager, F. Schröder, and K.H. Wohlfrom, 2002: Influence of fuel sulfur on the composition of aircraft exhaust plumes: The experiments SULFUR 1-7. *J. Geophys. Res. 107,* 1-28.

Schumann U., B. Mayer, K. Graf, and H. Mannstein, 2012: A Parametric Radiative Forcing Model for Contrail Cirrus. *J. App. Meteorol. Climatol. 51G*, 1391–406

Schumann, U., P. Jeßberger, and C. Voigt, 2013: Contrail ice particles in aircraft wakes and their climatic importance. *Geophys. Res. Lett. 40*, 2867-2872. doi: 10.1002/grl.50539.

Schumann, U., R. Baumann, D. Baumgardner, S.T. Bedka, D.P. Duda, V. Freudenthaler, J.-F. Gayet, A.J. Heymsfield, P. Minnis, M. Quante, E. Raschke, H. Schlager, M. Vázquez-Navarro, C. Voigt, and Z. Wang, 2017: Properties of individual contrails: a compilation of observations and some comparisons. *Atmos. Chem. Phys. 17,* 403-438. doi: 10.5194/acp-17-403-2017

Shine, K., J. Fuglestvedt, K. Hailemariam, and N. Stuber, 2005: Alternatives to the global warming potential for comparing climate impacts of emissions of greenhouse gases. *Clim. Change 68*, 281–302.

Shine, K. and D. Lee, 2021: COMMENTARY: Navigational avoidance of contrails to mitigate aviation's climate impact may seem a good idea —but not yet. *Green Air News of 22 July 2021*, https://www.greenairnews.com/?p=1421 as of 06 February 2022.

Spichtinger, P., K. Gierens, and W. Read, 2002: The statistical distribution law of relative humidity in the global tropopause region. *Meteorol. Z. 11*, 83-88.

Spichtinger, P., K. Gierens, and H. Wernli, 2005: A case study on the formation and evolution of ice supersaturation in the vicinity of a warm conveyor belt's outflow region. *Atmos. Chem. Phys. 5,* 973-987.

Spichtinger, P., K. Gierens, and A. Dörnbrack, 2005: Formation of ice supersaturation by mesoscale gravity waves. *Atmos. Chem. Phys. 5,* 1243-1255.

Striebich, R. C., L.M. Shafer, R.K., Adams, Z.J. West, M.J. DeWitt, and S. Zabarnick, 2014: Hydrocarbon group type Analysis of petroleum-derived and synthetic fuels using GCxGC. Washington, DC: Energy and Fuels ACS Publications

Ström, L. and K. Gierens, 2002: First simulations of cryoplane contrails. *J. Geophys. Res. 107*, doi:10.1029/2001JD000838.

Sussmann, R. and K. Gierens, 1999: Lidar and numerical studies on the different evolution of a contrail's vortex system and its secondary wake. *J. Geophys. Res. 104*, 2131-2142.

Teoh, R., U. Schumann, E. Gryspeerdt, M. Shapiro, J. Molloy, G. Koudis, C. Voigt, and M.E.J. Stettler, 2022a: Aviation contrail climate effects in the North Atlantic from 2016 to 2021. *Atmos. Chem. Phys. 22*, 10919–10935. doi: 10.5194/acp-22-10919-2022.

Teoh, R., U. Schumann, C. Voigt, T. Schripp, M. Shapiro, Z. Engberg, J. Molloy, G. Koudis, and M.E.J. Stettler, 2022b: Targeted Use of Sustainable Aviation Fuel to Maximise Climate Benefits. *Environ. Sci. Technol*. doi: 10.1021/acs.est.2c05781.

Timko, M.T., Z. Yu, T.B. Onasch, H.W. Wong, R.C. Miake-Lye, A.J. Beyersdorf, B. Anderson, K.L. Thornhill, E.L. Winstead, E. Corporan, M.J. DeWitt, C.D. Klingshirn, C. Wey, K. Tacina, D.S. Liscinsky, R. Howard, and A. Bhargava, 2010: Particulate Emissions of Gas Turbine Engine Combustion of a Fischer-Tropsch Synthetic Fuel. *Energy Fuels 24*, 5883-5896.

The Defense Energy Support Center ,2009: Petroleum Quality Information System Annual Report 2008. Fort Belvoir: The Defense Energy Support Center.

Thom, M. A. ,2018: Review of Existing Test Methods Used for Aviation Jet Fuel and Additive Property Evaluations with Respect to Alternative Fuel Compositions. Hg. v. COORDINATING RESEARCH COUNCIL, INC. (CRC Project No. AV-23-15/17). http://crcsite.wpengine.com/wp-content/uploads/2019/05/AV-23-15-17-Final-Report-defstan-rev-3-MAY-051618-1.pdf.

Tucker, J., C. Lewis, and A. Clark, 2011: Jet fuel desulphurization: An investigation into the impact of hydrotreatment on product quality, 12th International Conference on Stability, Handling and Use of Liquid Fuels, IASH 2011, Sarasota, Florida, USA.

Unterstrasser, S. and K. Gierens, 2010: Numerical simulations of contrail-to-cirrus transition -- Part 1: An extensive parametric study. *Atmos. Chem. Phys. 10,* 2017-2036.

Unterstrasser, S. and K. Gierens, 2010: Numerical simulations of contrail-to-cirrus transition -- Part 2: Impact of initial ice crystal number, radiation, stratification, secondary nucleation and layer depth. *Atmos. Chem. Phys. 10,* 2037-2051.

Unterstrasser, S., R. Paoli, I. Sölch, C. Kühnlein, and T. Gerz, 2014: Dimension of aircraft exhaust plumes at cruise conditions: effect of wake vortices. Atmos. Chem. Phys. 14, 2713-2733. doi: 10.5194/acp-14-2713-2014

Unterstrasser, S., K. Gierens, I. Sölch, and M. Lainer, 2016: Numerical simulations of homogeneously nucleated natural cirrus and contrail-cirrus. Part 1: How different are they? *Meteorol. Z. 26,* 621-642. doi: 10.1127/metz/2016/0777

Unterstrasser, S., K. Gierens, I. Sölch, and M. Wirth, 2016: Numerical simulations of homogeneously nucleated natural cirrus and contrail-cirrus. Part 2: Interaction on local scale. *Meteorol. Z. 26,* 643-661. doi: 10.1127/metz/2016/0780.

Urbanek, B., S. Groß, M. Wirth, M. Krämer, and C. Voigt, 2018: High Depolarization Ratios of naturally occurring Cirrus Clouds near Air Traffic Regions over Europe. *Geophys. Res. Lett.*, doi: 10.1029/2018GL079345.

Vander Wal, R.L., V.M. Bryg, and C.H. Huang, 2014: Aircraft engine particulate matter: Macromicro- and nanostructure by HRTEM and chemistry by XPS. *Combust Flame 161*, 602–11. doi: 10.1016/j.combustflame.2013.09.003.

Vázquez-Navarro, M., H. Mannstein, and S. Kox, 2015: Contrail life cycle and properties from 1 year of MSG/SEVIRI rapid-scan images. *Atmos. Chem. Phys. 15,* 8739-8749. doi: 10.5194/acp-15-8739-2015.

Voigt, C., et al., 2010: In-situ observations of young contrails - Overview and selected case studies from the CONCERT campaign. *Atmos. Chem. Phys. 10*, 9039–9056. doi: 10.5194/acp-10-9039-2010, 2010.

Voigt, C., U. Schumann, P. Jessberger, T. Jurkat, A. Petzold, J.-F. Gayet, M. Krämer, T. Thornberry, and D. Fahey, 2011: Extinction and optical depth of contrails. *Geophys. Res. Lett. 38*, L11806, doi: 10.1029/2011GL047189

Voigt, C., T. Jurkat, H. Schlager, D. Schäuble, A. Petzold, and U. Schumann, 2012: *Aircraft emissions at cruise and plume processes*. In: Atmospheric Physics: Background - Methods - Trends Research Topics in Aerospace. Springer-Verlag Berlin Heidelberg. Seiten 675-692. ISBN 978-3-642-30182-7. ISSN 2194-8240.

Voigt, C., et al., 2017: ML-CIRRUS: The Airborne Experiment on Natural Cirrus and Contrail Cirrus with the High-Altitude Long-Range Research Aircraft HALO. *Bull. Amer. Meteorol. Soc. 98*, 271-288. doi: 10.1175/BAMS-D-15-00213.1. ISSN 0003-0007.

Voigt, C., J. Kleine, D. Sauer, R.H. Moore, T. Bräuer, P. Le Clercq, S. Kaufmann, M. Scheibe, T. Jurkat-Witschas, M. Aigner, U. Bauder, Y. Boose, S. Borrmann, E. Crosbie, G.S. Diskin, J. DiGangi, V. Hahn, C. Heckl, F. Huber, J.B. Nowak, M. Rapp, B. Rauch, C. Robinson, T. Schripp, M. Shook, E. Winstead, L. Ziemba, H. Schlager, and B.E. Anderson, 2021: Cleaner burning aviation fuels can reduce contrail cloudiness. *Nature Commun. Earth Environ. 21,* 2, 1-10. doi: 10.1038/s43247-021-00174-y.

Wang, Z., L. Bugliaro, T. Jurkat-Witschas, R. Heller, U. Burkhardt, H. Ziereis, G. Dekoutsidis, M. Wirth, S. Groß, S. Kirschler, S. Kaufmann, and C. Voigt, 2023: Observations of microphysical properties and radiative effects of a contrail cirrus outbreak over the North Atlantic. *Atmos. Chem. Phys. 23,* 1941–1961. doi: 10.5194/acp-23-1941-2023.

Weibel, D., 2018: Techno-economic assessment of jet fuel naphthalene removal to reduce non-volatile particulate matter emissions [S.M. thesis, Massachusetts Institute of Technology]; DSpace@MIT. https://hdl.handle.net/1721.1/124174.

Wilhelm, L., K. Gierens, and S. Rohs, 2021: Weather variability induced uncertainty of contrail radiative forcing. *Aerospace 8,* 332. doi: 10.3390/aerospace8110332.

Wilhelm, L., K. Gierens, and S. Rohs, 2022: Meteorological conditions that promote persistent contrails. *Appl. Sci. 12,* 4450. doi: 10.3390/app12094450.

Wolf, K., N. Bellouin, and O. Boucher, 2023: Radiative effect by cirrus cloud and contrails – A comprehensive sensitivity study. EGUsphere, Preprint, 1–38. doi: 10.5194/egusphere-2023-155.

Wolters, F., 2022: Einfluss alternativer drop-in Flugturbinenkraftstoffe auf das Emissionsverhalten des globalen Luftverkehrs, Dissertation Ruhr-Universität Bochum, doi.org/10.13154/294-7624.

Yu, F. and R.P. Turco, 1998: The Formation and Evolution of Aerosols in Stratospheric Aircraft Plumes: Numerical Simulations and Comparisons with Observations. J. *Geophys. Res., Atmospheres 103 (D20*), 25915–25934. https://doi.org/10.1029/98JD02453.

Zschocke, A., 2014: Abschlussbericht zu dem Vorhaben Projekt BurnFAIR Arbeitspakete 1.1 bis 1.4. https://www.dbfz.de/fileadmin/user_upload/Referenzen/Berichte/Abschlussbericht_BurnFAIR.pdf.

Concawe
Environmental Science for
European Fuel Manufacturing

Concawe
Boulevard du Souverain 165
B-1160 Brussels
Belgium

Tel: +32-2-566 91 60
Fax: +32-2-566 91 81
e-mail: info@concawe.org
http://www.concawe.eu

ISBN 978-2-87567-181-3